NANOMEDICINE: MULTIFUNCTIONAL NANOPARTICLES OF BIODEGRADABLE POLYMERS FOR CANCER TREATMENT

LIU YUTAO

NATIONAL UNIVERSITY OF SINGAPORE

2011

NANOMEDICINE: MULTIFUNCTIONAL NANOPARTICLES OF BIODEGRADABLE POLYMERS FOR CANCER TREATMENT

LIU YUTAO

(B.Sc., Fudan University)

A THESIS SUBMITTED

FOR THE DEGREE OF DOCTOR OF PHILOSOPHY

DEPARTMENT OF CHEMICAL AND BIOMOLECULAR ENGINEERING

NATIONAL UNIVERSITY OF SINGAPORE

2011

ACKNOWLEDGEMENTS

First of all, I would like to take this opportunity to thank my supervisor, Professor Feng Si-Shen, for giving me the opportunity to conduct this research project and the enlightenment in the area of nanomedicine. I appreciate his support, advice and guidance throughout my postgraduate study. I also want to express my gratitude to Prof. Liu Bin, for her kindly support and guidance on my learning and research.

I am grateful of the research scholarship provided by NUS for supporting me to finish the study as well as the financial support from Singapore for the research projects. I would like to thank the professors in Department of Chemical & Biomolecular Engineering who have helped me for my work.

Moreover, I would thank my lab colleagues and my students for their help and directions run through my work. I would like to thank my collaborator, Mr. Li Kai for his support on my research works. The assistance from the professional officers, lab technologists and administrative officers in NUS, Dr. Yuan Zeliang, Mr. Chia Phai Ann, Mr. Zhang Jie, Ms. Lee Shu Ying, Mr. Zhang Weian, Mr. Boey Kok Hong, Ms. Lee Chai Keng, Mr. Mao Ning, Ms. Samantha Fam, Ms. Dinah Tan, Ms. Li Xiang, Mdm. Priya, Mdm. Li Fengmei, Ms. Doris How, Ms. Tan Hui Ting, and many others, is also appreciated.

Finally, the patience, guidance and help from my parents, friends, and classmates would be appreciated. I am also appreciative for the difficulties contributed by anyone who do not like me.

TABLE OF CONTENTS

SUMMARY

Multifunctional nanocarriers have been regarded as potent candidates for efficient cancer nanomedicine. Nanoparticles of biodegradable polymers were postulated as promising platforms to establish the multiple functions for anticancer purposes such as delivery of therapeutics, targeting the desired site, imaging the diseased cells, and monitoring the effects of treatment. In this PhD work, the proof-of-concept experiments were conducted based on the surface modified and functionalized PLGA nanoparticle systems in order to develop the multifunctional nanocarriers as novel formulations of cancer nanomedicine, especially for breast cancer. The desired properties of such developed nanoparticle formulations for drug delivery include small size, narrow size distribution, high stability, effective drug loading, sustained and controlled release of the drug, strong interaction with cells, specific uptake by cancer cells as well as efficient anticancer activity. Phospholipids were, at first, used to improve the features of polymeric nanoparticles through development of lipid shell polymer core nanoparticles. Optimization was carried out in order to identify the optimal type and amount of phospholipids for the fabrication of particles with desired properties in terms of particle size, size distribution, surface charge, shape and morphology, surface composition and drug loading. The feasibility of the optimal formulation for anticancer drug delivery was proved by the *in vitro* drug release, *in vitro* cellular uptake, and *in vitro* cytotoxicity studies. All the consistent results show that nanoparticles of DLPC shell and PLGA core could be a prospective drug delivery carrier which is able to provide greater cytotoxicity effect but at the same time alleviate the side effects. Subsequently, more advanced nanoparticles of lipid shell and polymer core was developed with the conjugation of molecular ligands to achieve

targeted nanomedicine by using the optimal formulation investigated in the previous work. An illustration of the formulation was shown to prove the potential of the designed nanocarrier as a versatile platform for targeted cancer nanomedicine.

Development of the strategy to precisely control the quantity of targeting ligands on nanocarriers and investigation on the impact of the quantity on the targeting effects, i.e. cellular uptake efficiency and cell inhibition performance was also included in this work. A copolymer blend of PLGA and PEGylated PLGA was used to achieve the quantitative control of the antibodies attached on the nanoparticles, after which the antibody conjugated polymeric nanoparticles with drug loaded was produced to show the prospect of the formulation to deliver drugs. The targeting effect on HER2-overexpressed breast cancer cells was presented by using the receptor overexpressed cancer cells. The development of cutting-edge nanoparticles of biodegradable polymers with overall fascinating performance demonstrates the progress in the field of nanomedicine for cancer treatment.

NOMENCLATURE

ACN	acetonitrile
ADME	absorption, distribution, metabolism and excretion
AUC	area under concentration-time curve
BBB	blood-brain barrier
CLSM	confocal laser scanning microscopy
CNS	central nervous system
CNTs	carbon nanotubes
CT	computed tomography
DCC	dicyclohexylcarbodiimide
DCM	dichloromethane
DCPC	1,2-dicapryl-*sn*-glycero-3-phosphocholine
DDS	drug delivery systems
DLPC	1,2-dilauroyl-*sn*-glycero-3-phosphocholine
DLS	dynamic light scattering
DMAP	4-(dimethylamino) pyridine
DMEM	Dulbecco's Modified Eagle's Medium
DMPC	1,2-dimyristoyl-*sn*-glycero-3-phosphocholine
DMSO	dimethyl sulfoxide
DNA	deoxyribonucleic acid
DPPC	1,2-dipalmitoyl-*sn*-glycero-3-phosphocholine
DSPC	1,2-distearoyl-*sn*-glycero-3-phosphocholine
DSPE	1,2-distearoyl-*sn*-glycero-3-phosphoethanolamine
EDAC	*N*-(3-Dimethylaminopropyl)-*N′*-ethylcarbodiimide hydrochloride
EE	encapsulation efficiency

EGFR	epidermal growth factor receptor
EPR	enhanced permeability and retention
FBS	fetal bovine serum
FDA	Food and Drug Administration
FESEM	field emission scanning electron microscopy
FITC	fluorescein isothiocyanate
FR	folate receptor
GI	gastro-intestinal
HER	human epidermal growth factor receptor
HER2	human epidermal growth factor receptor type 2
HLB	hydrophile-lipophile balance
^{1}H NMR	proton nuclear magnetic resonance
HPLC	high performance liquid chromatography
HPMA	*N*-(2-hydroxypropyl)methacrylamide
HSA	human serum albumin
IC_{50}	concentration at which 50% cell population is suppressed
IgG	Immunoglobulin G
IOs	iron oxides
LCST	lower critical solution temperature
LLS	laser light scattering
LPNPs	lipid-shell and polymer-core nanoparticles
mAb	monoclonal antibody
MBC	metastatic breast cancer
MDR	multi-drug resistance
MPS	mononuclear phagocyte system

MRI	magnetic resonance imaging
MTD	maximum tolerable dose
MTT	3-(4,5-dimethylthiazol-2-yl)-2,5-diphenyltetrazolium bromide
NP	nanoparticle
NIRF	near infrared fluorescence
NHS	*N*-hydroxysuccinimide
OI	optical imaging
PAMAM	polyamidoamine
PBCA	poly(butylcyanoacrylate)
PBS	phosphate buffer saline
PCL	poly(ε-caprolactone)
PDI	polydispersity index
PDT	photodynamic therapy
PEG	poly(ethylene glycol)
PEG-PE	polyethylene glycol-phosphatidylethanolamine
PET	positron emission tomography
P-gp	P-glycoprotein
PI	propidium iodide
PLA	poly(lactide)
PLGA	poly(D,L-lactide-co-glycolide)
PVA	poly(vinyl alcohol)
PVDF	poly(vinylidene fluoride)
QDs	quantum dots
RES	reticuloendothelial system
RME	receptor-mediated endocytosis

RNA	ribonucleic acid
SD	standard deviation
SE	standard error
Sulfo-NHS	*N*-hydroxysulfosuccinimide
TEA	triethylamine
TPGS	D-α-tocopheryl polyethylene glycol succinate
trypsin-EDTA	trypsin-ethylenediaminetetraacetic acid
Tween 80	polyoxyethylene (20) sorbitan monooleate (or polysorbate 80)
XPS	X-ray photoelectron spectroscopy

LIST OF TABLES

LIST OF FIGURES

Chapter 1 : Introduction

1.1 Background

Cancer is one of the most dreaded diseases today (Jemal et al., 2009). Nevertheless, there has been no substantial progress in fighting against cancer in the past 50 years. The mostly used cancer therapies in the current stage have still been surgery followed by chemotherapy and/or radiotherapy, which are not satisfactory enough to suppress the disease and the survival rate of the patients is still not favorable. As a result, reevaluation of basic assumptions concerning the nature of cancer and how to better assess risk, prevent, and medically manage is a high priority. While it is quite old already, chemotherapy has still been one of the most important components in cancer therapies due to the systemic property. Although chemotherapy is a complicated procedure and carries a high risk due to dosage form, drug toxicity, restricted pharmacokinetics and pharmacodynamics (ADME), severe side effects and drug resistance at various physiological levels (Feng, 2006), the problems could be readily solved by chemotherapeutic engineering, which was defined as application and further development of engineering especially chemical engineering principles to solve the problems in the current regimen of chemotherapy to achieve the best efficacy with the least side effects (Feng and Chien, 2003).

As a major technology for engineering chemotherapy, nanotechnology has been regarded as one of the most promising approaches to deal with cancer and has been extensively exploited to improve conventional chemotherapy in the recent years (Farokhzad and Langer, 2009; Ferrari, 2005; Sinha et al., 2006). Nanoparticles (NPs) of biodegradable polymers have become promising platforms for sustained, controlled

and targeted drug delivery to improve the therapeutic effects and reduce the side effects against cancer (Kataoka et al., 2001; Farokhzad and Langer, 2006; van Vlerken et al., 2007). They may provide an ideal solution for the problems encountered in current regimen of chemotherapy owing to their unique properties such as the small size, acceptable biocompatibility, high drug encapsulation efficiency especially for hydrophobic drugs, controlled and sustained drug release manner, high cellular uptake efficiency, desired pharmacokinetics, long circulation half-life, and highly tailored functions (Cho et al., 2008; Tong and Cheng, 2007; Zhang et al., 2008a). With the aid of NPs, the problems of traditional chemotherapy, i.e. the dosage form, toxicity, severe side effects, and unfavorable pharmacokinetics could be settled with satisfaction.

Nanomedicine is designed to provide an ideal method by application of nanotechnology to solve the problems in medicine, which means to diagnose and treat the disease at cellular and molecular level and thus will radically change the way we diagnose, treat and prevent diseases. Nanoparticles of biodegradable polymers as delivery carriers for transportation of therapeutic agents are one of the promising platforms to fulfill the purpose. To achieve optimized anticancer effect, the NPs should be properly tailored by the selection of biomaterials and the engineering of the nanoparticulate systems that are able to be efficiently carry desired payloads, specifically taken up by targeted diseased cells and subsequently release the payloads at a plasma concentration between the minimum effective level and the maximum tolerable level in a sustained manner (Gref et al., 1994; Langer, 2001; Ferrari, 2005).

In addition, by using nanotechnology, multifunctional NPs with multiple functions to treat cancers are also able to be produced. Since cancer is a very complicated system, powerful anticancer weapons equipped with a variety of functions are highly desired.

The functions such as targeting, diagnosing, therapy-delivering, long circulating and result-reporting could be developed for cancer diagnosis and treatment. Cancer will thus become curable at its earliest stage by molecular imaging guided, targeted and sustained chemotherapy since high drug concentration could be delivered to a very limited area and the needed amount of the drug could be minimized.

The screening of biomaterials to build up the matrix (or core) of the NPs is the first issue that should be addressed. The favorable features from the NPs, to large extent, depend on the properties of the materials. In the past a few years, PLGA approved by FDA for therapeutic devices has been one of the most widely used biodegradable polymers for anticancer drug delivery. Through engineering methods, the NPs can be easily produced from the polymers to load hydrophobic anticancer drugs like docetaxel, which is a potent drug used in the treatment of a wide spectrum of cancers like breast cancer, ovarian cancer, small and non-small cell lung cancer, prostate cancer, etc. PLGA NPs were proved to possess the advantages such as accepted low toxicity, high stability in storage, high drug loading capability, controlled and sustained drug release behavior, high cell penetration ability and favorable pharmacokinetics (Feng et al., 2007; Win and Feng, 2006). Moreover, polymeric nanoparticles show some advantages with respect to other drug delivery systems besides the stability during storage (Müller et al., 2001). After intravenous administration, they may extravasate solid tumors and into inflamed or infected sites, where the capillary endothelium is defective thus passively targeting drug loaded nanoparticles to the tumor site (Musumeci et al., 2006).

However, at present, NPs should be appropriately engineered prior to taking effect in practical cancer chemotherapy in that there are several fundamental problems and

technical barriers that must be overcome for anticancer nanomedicine (Nie, 2010), which include opsonization and phagocytosis of NPs (Owens and Peppas, 2006), capture and retention of NPs in RES (Jain, 1990), difficulties in nanoparticle accumulation in vicinity of solid tumors and targeting the cancerous cells followed by penetration into solid tumors (Dreher et al., 2006; Minchinton and Tannock, 2006). The effective solution is to engineer NPs by tuning their size, polydispersity, surface area, surface charge, morphology, as well as surface chemical property through introducing versatile materials on NPs to meet the needs. Among those characteristics of NPs, surface property plays a key role in determining the performance on nanomedicine in the aspects of 1) enhancing the circulation time of the NPs, which results by avoiding the recognition by phagocytic system and escaping from the adsorption of proteins in bloodstream; 2) prompting cellular uptake efficiency benefiting from higher interaction of the surface of NPs with the cell membrane; and 3) decorating NPs surface to achieve favorable chemotherapy by coating with various functional materials and/or conjugating desired molecules.

Furthermore, targeted drug delivery or tumor specific drug delivery using NPs is of paramount importance since the therapeutic agents can be concentrated in the diseased tissues or cells which results in higher anticancer effect with lower side effects exposed in healthy organs or normal cells with the aid of accurate guidance to the specific sites by targeted molecular imaging to visualize tumors and cancer cells. Once the NPs have been attached with targeting ligands, the payloads inside the particles can thus, ideally, be only released in the desired sites with the protection from the exposure of physiological fluids and plasma components, and subsequently, destroy the targeted

enemies, as like the magic bullets (Strebhardt and Ullrich, 2008) or missiles (Barbe et al., 2004).

1.2 Objective of the PhD work

To sum up the objective of this PhD work, we dedicated to developing new nanomedicine formulations based on nanoparticles of biodegradable polymers, as more powerful weapons with more advanced overall performance, for cancer treatment with multiple functions, especially for breast cancer after Stage 1. The focus lies on the modification of surface properties of the NPs to achieve the purpose of desired surface properties, higher cellular uptake efficiency, better therapeutic effects, targeted therapy on cancer, and finally controlling the targeting effect.

The main body of this thesis includes four chapters. The first one starts from the report of proof-of-concept study on the feasibility of using phospholipids to produce lipid shell polymer core NPs, which are novel alternative drug formulations with the combined merits of liposomes and polymeric nanoparticles. The characterization and evaluation on the cellular level exhibits solid evidence of the possibility of developing the novel nanocarriers for drug delivery as well as the advantages over commercial drug formulations and traditional drug delivery carriers. The study creates a new platform of nanotechnology based nanomedicine formulation possessing the high potential of further modification for various anticancer applications. Followed by the pioneering work, a derived nanoparticle of lipid shell and polymer core with molecular ligand attached for targeted cancer nanomedicine is reported in the next chapter. The more advanced nanocarrier was fabricated based on the previous optimization study

and equipped with more functions to achieve more superior properties and targeted drug delivery with the aid of versatile targeting ligands conjugated on the lipid shell. Afterwards, the emphasis of the work is still on the research of biomaterials that are appropriate to coat on polymeric particles to obtain more desired surface properties. In the third part, new PEGylated vitamin E analogues were synthesized as new-generation surfactants and applied to fabricate nanoparticles. The new and functional materials impart advantages to the particles over those coated by traditional surfactants. The preliminary research opens a new area of customizing surface functions of nanocarriers by simply using the tailored materials to coat on the particle surafce.

The last chapter displays a preliminary proof-of-concept study on the precision engineering of polymeric nanoparticles for quantitative control of targeted drug delivery. In other words, we proposed a "post-conjugation" strategy to achieve the purpose of precisely control the targeting ligands conjugated on the nanocarriers in a quantitative maner. By realization of the objective, it is possible to tune the targeting effects for cancer nanomedicine. Moreover, it was proved that the quantity of the targeting ligands do have great impact on the anticancer performance of the nanocarriers on cellular level. It is thus anticipated to make personalized cancer therapy come true in terms of optimal therapeutic effect while least side effects.

Chapter 2 : Literature Review

2.1 Cancer

Cancer is defined as diseases in which abnormal cells divide without control and that are able to invade other tissues. Up to date, cancer is the number one cause of death in the United States for people less than 75 years old (Mbeunkui and Johann, 2009). The recent statistics reported that about 25% of death is due to cancer in US, although the combined death rates for men decreased by 21.0% between 1990 and 2006 and for women, overall cancer death rates between 1991 and 2006 decreased by 12.3% (Jemal et al., 2010). Every year, more than 11 million people are diagnosed with cancer throughout the world and it may likely increase to 16 million by 2020. In 2005, cancer accounted for 7.6 million deaths from a total of 58 million deaths worldwide (Jemal et al., 2011). Currently, more than 200 different types of cancer have been discovered, most of which are named for the organ or type of cell in which they start. For example, cancer that begins in the breast is called breast cancer; cancer that begins in ovarian is called ovarian cancer. Cancer types can be grouped into broader categories, mainly including carcinoma (cancer that begins in the skin or in tissues that line or cover internal organs), sarcoma (cancer that begins in bone, cartilage, fat, muscle, blood vessels, or other connective or supportive tissue), leukemia (cancer that starts in blood-forming tissue such as the bone marrow and causes large numbers of abnormal blood cells to be produced and enter the blood), lymphoma and myeloma (cancers that begin in the cells of the immune system) and glioma (cancers that begin in the tissues of the brain and spinal cord) (http://www.cancer.gov/cancertopics/cancerlibrary/what-is-cancer).

Cancer cells develop because of damage to DNA commonly caused by external factors (chemicals, viruses, tobacco smoke, radiation, too much sunlight and infections) and internal factors (inherited metabolism mutations, hormones and immune conditions). When DNA is damaged or changed, producing mutations that affect normal cell growth and division, cells do not die when they should and new cells form while the body does not need them. The reason of the damage in DNA, although the exact mechanism behind has not been clearly elucidated yet, can be attributed to the activation of telomerase that was discovered by Carol W. Greider and Elizabeth Blackburn in 1984 who are the Nobel Prize Laureates in Physiology or Medicine 2009. For the normal cells, telomeres, which are found at the ends of chromosomes, will be shortened after each replication cycle, resulting in the programmed death (apoptosis) of the cells. While for the cancerous cells, due to the presence of telomerase which is an enzyme that adds DNA sequence repeats to the 3' end of DNA strands in the telomere regions, the telomeres will be elongated and will not be shortened after cell replication. As a result, the cancerous cells will become immortal (Blackburn, 2005).

Subsequently, the extra cells may form a mass of abnormally grown tissue in the vicinity of blood vessels called a tumor. Among tumors, benign tumors are not cancerous, which can often be removed, and, in most cases, do not come back. Cells in benign tumors do not spread to other parts of the body. But malignant tumors are cancerous, cells in which can invade nearby tissues and spread to other parts of the body. The spreading process that cancer cells travel from one part of the body to another through bloodstream or lymph system where they begin to grow and replace normal tissue is called metastasis (Klein, 2008).

The special property of tumor tissues leads to the difficulty of transporting therapeutic agents into the matrix and the agents will be usually eliminated from the tissue. Unlike most normal tissues, the interstitium of tumor tissues has high hydrostatic pressure, leading to an outward convective interstitial flow that can flush the drug away from the tumor. Even if the drug is successfully penetrated into the tumor interstitium, it may also be removed by multi-drug resistance (MDR) (Brigger et al., 2002). MDR is mainly attributed to overexpression of P-glycoprotein (P-gp) on the plasma membrane, which is capable of pumping drugs out of the cell (Figure 2.1). Several strategies for circumventing P-gp-mediated MDR have been proposed, including the co-administration of P-gp inhibitors and anticancer drugs encapsulated in nanoparticles (Krishna et al., 2000; Patil et al., 2009).

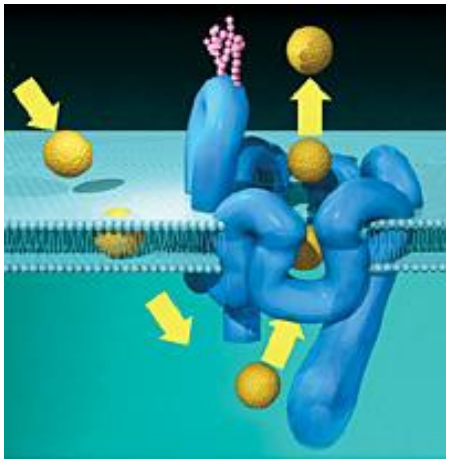

Figure 2.1 Structure of the drug efflux transporter: drug molecules (the balls) encounter MDR pumps (the knot) after passing through a cell membrane (adapted from http://publications.nigms.nih.gov/medbydesign/chapter1.html, copyright of Nye L.S.).

2.2 Treatments of cancer

Nowdays, death rates for the four most common cancers (prostate, breast, lung, and colorectal), as well as for all cancers combined, continue to decline; the rate of cancer incidence has declined since the early 1990s (http://progressreport.cancer.gov/).

Generally, there are several major types of treatment for cancer diseases: surgery, chemotherapy, radiotherapy, immunotherapy, anti-angiogenesis therapy, gene therapy, and photodynamic therapy, and usually, the combination of those therapies.

2.2.1 Surgery

Surgery is the oldest form of cancer treatment, whose primitive manner can be traced back to more than hundred years ago. The majority work of surgery to treat cancer is to excise tumors or the tissues invaded by cancer cells. It also has a key role in diagnosing cancer and finding out how far it has spread (staging). Advances in surgical techniques have allowed surgeons to successfully operate on a growing number of patients. Today, less invasive operations often can be done to remove tumors while saving as much normal tissue and function as possible. Surgery offers the greatest chance to cure for many types of cancer, especially those that have not spread to other parts of the body.

2.2.2 Chemotherapy

Chemotherapy is usually defined as the use of any medicine to treat any disease. Contemporarily, chemotherapy, or "chemo" for short, is most often narrowly regarded as taking certain types of drugs to kill or control cancer. Commonly the chemotherapeutic agents will be taken combined with surgery and/or radiotherapy.

Chemotherapy is also one of the most important therapies due to its systemic character which is able to treat the metastatic cancer cells. Cancer chemotherapy has been helping people beat cancer since the early 1950s. So far there have been hundreds of anticancer drugs available for clinical cancer defeating (Feng and Chien, 2003) and proved to be effective.

2.2.3 Radiotherapy

Radiotherapy has been made an important part of cancer treatment today. In fact, about half of all people with cancer will get radiation as one part of their cancer treatment, usually after surgery and combined with chemotherapy. Radiation is energy that is carried by waves or a stream of particles. It can change the genes (DNA) and some of the molecules of a cell. These genes control how cells in the body grow and divide. In cell cycle, radiation usually kills the cells that are actively or quickly dividing to inhibit cell mitosis.

2.2.4 Immunotherapy

Immunotherapy, also called biologic therapy or biotherapy, is a treatment that uses certain parts of the immune system to fight disease, including cancer. This can be done by stimulating own immune system to work harder or smarter, or giving immune system components, such as man-made immune system proteins. It is most likely to be effective when treating smaller, early stage cancers, whose main role at this time is making other forms of treatment better or providing cancer patients with another, often less toxic, treatment option.

2.2.5 Angiogenesis therapy

Angiogenesis is the creation of new blood vessels. Normally, it is a healthy process. As the human body grows and develops, it needs to make new blood vessels to deliver blood to all of its cells. But in a person with cancer, this same process creates new, very small blood vessels that provide a tumor with its own blood supply and allow it to grow. Anti-angiogenesis is a form of targeted therapy that uses drugs or other substances to inhibit the creation of new blood vessels for tumors. Without a blood supply, tumors cannot grow. Anti-angiogenesis drugs do not attack cancer cells directly. Instead, they target the blood vessels these cells need to survive and grow. By this mean, they may prevent new tumors from growing or shrink large tumors as long as their blood supply is cut off.

2.2.6 Gene therapy

Gene therapy involves inserting genetic material (DNA or RNA) into cells to restore a missing function or to give the cells a new function. Because missing or damaged genes cause certain diseases such as cancer, it makes sense to try to treat these diseases by adding the missing gene(s), fixing those which are damaged or replacing the abnormal ones by normal ones. Gene therapy is being used to treat cancers by adding functioning genes to cells that have diseased or missing genes, stopping oncogenes or other genes important to cancer from working, adding or changing genes to make cancer cells more unstable, adding or changing cancer cell genes to make them more vulnerable to cancer treatments, making tumor cells more easily detected and destroyed by the body's immune system and stopping genes that play a role in new blood vessel formation (angiogenesis) or adding genes that stop it.

2.2.7 Photodynamic therapy

Photodynamic therapy is also called photoradiation therapy, phototherapy, or photochemotherapy. The photosensitizing agents are used along with light to kill cancer cells in this treatment. The drugs only work after they have been activated or "turned on" by certain kinds of light. Depending on the part of the body being treated, the photosensitizing agent is either injected into the bloodstream or put on the skin. After the drug is absorbed by the cancer cells, light is applied only to the area to be treated. The light causes the drug to react with oxygen, which forms singlet oxygen that kills the cancer cells. PDT may also work by destroying the blood vessels that feed the cancer cells and by alerting the immune system to attack the cancer.

2.3 Problems of cancer therapies

With the more biological knowledge of cancer, deeper research in current treatments of cancer and the discovery of “better” anticancer weapons, those therapies will be undoubtedly much stronger, more specific and more effective in the future. However, presently, there are still some worrying statistics here. The incidence rates of cancer of the liver, pancreas, kidney, esophagus, and thyroid have continued to rise, as have the rates of new cases of non-Hodgkin lymphoma, leukemia, myeloma, and childhood cancers. The incidence rates of cancer of the brain and bladder and melanoma of the skin in women, and testicular cancer in men, are rising. Lung cancer death rates in women continue to rise, but not as rapidly as before. Death rates for cancer of the esophagus and thyroid in men, as well as of the liver, are increasing (http://progressreport.cancer.gov/).

One of the reasons that cancer therapies are still not ideal is that there are various problems, drawbacks and side effects in those therapies. To some extent, surgery is severe to human bodies. Possible complications during surgery may be caused by the surgery itself, the anesthesia, or an underlying disease, such as externally bleeding, damage to internal organs and blood vessels, reactions to anesthesia or other medicines. Also, problems after surgery are fairly common, like pain, infection, pneumonia, internally bleeding, blood clots and slow recovery of other body functions. Besides, long-term side effects depend on the type of procedure done. For example, people who are having colorectal cancer surgery may need a colostomy (an opening in the abdomen to which the end of the colon is attached). Men undergoing radical prostatectomy (removal of the prostate) are at risk for losing control of urination or becoming impotent. But what is worse is that surgery sometimes cannot cut the tumors completely, kill all spread cancer cells or prevent metastasis. Radiotherapy attacks cancer cells that are dividing, but it also affects dividing cells of normal tissues. The damage to normal cells is what causes side effects. Each time radiotherapy is given it involves a balance between destroying the cancer cells and sparing the normal cells. For instance, fatigue, damage of skin, inflammation of mouth or throat, changes in brain function that can lead to memory loss, poor tolerance for cold weather, nausea, unsteadiness, and changes in vision are usual symptoms caused by radiation. Moreover, radiotherapy, one of the local therapies, might only be effective to local tumors but not spread cancer cells. The systemic treatment, anti-angiogenesis, similar to chemotherapy, for the most part, tends to have milder side effects than chemotherapy drugs because the anti-angiogenesis drugs only act where new blood vessels are forming. But they can still have serious or even life-threatening side effects such as

bleeding or holes in the digestive tract, raised blood pressure, surgery risks (affect wound healing), and pregnancy risks (affect a developing fetus). For the immunotherapy, the idea of using one's own immune system to fight cancer is tempting, but it still has a fairly small role in treating most cancers since it is too specific and only a few immunotherapies have been proved by FDA. So far, in most cases, it has not been shown to be clearly better than other forms of treatment. And it may be less helpful for more advanced diseases. Although the ideas of gene therapy are promising, figuring out how to insert specific genes into specific sites to solve specific problems has not been simple and has not been used for common clinical trials. Studies have shown that PDT can work as well as surgery or radiotherapy in treating certain kinds of cancers and pre-cancerous conditions. The definite advantages cannot be neglected, such as it has no long-term side effects when used properly; it is less invasive than surgery; it can be targeted very precisely; it can be repeated many times at the same site if needed; there is little or no scarring after the site heals. However, the limits of PDT are inclusive. It can only treat areas where light can reach, so it is mainly used to treat problems on or just beneath the skin, or in the lining of internal organs. While the drugs may travel throughout the body, the treatment only works at the area exposed to light, so PDT cannot be used to treat advanced cancers. Also, the drugs that are now in use leave people very sensitive to light, and during this time special precautions must be taken.

2.4 Chemotherapy and challenges

Chemotherapy is a complicated procedure. The general working process of chemotherapy drugs, which are very strong and carry high risk due to the toxicity, against cancer cells, is by attacking cells in the body that divide quickly. But meanwhile they can also harm other normal, healthy cells that divide quickly, such as those in the bone marrow, the skin, and in the mouth and intestines. This can lead to serious side effects like low blood cell counts (which can cause fatigue, infections, and bleeding), hair loss, mouth sores, nausea, and diarrhea. However, unfortunately, chemotherapy still is of paramount importance to fight against cancer due to the systemic feature, effects to a spectrum of cancers, easily to be treated and some proven successful trails although patients have to tolerate severe side effects and sacrifice the life quality. What is worse is that the effectiveness of chemotherapy depends upon many factors which are not easily to compromise (Feng and Chien, 2003).

The first factor is the dosage form. Most anticancer drugs are highly hydrophobic, and hence are not soluble in water and most pharmaceutical solvents. Adjuvants such as Cremophor EL for paclitaxel and Tween-80 for docetaxel have to be used for the clinical administration of the anticancer drugs, which may cause serious side effects, some of which are life-threatening (Rowinsky et al., 1992; Webster et al., 1993; Fjallskog et al., 1993).

The second is the pharmacokinetics. In order to achieve successful anticancer effect, the cancer cells should be exposed to sufficiently high concentration of the drug for long enough duration. It would be ideal if a single administration can lead to effective chemotherapy that can last for days, weeks, or even months (Feng and Chien, 2003). Additionally, the ideal goal for chemotherapy is to deliver the drugs of high efficacy at

the right time to the desired location with a high enough concentration over a sufficiently long period (Feng and Chien, 2003). However the problems are that the principles, theories, and devices in chemotherapy are difficult to be modified and developed to meet those requirements to achieve effective delivery of drugs.

The third one is the toxicity. Anticancer drugs can also affect healthy cells. Certain cells with rapid turnover, such as bone marrow cells and intestinal epithelium cells, however, may also be seriously affected (Feng and Chien, 2003). The important organs for metabolism and excretion, liver and kidney may also be damaged by chemotherapy. It would be ideal if the chemotherapeutic agents could exert their actions only on the cancerous cells.

The fourth factor is the drug resistance. Chemotherapy often fails in the long-term because of the development of drug resistance, like MDR, by the cancer cells. There are three major categories of drug resistance: pharmacokinetic resistance due to the low concentration of drug in the tumor, kinetic resistance due to the presence of only a small fraction of cells in a susceptible state, and genetic resistance due to the biochemical resistance of the tumor cells to the drug (Feng and Chien, 2003). Another problem is the microcirculatory barrier. The therapeutic molecules must penetrate into the blood vessels of the tumor to reach the cancer cells. Unfortunately, tumors often develop in ways that hinder the penetration (Jain, 2001).

2.5 Taxanes, the potent anticancer drugs

Taxanes, including paclitaxel and docetaxel, are one family of plant alkaloids which are nitrogen containing organic bases that are naturally occurring. This group of

compounds is often characterized by their bitter tastes as well as their physiological activities (Manske and Holmes, 1952).

2.5.1 Paclitaxel

Paclitaxel (Figure 2.2) is one of the antineoplastic drugs discovered from nature in the early 1960s. It is identified as the crude extract from the bark of the North American pacific yew tree, Taxus Brevifolia (Lopes et al., 1993). It was found to have excellent therapeutic efficacy against a spectrum of cancers, such as breast cancer, ovarian cancer, small and non-small cell lung cancer, colon cancer, head and neck cancer multiple myeloma, melanoma, and Kaposi's sarcoma (Feng et al., 2004). It was approved by US FDA to treat a range of cancers in 1990s (Feng and Chien, 2003). The action mechanism of paclitaxel is that is inhibits mitosis in tumor cells by binding to microtubules, which involve in various cellular functions, such as movement, nutrition ingestion, shape control, and spindle formation during cell division. The microtubules formed by paclitaxel action are stable, thus dysfunctional, leading to cell death (Lopes et al., 1993; Rowinsky et al., 1990; Donehower et al., 1987).

However, there are several limitations for clinical applications of paclitaxel (Feng and Chien, 2003). One is its availability. Four yew trees more than 100 years old have to be sacrificed to produce 2 gram of the drug. Another limitation is its difficulty in clinical administration. Due to the high hydrophobicity of paclitaxel, the dosage form available for the current clinical administration uses an adjuvant consisting of Cremophor EL (polyoxyethylated castor oil) and dehydrated alcohol. It has been shown that Cremophor EL causes serious side effects, including hypersensitivity reactions, nephrotoxicity, neurotoxicity and cardiotoxicity (Feng and Chien, 2003).

Moreover, the delivery of clinical formulation of paclitaxel, Taxol® cannot be specific to the cancer cells in appropriate time with sufficient amount kept in a long enough duration in administration. Furthermore, due to the existence of some biological barriers, like GI barrier and blood-brain barrier, paclitaxel cannot be effectively delivered to intestines and brains.

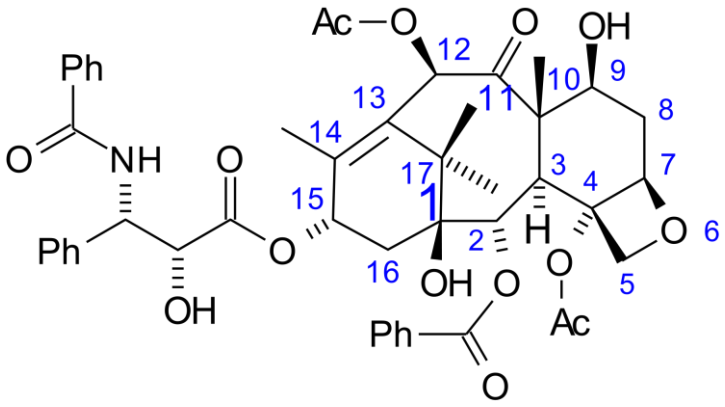

Figure 2.2 Chemical structure of paclitaxel.

2.5.2 Docetaxel

Docetaxel (Figure 2.3) is a more advanced taxane analogue commonly used, similar to paclitaxel, in the treatment of a wide spectrum of cancers such as breast cancer, ovarian cancer, small and non-small cell lung cancer, prostate cancer. It is a semisynthetic compound produced from 10-deacetylbaccatin-III, which is found in the needles of the European yew tree, Taxus baccata (Gelmon, 1994). The semisynthetic production process of docetaxel circumvented the availability problems of taxnes. Docetaxel is slightly more water soluble than paclitaxel (Hennenfent and Govindan, 2006). It also acts by disrupting the microtubular network and promotes the assembly

of tubulin into stable microtubules and inhibits their disassembly, resulting in inhibition of cell division and eventual cell death. Pre-clinical studies and a clinical randomized Phase III study demonstrated that docetaxel have greater efficacy than paclitaxel (Jones, 2006; Jones et al., 2005). Docetaxel shows 1.9-fold higher affinity than paclitaxel for microtubule (Musumeci et al., 2006). Docetaxel also shows wider cell-cycle bioactivity and slower efflux from the tumor cells (Riou et al., 1992; Riou et al., 1994; Brunsvig et al., 2007). Docetaxel was reported to exhibit 11-fold higher cytotoxic activity than paclitaxel (Riou et al., 1992; Hanauske et al., 1994; Lavelle et al., 1995).

Due to the low water solubility of docetaxel, the commercial formulation, Taxotere® consists of a solution (40 mg/ml) in a vehicle containing high concentration of Tween-80. The adjuvant has been associated with several hypersensitivity reactions and has shown incompatibility with common polyvinyl chloride intravenous administration sets (Gelderblom et al., 2001). Therefore, alternative drug formulations deserve to be developed to avoid the problems and increase the therapeutic effects.

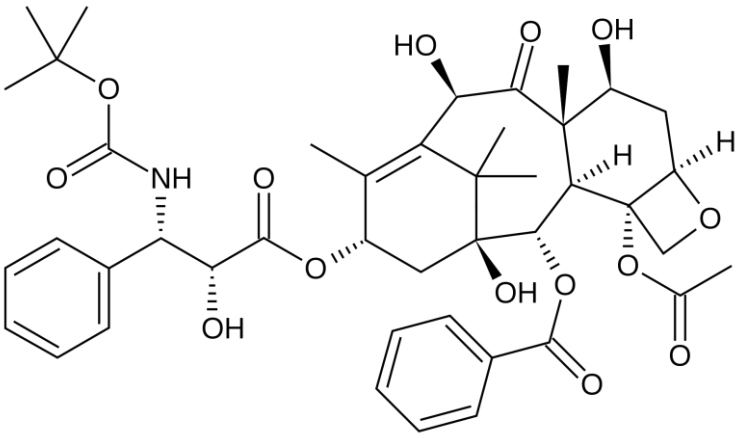

Figure 2.3 Chemical structure of docetaxel.

2.6 Nanotechnology for drug delivery and nanomedicine

Are there any effective solutions for those problems? Fortunately, nanotechnology and emerged nanomedicine provides strong weapons for cancer treatment. Nanotechnology is making an intensive and significant impact on drug delivery in the past decades. Nanotechnology, featured by the technology on nanoscale, provides a new way for human beings to visualize the human body, which can make dramatic differences in medical treatments. Contemporarily, there is a growing interest in integrating nanotechnology with medicine, creating so-called nanomedicine aiming for disease diagnosis and treatment with unprecedented precision and efficacy (Farokhzad and Langer, 2006). Specifically, in drug delivery area, nanomedicine is a recently developed term to describe nanometer sized, multi-component drug or drug delivery systems for disease treatment (Duncan, 2006).

Analogically, a nanocarrier for cancer treatment is just like a missile (Barbe et al., 2004). The anticancer drugs loaded in the carrier resembles the explosive in the warhead of the missile, which should have enough amounts and high efficacy to destroy targets (cancer cells). The following key step is to find the hit target and avoid being detected by radars and intercepted by defense system. The overall human body is large radar to detect intrusion and leucocytes are guards to protect body. Therefore the carrier needs to quickly receive the ‘signals’ from the receptors on the targeted cells and accurately locate the targets by its own ‘GPS’ by the molecular ligands attached and ‘swim’ to the specific site safely by the protection of, for instance, polyethylene glycol. After reaching the target, the carrier will release the loads to kill cancer cells just like the missile explodes. But what is more complex, the carrier should penetrate into cell membranes to sustainably release drugs towards intracellularly. That is the

pharmacokinetics matter: how to reach the controlled release. The distinctive advantage of controlled release systems is increasing the overall efficacy of the drug by maintaining the drug concentration in the body within the optimum therapeutic range and under the toxicity threshold. For the better carriers, after fulfilling the task, they can be properly disposed by body.

The existing challenge of drug delivery is to design vehicles that can carry sufficient drugs, efficiently cross various physiological barriers to reach disease sites, image the diseased tissues, and cure diseases in a less toxic and prolonged manner. A few decades ago, Paul Ehrlich, the founder of chemotherapy, postulated the creation of 'magic bullets' for use in the fight against human diseases inspired generations of scientists to devise powerful drug delivery carriers of molecular cancer therapeutics (Strebhardt and Ullrich, 2008). As most physiological barriers prohibit the permeation or internalization of particles or drug molecules with large sizes and undesired surface properties, the main input of nanotechnology on nanomedicine is to miniaturize and multi-functionalize drug carriers for improved drug delivery in a time- and disease-specific manner. In sum, the desired features of ideal drug delivery systems for nanomedicine include the small size, optimal morphology, biodegradability and biocompatibility, appropriate surface coatings, high content of a drug inside the system, sustained circulation in the blood, and, ideally, the ability to target required areas passively (via the EPR effect) or actively (via receptor-ligand interaction) (Agarwal et al., 2008).

2.7 Nanotechnology based drug carriers

Although nanomedicine was conceptualized only recently (Farokhzad and Langer, 2006; Duncan, 2006; Ferrari, 2005; Nishiyama and Kataoka, 2006; Moghimi et al., 2005), nanotechnology has been employed in drug delivery for decades (Bangham et al., 1965; Marty et al., 1978). For example, nanoparticulate liposomes were first introduced more than 40 years ago (Bangham et al., 1965). The use of colloidal nanoparticles in drug delivery can date back to almost 30 years (Marty et al., 1978). Nowadays, a handful of liposome based, nanoparticulate delivery vehicles have been approved by the FDA for clinical applications (Barenholz, 2001; Duncan, 2006). They became clinically promising when long circulating, stealth polymeric nanoparticles were developed (Gref et al., 1994). Both micelles and polymer-drug conjugates have been investigated for more than two decades for the treatment of various diseases including cancer (Nishiyama and Kataoka, 2006; Lavasanifar et al., 2002).

The application of nanotechnology to clinical cancer therapy, also known as cancer nanotechnology, was recently detailed (Ferrari, 2005). There are several categories of promising drug carriers for anticancer nanomedicine: liposomes, micelles, nanoparticles, polymeric vesicles, polymer-drug conjugates, dendrimers, hydrogels, nanotubes, etc (schemed in Figure 2.4).

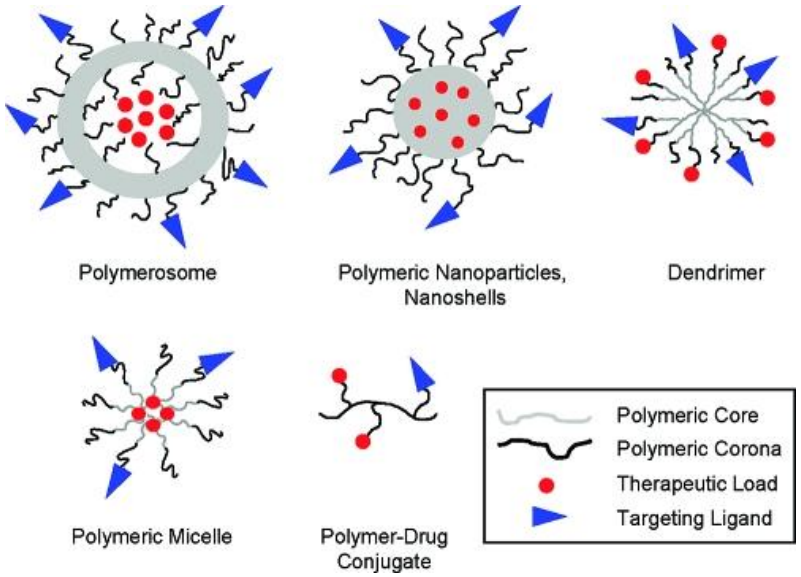

Figure 2.4 Illustration of typical drug delivery carriers (Alexis et al., 2008).

2.7.1 Liposome

Liposomes, which are phospholipid bilayer vesicles with aqueous center, have been extensively reviewed (Park et al., 2004; Noble et al., 2004; Cattel et al., 2003; Patel et al., 1999). They have received a lot of attention during the past 30 years as pharmaceutical carriers of great potential since the pioneering observation of Alec Bangham roughly forty years ago (Bangham et al., 1965). Although they were just regarded as one of exotic objects of biophysical research originally, they have been gradually become a pharmaceutical carrier for numerous practical applications. The real breakthrough developments in the area during the past 15 years have resulted in the approval of several liposomal drugs, and the appearance of many unique biomedical products and technologies involving liposomes (Torchilin, 2005). More recently, a variety of new developments have been seen in the area of liposomal drugs: from clinically approved products to new experimental applications, with gene

delivery and cancer therapy as the principal areas of interest. The reasons that liposomes can be applied for drug delivery are the several attractive biological properties, including their biocompatibility, the entrapment of water-soluble (hydrophilic) pharmaceutical agents in their internal water compartment and water-insoluble (hydrophobic) pharmaceuticals into the lipid wall, the protection of liposome-incorporated pharmaceuticals from the inactivating effect of external conditions, yet without undesirable side reactions, the unique opportunity to deliver pharmaceuticals into cells or even inside individual cellular compartments, as well as the size, charge and surface properties of liposomes that can be easily changed simply by adding new ingredients to the lipid mixture and/or by variation of preparation methods (Torchilin, 2005). Nevertheless, one of the drawbacks of liposomes is the fast elimination by the blood circulation and reticuloendothelial system, primarily in the liver. A number of developments have aimed to reduce this problem. To increase liposomal drug accumulation in the desired tissues and organs, the use of targeted liposomes with surface-attached molecules capable of recognizing and binding to cells of interest (immunoliposomes) has been suggested. IgG class and their fragments are the most widely used targeting moieties for liposomes, which can be attached to liposomes, without affecting liposomal integrity or the antibody properties, by covalent binding to the liposome surface or by physical adsorption onto the liposomal membrane after modification with hydrophobic residues (Torchilin, 2005). HER2 directed immunoliposomes were investigated and shown a distinct mechanism for the drug delivery to tumor cells *in vivo*, which exploits mAb-dependent binding and internalization in tumor cells (Kirpotin et al., 2006). The results suggest that HER2 immunoliposomes are capable of penetrating tumor tissue, internalizing specifically in

HER2-overexpressing cancer cells and intracellularly releasing encapsulated drugs, representing a potentially advantageous strategy for molecularly targeted drug delivery. Still, despite improvements in targeting efficacy, the majority of immunoliposomes accumulate in the liver as a consequence of insufficient time for the interaction between the target and targeted liposome. Better target accumulation can be expected if liposomes can be made to remain in the circulation long enough. Therefore, different methods have been suggested to achieve long-circulating liposomes (stealth liposomes), including coating the liposome surface with inert, biocompatible polymers, such as PEG, which form a protective layer over the liposome surface and slow down liposome recognition by opsonins and subsequent clearance of liposomes (Klibanov et al., 1990; Blume and Cevc, 1993). Long-circulating liposomes are now being investigated in detail and are widely used in biomedical *in vitro* and *in vivo* studies (Gabizon, 2001). An important feature of protective polymers is their flexibility, which allows a relatively small number of surface-grafted polymer molecules to create an impermeable layer over the liposome surface (Torchilin and Trubetskoy, 1995). Long-circulating liposomes demonstrate dose-independent, non-saturable, log-linear kinetics and increased bioavailability (Allen and Hansen, 1991). Current research on PEG liposomes focuses on attaching PEG in a removable fashion. Novel detachable PEG conjugates have been described (Zalipsky et al., 1999), in which the detachment process is based on the mild thiolysis of the dithiol linkage. Continuing interest in using long-circulating liposomes in cancer chemotherapy is supplemented by their potential use for other purposes, such as carrying imaging agents and the treatment of infection (Gabizon, 2003; Bakker-Woudenberg, 2002). The further development of liposomal carriers involved the attempt to combine the properties of long-circulating

liposomes and immunoliposomes in one preparation (long-circulating immunoliposomes) (Abra, 2002). To achieve better selectivity of PEG-coated liposomes, it is advantageous to attach the targeting ligand via a PEG spacer arm, so that the ligand is extended outside of the dense PEG layer, which reduces steric hindrance of binding to the target.

2.7.2 Micelle

Micelle is a core-shell structured aggregation with a hydrophobic core and a hydrophilic shell, created by a spontaneous self-assembly of amphiphilic molecules. The core is an ideal reservoir for potential application, such as microreactor, microelectric unit and drug carrier. Meanwhile, the shell provides the solubility of micelle in solvent and serves as the steric barrier to core-core interaction and agglomeration. The aggregated shapes are various, including spherical, as the most common, and cylindrical, rod-like, worm-like, disc-like, flower-like, etc. The sizes of polymeric micelles (no swollen) are typically nanosized, from 10 to 100 nanometers, some of which are several hundred nanometers. Polymeric micelles were first introduced as drug delivery vehicles in the early 1980s by Helmut Ringsdorf (Gros et al., 1981; Pratten et al., 1985). Polymeric micelles have a condensed, compact inner core, which serves as the nanocontainer of hydrophobic compounds. As polymer micelles are generally more stable than hydrocarbon based micelles, sustained drug release from polymeric micelles becomes possible. Numerous types of amphiphilic copolymers have been employed to form micelles (Lavasanifar et al., 2002; Kakizawa and Kataoka, 2002; Nishiyama and Kataoka, 2006; Torchilin, 2005; Huang and Remsen, 1999; Hagan et al., 1996; Kabanov et al., 2002). Polymeric micelles can

accumulate in tumors after systemic administration. Their biodistributions are largely determined by their physical and biochemical properties, such as sizes, hydrophobicity, and hydrophilicity of the polymers and drugs, and surface biochemical properties (Avgoustakis, 2004). A major issue that limits the systemic application of micellar nanocarriers is the non-specific uptake by the RES. It is critical to have systems that can circulate for a long time without significant accumulation in the liver or the spleen. The sizes and the surface features of micelles have to be controlled for favored biodistribution and intracellular trafficking (Gref et al., 1994). The hydrophilic shells of micelles usually consist of PEG which prevents the interaction between the hydrophobic micelle cores and biological membranes, reduces their uptake by the RES, and prevents the adsorption of plasma proteins onto micelles (Kataoka et al., 2001). Polymeric micelles that are responsive to pH, temperature or light are potentially exciting nanomedicine modalities (Tong and Cheng, 2007). The stimuli-responsive capacity is advantageous for both targeted delivery and controlled release. Basically, the stimuli to micelles are the tools to control the micellization (keep stability) and micelle disruption (release contents) in proper time and site. The first category is pH-responsive micelles. The mildly acidic pH in tumor and inflammatory tissues (pH~6.5) as well as in the endosomal intracellular compartments (pH~4.5-6.5) (lower than that in normal tissues (pH~7.2)) (Rapoport, 2007), may trigger drug release from pH sensitive micelles upon their arrival at the targeted disease sites. One process is that the core which is stable in one pH value will be swollen even disrupted when exposed to other pH values, thus release encapsulated cargos faster. This phenomenon has been employed in the design of numerous pH-sensitive polymeric micellar systems for the delivery of anticancer drugs to tumors (Bae et al., 2003; Lee et al., 2003; Bae et al.,

2005; Sethuraman and Bae, 2007). Another type of responsive micelles is thermo-sensitive micelles. Developing this kind of polymeric micelles as intelligent drug carriers that would react by a sharp change of properties in response to a small change of temperature is perspective (Rapoport, 2007). The thermo-responsive fragment can be incorporated to either micelle core or shell. In particular, LCST polymers such as poly (N-isopropylacrylamide) with a transition temperature around 32 ℃ are one of candidates (Neradovic et al., 2004). Also a synthesized thermo-sensitive micellar drug delivery system with an increased physical stability but with a retained biodegradability was proven to be due to the core-crosslinking (Rijcken et al., 2007). Moreover, lipid based polymeric micelles, like PEG-PE, can increase the tumor penetration and accumulation, thus the antitumor efficacy *in vivo* (Tang et al., 2007). Alternatively, the ultrasound-responsive micelle is another kind of external stimuli-responsive micelles. Ultimately, by using convenient ultrasonic dispersion, intracellular uptake of drugs will be increased as well as the distribution of the micelles and drug throughout the tumor volume will be more uniform resulting in effective tumor targeted drug delivery and suppression of tumor growth for drug sensitive and multidrug-resistant tumors (Rapoport, 2007). The light-responsive micelles, by the use of light, including infrared, ultraviolet and fluorescence, as an external stimulus to control micellization/micelle disruption processes, has just started being exploit. Pyrene and azo are ideal light sensitive molecules, though biocompatibility still need to be investigated (Jiang et al., 2005). The light irradiation will destabilize the micelles and cause drug releasing. This design may potentially be used to control drug release in deep tissues harmlessly.

2.7.3 Nanoparticle

NPs are colloidal systems with the size range from 10 to 1000nm. Drug safety and efficacy can be greatly improved when a pharmaceutical agent is encapsulated within nanoparticles or attached onto surface of nanoparticles (Langer, 1998). This may lead new therapies, and change the way we diagnose and treat cancers. Nanoparticles have been regarded as perspective drug delivery carriers years ago and there are a lot of investigations and inventions on design of ideal nanoparticles these years. Inorganic nanoparticles, such as gold and silica nanoparticles (Barbe et al., 2004), are good candidates because of their biocompability and stability in blood circulation. Nonetheless, the rapid clearance by RES and non-biodegradability may cause confusion on the sustained efficacy and prolonged safety issues. Therefore, biodegradable polymeric nanoparticles might be better choice. The polymers used for the formulation of nanoparticles will be degraded into harmless molecules such as carbon dioxide and water and excreted from the body (Parveen and Sahoo, 2008). A hydrophobic drug can be introduced into the nanoparticle matrix, thereby improving its bioavailability. These formulations can also be bound with biocompatible and non-biodegradable polymers like PEG to keep them in circulation for longer periods. Moreover, the problem of sustained, controlled release of anticancer drugs can be addressed by various nanoparticle formulations. The drug release from nanoparticles can be controlled by modulating the polymer characteristics to achieve the desired therapeutic level in target tissues for required durations with optimal therapeutic efficacy and release of a constant amount of drug per unit time (Parveen and Sahoo, 2008). In the case of central nervous system cancers, many drugs have difficulty in reaching the therapeutic site due to BBB. Drug loaded nanoparticles, with appropriate size and surface decoration, have potential to breach this barrier and thus show greatly

increased therapeutic concentrations of anticancer drugs in brain. Those nanoparticles can also solve the multidrug resistance problem caused by P-gp and the characteristics of higher hydrostatic pressure of tumors. Recently, nanoparticles for cancer chemotherapy have been extensively investigated. A number of biodegradable polymers, such as PLGA, PLA, PCL, chitosan, and HSA have been employed to produce nanoparticles for controlled delivery of various effective anticancer agents to avoid the using of toxic adjuvants, to realize the desired pharmacokinetics, and to enhance their uptake by cancer cells (Feng and Chien, 2003).

2.7.4 Polymersome

Apart from forming micelles, amphiphilic block copolymers can also construct vesicles when the fraction of the hydrophobic domain relative to the hydrophilic domain is controlled within a certain range (0.2-0.42) (Discher and Eisenberg, 2002; Discher and Ahmed, 2006). The liposome-like structures possess a hydrophobic membrane and a hydrophilic inner cavity; therefore they are also called polymersomes. Compared to liposomes, polymeric vesicles are more stable because their membrane-making polymers form much stronger hydrophobic interactions than the short hydrocarbon segments of liposomes (Tong and Cheng, 2007). Although polymeric vesicles have only been studied for a few years, they have shown great promise in controlling drug loading, systemic biodistribution, and drug release (Ahmed and Discher, 2004; Geng et al., 2007). In polymeric vesicles, precise tuning of the drug release rates can be achieved through blending vesicle-forming copolymers with a hydrolyzable copolymer. Recently, a polyarginine-polyleucine copolymer vesicle was

demonstrated to have excellent intracellular trafficking properties (Holowka et al., 2006).

2.7.5 Polymer-drug conjugation

Polymer-drug conjugation (prodrug) was seen as a mean of improving the cell specificity of low molecular-weight drugs. It is needed to design an effective polymer-drug conjugate with the desired features: a bio-responsive polymer-drug linker that is stable during conjugate transport and able to release drug (via broken of the linking bond) at an optimum rate on arrival at the target site; adequate drug carrying capacity in relation to the potency of the drug being carried; and the ability to target the diseased cell or tissue. As the drugs carried often exert their effects via an intracellular pharmacological receptor, it is essential that they eventually access the correct intracellular compartment (Duncan, 2003). A number of polymer-drug conjugates have been tested clinically (Duncan, 2003). Covalent attachment of drug to a polymeric vehicle is particularly attractive, as the increased molecular weight produces a radical change in the pharmacokinetics at both the whole body and cellular levels (Duncan, 2003). Careful tailoring of polymer-drug linkers is essential to the creation of a polymeric prodrug that is inert during transport but allows drug liberation at an appropriate rate intratumorally. Polymer-drug linkers were popularized by the successful design of HPMA copolymer-doxorubicin conjugates which is stable in the circulation, but is cleaved by the lysosomal thiol-dependent protease cathepsin B following endocytic uptake of conjugate from the tumor interstitium (Duncan et al., 1992; Vasey et al., 1999; Seymour et al., 2002). HPMA copolymer conjugates of paclitaxel have also emerged into clinical evaluation (Meerum et al., 2001). PLA and

PEG have also been used to produce drug conjugates via ester bonds which are rather interesting and attractive (Li et al., 1998; Denis et al., 2000; Greenwald et al., 2003).

2.7.6 Dendrimer

A dendrimer is a synthetic polymeric macromolecule of nanometer dimensions, composed of multiple highly branched monomers that emerge radically from the central core (Cho et al., 2008), which was first reported in the late 1970s and early 1980s (Tong and Cheng, 2007). Properties associated with these dendrimers such as their monodisperse size, modifiable surface functionality, multivalency, water solubility, and available internal cavity make them attractive for drug delivery (Svenson and Tomalia, 2005). Dendritic polymers also have a number of beneficial attributes for biomedical applications, including biodistribution and pharmacokinetic properties that can be tuned by controlling dendrimer size and conformation, high structural and chemical homogeneity, ability to be functionalized by multiple copies of drugs or ligands, high conjugation density and controlled degradation (Lee et al., 2005). In the past decade, significant efforts have been devoted to exploiting the potential applications of dendrimers as drug carriers (Lee et al., 2006; Qiu and Bae, 2006; Esfand and Tomalia, 2001). Drug molecules can either be conjugated onto the surface of dendrons or encapsulated inside the branches. The periphery of a dendrimer usually contains multiple functional groups for the conjugation of drug molecules or targeting ligands. Drugs are majorly covalently conjugated onto the surface because of the straightforward attachment and easy control (Tong and Cheng, 2007). Despite numerous designs of dendrimer based carriers, only a few of them have been evaluated for their *in vivo* antitumor activities (Malik et al., 1999; Maeda et al., 2000; Kukowska-

Latallo et al., 2005). One early example is a sodium carboxyl-terminated PAMAM dendrimer for the conjugation of cisplatin. The drug-dendrimer conjugation displayed ten-fold enhancement of anticancer activity when administered intravenously to treat a subcutaneous B16F10 melanoma, compared to free cisplatin (Malik et al., 1999). Moreover, dendrimer-doxorubicin displayed comparable *in vivo* antitumor efficacy as Doxil®, an FDA approved, liposome-based doxorubicin delivery vehicle (Tong and Cheng, 2007). Compared to liposomes and micelles, dendrimer-drug conjugates may be more stable owning to their covalent attachment and uniform molecular structures, thus are easier to be formulation, sterilization, transportation and storing. However, in spite of the benefits as well as high biocompatibility of dendrimers, the toxicity issues still need to be investigated and the multistep precise synthesis and accompanied higher preparation costs hinder the moving from the laboratory to the clinic. In addition, improved quality control assays need to be devised to ensure that multicomponent dendritic polymers contain the correct components in the correct ratios (Lee et al., 2005).

2.7.7 Hydrogel

Hydrogels are water-swollen polymeric materials that can retain a significant amount of water while maintaining a distinct three-dimensional structure (Xu and Kopecek, 2007; Kopecek, 2007). It has been proposed that hydrogels can be used as biomaterials as early as 1960 (Wichterle and L ím, 1960). They are also the first biomaterials designed for use in the human body (Kopecek, 2007a). Nowadays, numerous applications have been proposed and investigated for the self-assembled hydrogels in drug delivery area (Xu and Kopecek, 2007). Especially, hydrogels that can respond to

environmental stimuli, such as temperature, pH, electric field, light, or chemical signals are catching more and more attraction. N-Isopropylacrylamide-based hydrogel systems are the most intensively investigated thermo-responsive systems, including their use for drug delivery (Liu et al., 2006; Yin et al., 2006), cell encapsulation and delivery (Na et al., 2006) and cell culture surfaces (Hatakeyama et al., 2006). These hydrogels can swell in situ under physiological conditions and provide the advantage of convenient administration (Klouda and Mikos, 2008). However, several challenges remain to be improved. One of the major challenges relates to the ease of clinical usage. There are also persistent challenges in expanding the types of kinetic release profiles which can be achieved using hydrogels. There is also a need for continued improvement in the delivery of not only hydrophobic molecules, but also the delivery of more sensitive molecules such as proteins, antibodies, or nucleic acids which can readily be deactivated or unfolded by interactions with the hydrogel delivery vehicle (Hoare and Kohane, 1993).

2.7.8 Carbon nanotube

CNTs belong to the family of fullerenes, the third allotropic form of carbon along with diamond and graphite. They are comprised exclusively of carbon atoms arranged in a condensed polyaromatic surface rolled-up in a tubular structure with their ends closed (Bianco et al., 2005). They are unique materials with exceptional chemical and electronic properties and have been applied in biology as sensors for detecting DNA and protein, diagnostic devices for the discrimination of different proteins from serum samples, and carriers to deliver vaccine or protein (Bianco et al., 2005a). Due to their high stability, they also are regarded as promising drug carriers. However, concerns on

health and toxicity problems as well as the biocompatibility of CNTs generated. Recently, experimental evidence clearly indicates that long, rigid CNTs should be avoided for *in vivo* applications and that chemical functionalization should be optimized to ensure adequate dispersibility, individualization and excretion rates sufficient to prevent tissue accumulation (Kostarelos et al., 2008). But increasing the solubility and preventing aggregation to facilitate urinary excretion and decrease tissue aggregation might enhance the safety of CNTs *in vivo* (Kostarelos et al., 2008). In addition, early biocompatibility data for CNT and novel nano-structured biomaterials suggest that the scientific community could remain cautiously enthused by potential biomedical applications of CNT-based materials (Smart et al., 2006). In fact, the introduction of chemical modification to CNTs can render them water-soluble and functionalized so that they can be linked to a wide variety of anticancer drugs and active molecules such as peptides, proteins, and nucleic acids (Bianco et al., 2005b). For potential *in vivo* applications, the significant limitation of CNTs, owing to their rapid clearance or high hepatic uptake has been resolved by using PEG to covalently bind on the surface of CNTs to escape the capture of reticuloendothelial system, making them stealth nanotubes (Yang et al., 2008). Dai's group have shown in their current work by Raman Spectroscopy that surface chemistry is crucial to the behavior of CNTs *in vivo*, pegylation of CNTs could block the hydrophobicity and enable longer blood circulation time and lower RES uptake, and no obvious toxic effect was found (Liu et al., 2008). Other studies have demonstrated that the functionalized CNTs with aqueous solubility and cationic surface are able to cross the plasma membrane and distribute throughout the cellular compartments (Bianco et al., 2005a). In the diagnosis area, combining the optical properties of quantum dots with the ability of

CNTs to carry pharmaceutical cargos could provide high benefits (Zerda et al., 2007). Even though the safety issue of CNTs for clinical application still deserves huge investigation, promising biomedical applications of functionalized CNTs are obvious, if the toxicity can be well defined. More recently, an *in vivo* tumor uptake study using graphene, a two-dimensional structure of CNT was conducted, announcing the potential anticancer effects of the rising star material (Yang et al., 2010).

2.8 Polymeric nanoparticles

In particular, polymeric nanoparticles fabricated by biodegradable polymers as drug carriers have been extensively investigated over the past 30 years. One of the most distinctive advantages of those polymers over other materials is that the behavior of drug release is able to be finely tuned by precise control on the molecular structure of the polymers. Ideally, a zero-order drug release is desired that can maintain a constant drug concentration over long period, which was termed as controlled and sustained release. Among various synthetic biodegradable polymers with biocompatibility, PLGA is the mostly used one for clinical use (Anderson and Shive, 1997) as drug delivery carrier and therapeutic devices with confirmed biocompatibility (Shi et al., 2002).

PLGA is a block copolymer composed of polylactic acid block and polyglycolic acid block (Figure 2.5). The common synthesis route is by means of random ring-opening copolymerization of the monomers glycolic acid and lactic acid. During polymerization, successive monomeric units (of glycolic or lactic acid) are linked together in PLGA by ester linkages, thus yielding a linear, aliphatic polyester as a

product (Astete and Sabliov, 2006). The characteristics of PLGA can be easily obtained by engineering the molar ratio of lactide to glycolide used in the polymerization. For example, PLGA 50:50 identifies a copolymer whose composition is 50% lactic acid and 50% glycolic acid. PLGA is amorphous rather than crystalline and shows a glass transition temperature in the range of 40-60 ℃. From the polymer chemistry point of view, the polylactic acid block is more hydrophobic while the polyglycolic acid block is more crystalline. Hence the degradation properties of PLGA and the drug release behavior from the PLGA nanoparticles is in close relationship with the ratio of those two blocks.

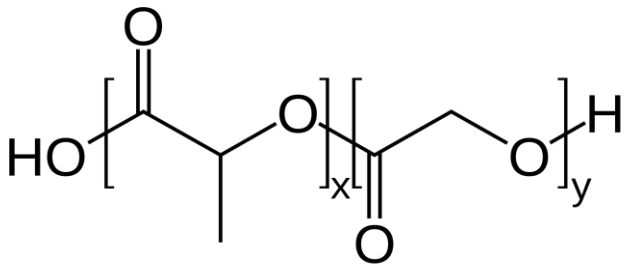

Figure 2.5 Chemical structure of PLGA. x= number of units of lactic acid; y= number of units of glycolic acid.

The dominant process of the degradation of PLGA in water depends on the hydrolysis of ester linkages (Figure 2.6). The ratio of the blocks or say net hydrophobicity of the copolymers controls the rate of degradation. Higher glycolide ratio results in lower hydrophobicity, thus faster degradation. Generally, the half-time of degradation takes 12-16 weeks (Alexis, 2005; Zweers et al., 2004). The process involves the by-products of various metabolic pathways in the body for PLGA and hence causes low systemic toxicity, which makes it an ideal drug carrier.

For the release of the drugs encapsulated in PLGA spheres, it is very possible to tailor the release rate by controlling the degradation time which can be achieved by altering the ratio of the monomers used during synthesis. The mechanism of drug release can be summarized as the involvement of six main steps: desorption of the surface bounded drugs, diffusion of the drugs through the matrix pores, diffusion through the polymer barrier, next to the release of drug when the polymer degrades and eventually bulk degradation (Jalil and Nixon, 1990; Soppimath et al., 2001).

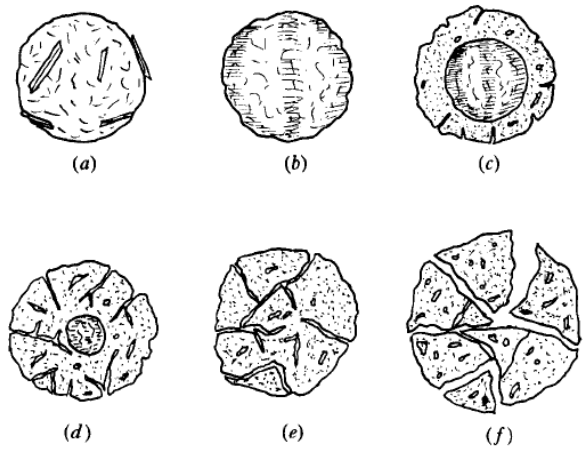

Figure 2.6 Schematic diagram showing the swelling and degradation of a microcapsule when dissolve in aqueous solution (Jalil and Nixon, 1990): (a) Microcapsule containing the therapeutic drug. (b) Attached surface drugs dissolve by the aqueous environment. (c) Swelling and onset of the erosion. (d) Gradual size reduction of the central matrix proportion with extensive erosion and pore formation. (e) Formation of fully hydrated microcapsule with the disappearance of the core. (f) Fragmentation and degradation into its monomers.

PLGA based nanoparticles have also been deeply investigated in our groups in the past ten years for drug delivery (Mu and Feng, 2002; Mu and Feng, 2003; Win and Feng, 2006; Feng et al., 2007). By using paclitaxel as a prototype anticancer drug encapsulated in PLGA NPs, it was concluded that the NP formulation of paclitaxel has great advantages versus the commercial paclitaxel formulation. The side effects

associated with toxic adjuvant contained in the commercial formulation can be avoided. *In vitro* cell viability experiment on cancer cells showed much higher cytotoxicity of paclitaxel in the NP formulation than that in the commercial formulation. The NP formulation can result much greater therapeutic effects and sustained chemotherapy *in vivo* of the drug in the NP formulation.

However, sometimes, using PLGA alone to fabricate NPs is not satisfactory enough in terms of, for example, the hydrophilicity and bioavailability. The rapid uptake of nanoparticulate drug carriers by the MPS is the main limitation for drug carrier to reach tumor sites after circulating in human body (Klibanov et al., 1990). PEG is at present the most popular materials to modify particulate surfaces in order to avoid recognition by MPS (by decreasing the protein adsorption). PEG presents unique properties such as (i) soluble in water; (ii) lack of immunogenicity, antigenicity and toxicity; (iii) high hydration and flexibility of the polymer chain; and (iv) approval by FDA for human use (Pasut and Veronese, 2007). In order to equip the stealth and long circulating properties for the particles in bloodstream, which indicates the escape from the recognition by MPS cells, pegylation is a necessary process to decorate the particles that is a preferred method of imparting stealth, or sterically stabilized properties to nanoparticles (Gref et al., 1994; Owens and Peppas, 2006). PEGylation simply refers to the decoration of a particle surface by the covalently grafting, entrapping, or adsorbing of PEG chains. PEGylation changes the physicochemical properties such as conformation, electrostatic binding, and hydrophobicity, resulting in an improvement in the pharmacokinetic behavior of the drug carrier (Veronese and Mero, 2008). PEGylation also improves the stability and the retention time of the carriers in blood, thereby allowing the prolonged circulation and lifetime of the drug

loaded carriers. PEGylation has already become a commonly used strategy to modify the biodegradable polymers for better performed drug carriers, such as PLGA-b-PEG copolymer. For instance, functional PEG was conjugated with PLGA by covalent bonding to form amphiphilic block copolymers which would be used to produce polymeric micelles or particles. The other end of functional group on PEG chains would be free by applying this strategy which can be reserved to attach with molecular ligands for targeted delivery. A few similar studies using paclitaxel or docetaxel incorporating in PEGylated PLGA nanocarriers have been reported in recent years (Zhao and Yung, 2008; Zhao and Yung, 2009; Esmaeili et al., 2008; Murugesan et al., 2008; Senthilkumar et al., 2008; Danhier et al., 2009). The results contributed by one group demonstrate that the PEGylated NPs strongly enhances the cytotoxicity of the drug through sustained delivery. The pharmacokinetic result shows the long circulating properties of PEGylated NPs, which could increase the possibility of the NPs to penetrate into the tumor tissues. Furthermore, PEGylated NP formulations shows a much better tumor suppression effect than docetaxel solution and corresponding PLGA NP formulations (Senthilkumar et al., 2008).

2.9 Multifunctional nanoparticles

The concept of nanoscale devices has led to the development of biodegradable self-assembled nanoparticles, which can be highly tailored and are being engineered for the targeted delivery of anticancer drugs and imaging contrast agents (Sinha et al., 2006). Nanocarriers should serve as customizable, targeted drug delivery vehicles capable of ferrying large doses of chemotherapeutic agents or therapeutic genes into malignant

cells while sparing healthy cells. Such ‘smart’ multifunctional nanodevices hold out the possibility of radically changing the practice of oncology, allowing easy detection and then followed by effective targeted therapeutics at the earliest stages of the disease.

2.9.1 Targeting

Targeting, including passive targeting and active targeting, is the first essential function to achieve the desired delivery that differentiates tumors from normal tissues. Ideally, for anticancer agents to work, they should be able to reach the desired tumor location through the various routes and barriers with minimal loss of their volume and functional integrity. Upon reaching the tumor site, they should be able to selectively kill the cancerous cells without affecting the surrounding healthy cells via controlled and targeted release mechanisms, which would drastically improve patient survival, mitigate adverse side effects of the drugs, minimize expensive drug wastage and improve the overall therapeutic effect. Combinations of physical and chemical properties can be utilized to design targeted drug carrier systems. Such properties include surface hydrophobicity, surface charge, size and morphology, tumor properties and possible biochemical interactions such as ligand-receptor interactions.

Passive targeting takes advantage of the permeability and unique microenvironment of tumor tissue (Wang et al., 2008).

Rapid neovascularization to serve fast-growing cancerous tissue leads itself to a leaky and defective architecture, which in turn, can be easily accessible to chemotherapeutic drugs. Tumor blood vessels are generally characterized by abnormalities such as a relatively high proportion of proliferating endothelial cells, increased tortuosity, pericyte deficiency and aberrant basement membrane formation. Proliferating cancer

cells demand the recruitment of new vessels (neovascularization) or rerouting of existing vessels near the tumor mass to supply them with oxygen and nutrients (Carmeliet and Jain, 2000). The resulting imbalance of angiogenic regulators such as growth factors and matrix metalloproteinases makes tumor vessels highly disorganized and dilated with enlarged gap junctions between endothelial cells and thus more permeable towards macromolecules than the capillary endothelium in normal tissues as well as compromised lymphatic drainage resulting in drug accumulation (Carmeliet and Jain, 2000). Because of the decreased lymphatic drainage, the permeate nanocarriers are not removed efficiently, and are thus retained in the tumor. This is the EPR effect (Matsumura and Maeda, 1986; Maeda, 2001). Most polymeric nanoparticles can be used to target such effect due to their small size and large surface area (Figure 2.7). If a chemotherapeutic agent is loaded in a suitable polymeric carrier, the system then has the potential of increasing the concentration of the chemotherapeutic agent accumulated in the tumor tissue. However, it should be noted that the vessel permeability that forms a cornerstone of the EPR effect varies during tumor progression and tumor types. In addition, extravasation of polymeric nanomedicines will depend on the tumor type and anatomical location, as well as the physicochemical properties of the utilized polymers (Koo et al., 2006).

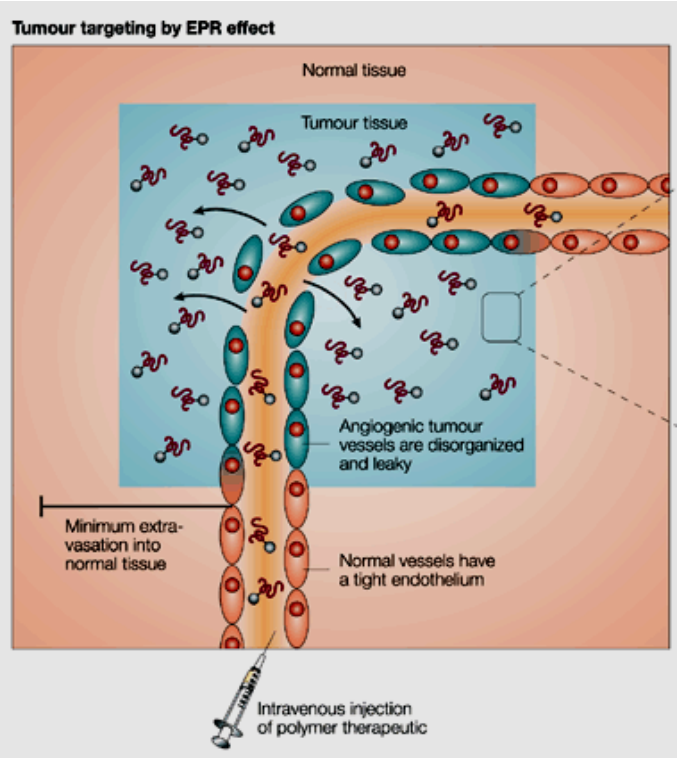

Figure 2.7 Tumor targeting of nanoparticles passively by EPR (Duncan, 2003).

Meanwhile, the unique microenvironment surrounding tumor cells, which is different from that of normal cells also contributes to passive targeting. Hyperproliferative cancer cells possess a high metabolic rate, and the supply of oxygen and nutrients is usually not sufficient for them to maintain this. Therefore, tumor cells use glycolysis (hypoxic metabolism) to obtain extra energy for tumor migration, invasion, and metastasis, resulting in an acidic environment (Yatvin et al., 1980; Pelicano et al., 2006). The drug can be conjugated to a tumor-specific molecule and is administered in an inactive state, and once it reaches its destination, the tumor microenvironment is able to convert it to an active and volatile substance by pH and/or specific enzymes, so-called tumor-activated prodrug therapy (Sinha et al., 2006). Also, direct local application allows the drug to be given directly to tumor tissue, avoiding systemic

circulation. Direct delivery of drugs into the tumor tissue prevents the drug from circulating throughout the body and rendering itself to metabolism by various systems. The disadvantage of direct inoculation of drug into tumors is that this method can be highly invasive, tumor localization is not feasible, and accessibility to certain tumors, for example lung cancer, can be problematic (Sinha et al., 2006).

Passive targeting systems which use a binary structure conjugate inevitably have intrinsic limitations to the degree of targeting specificity they can achieve. In the case of the EPR effect, while poor lymphatic drainage on the one hand helps the extravasated drugs to be enriched in the tumor interstitium, on the other hand, it induces drug outflow from the cells as a result of higher osmotic pressure in the interstitium, which eventually leads to drug redistribution in some portions of the cancer tissue. As a consequence, the efficacy is not as high and there is precious drug wastage to an extent (Wang et al., 2008; Stohrer et al., 2000). Apart from that, passive targeting strategy is not adaptable on the molecular or cellular level, leading the non-specific interaction of the drug carriers with cells.

Therefore, to overcome these limitations, a prudent approach is the inclusion of a targeting moiety which has molecular recognition and interaction with the cancerous cells. Active targeting is usually achieved by conjugating the nanoparticle to a targeting moiety, thereby allowing preferential accumulation of the drug within individual cancer cells, intracellular organelles, or specific molecules in cancer cells. The success of active targeting depends on the selection of the targeting agent, which should be abundant, have high affinity and specificity of binding to cell membrane receptors and be well suited to chemical modification in conjugation. The receptors should be expressed uniquely in diseased cells only or exhibit a differentially higher

expression in diseased cells as compared with normal cells (Cho et al., 2008). The commonly used molecular ligands for active targeting include folic acids (Yoo and Park, 2004), peptides (Brown, 2010), antibodies (Adams and Weiner, 2005), aptamers (Farokhzad et al., 2006), and affibodies (Ahlgren et al., 2009). Folic acid is a classical targeting moiety that binds the folate receptors on tumor cells. The overexpression of receptors in human cancer cells leads it to efficient uptake via receptor-mediated endocytosis. This is a process whereby extracellular particles gain entry into the intracellular environment (Figure 2.8). In general, the drug bound to a polymer carrier is taken into the cell via ligand-receptor interactions. Once localized at the cell surface, the targeted drug-polymer carrier complexes may exert its cytosolic action either at the plasma membrane or following internalization. Dissociation of the drug from its polymer can occur in lysosomes by lysosomal enzymes, resulting in the release of free drug into the cytosol. The receptors or antigens should be recycled and take their place on the cell membrane after transportation is complete (Sinha et al., 2006).

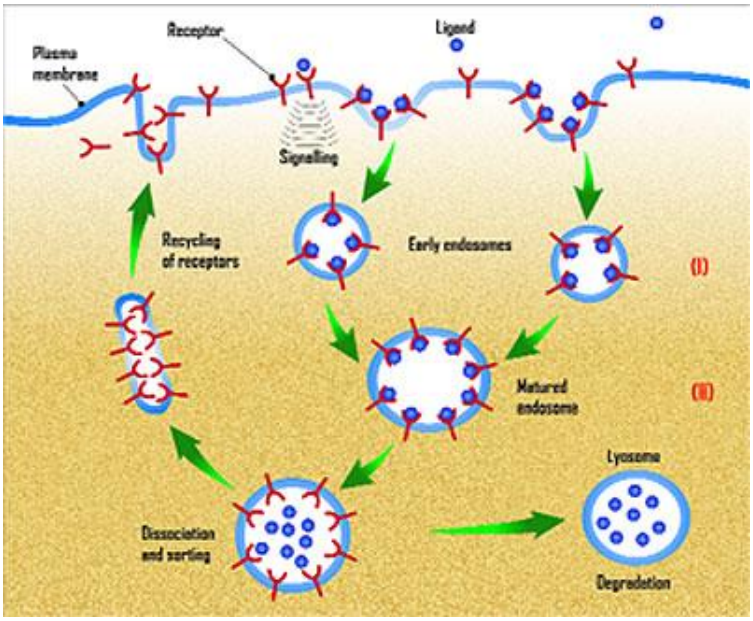

Figure 2.8 The pathway for receptor-mediated endocytosis (adapted from http://www.expresspharmaonline.com/20060815/research03.shtml).

2.9.2 Imaging

It is straightforward to understand that precaution is more important than treatment for cancer as there is virtually no specifically effective therapy to such a leading killer disease up to now. Therefore how to detect the symptoms of the disease or visualize the tumor skeleton as early as possible by means of practical and simple methods, desirably, in routine health check should be addressed as the first issue. Modern techniques, in recent years, have provided several diagnosis solutions for the detection of cancer indications, particularly, imaging the cancerous cells.

During the past decades, scientists and engineers have dedicated to developing quite a few of practical imaging techniques applicable to clinical imaging, diagnosis and treatments. Typically, optical imaging based on eye-visible fluorescence or near infrared fluorescence, magnetic resonance imaging, radionuclide imaging such as positron emission tomography and single photon emission computed tomography, computed tomography, and ultrasound have been widely applied and made superb performance in practical medicine. Basically, fluorescent dyes, paramagnetic materials, radioactive materials, heavy atom substances, and acoustically active microbubbles have been used as imaging agents for OI, MRI, PET, CT, and ultrasound, respectively.

Practically, each imaging techniques and imaging modalities possesses their merits and limitations. In detail, optical imaging or NIRF probes offer sensitivity enhancements while compromise tissue penetration depth. On the contrary, MRI provides great contrast and spatial resolution among different soft tissues of the body, making it

especially useful in neurological, musculoskeletal, cardiovascular and oncological imaging, yet the sensitivity is not as high as fluorescence imaging. PET is a radionuclide imaging technique which provides high target sensitivity but poor spatial resolution. CT, like MRI, is a noninvasive technique and generates three-dimensional images of a body object, providing good spatial resolution while sacrificing target sensitivity. The major advantage of ultrasound imaging is low cost, high safety but both resolution and sensitivity are low.

For the purpose of diagnosing tumors, imaging agents such as colloidal Au particles (Bardhan et al., 2008), IO contrast particles (Huh et al., 2005; Kopelman et al., 2005), and QDs (Gao et al., 2004), have been widely used. Loading those agents into nanoparticulate carriers may enhance detection sensitivity in medical imaging, improve imaging effectiveness, and decrease side effects (Moghimi et al., 2005). For imaging modalities with low sensitivity, nanoparticles bearing multiple contrast agents provide signal amplification. Nanotechnology can also enhance the colloidal stability of the nanosized imaging agents as well as prolong the circulation time in blood by protection of polymers to prevent the excretion from the bodies.

2.9.3 Multifunction

One nanoparticle can in principal deliver both reporting agents like peptides, genes, or dyes and drugs, allowing monitoring of biodistribution and reporting therapeutic activity simultaneously (theranostics) (Debbage and Jaschke, 2008). This ‘therapy’ plus ‘diagnostics’, or ‘theranostics’ holds the promise in future of monitoring or reporting the effectiveness of therapy simultaneously with delivering the therapy, and

thus of tailoring the therapy to the individual needs of a patient (personalized medicine).

Combining the targeting, imaging, reporting functions with the long circulating therapeutics delivery systems, it is a potent tool for thorough cancer therapy (schemed in Figure 2.9). It is clear that the development of multifunctional nanoparticles is luring, although has a long way to go and relies on the progress of cellular and molecular biology. Moreover, the feasibility to approach to the ultimate multifunctional systems should be based on the satisfied performance on single specific functions (Feng, 2006).

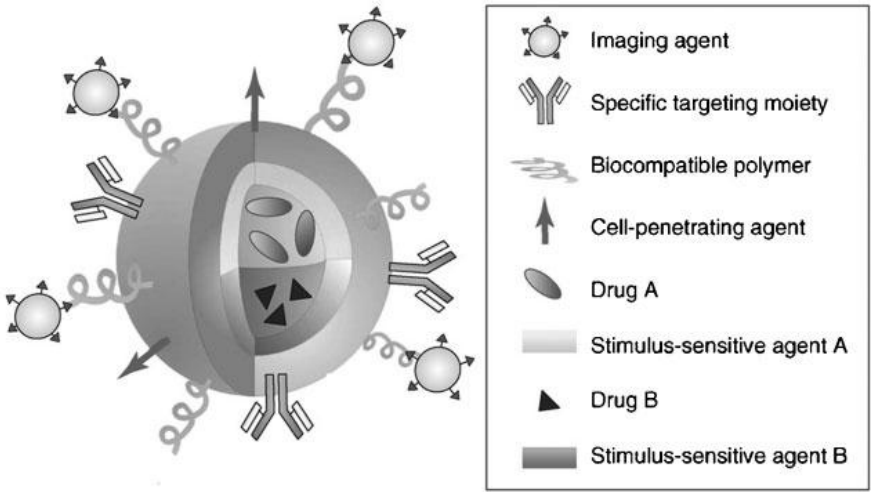

Figure 2.9 Schematic image of multifunctional nanoparticulate platform (Park et al., 2009).

2.10 Methods of producing polymeric nanoparticles

Nanoparticles can be fabricated by various methods (Feng and Chien, 2003; Hans and Lowman, 2002). The two main types are one-pot producing from monomer polymerization and dispersion of polymer solutions in water. Due to the difficulties on

strictly precise control factors to produce biodegradable polymers with desired molecular weight, one-pot polymerization method is not ideal. In the dispersion methods, some major routes can be utilized. The solvent extraction/evaporation technique might be the most important one. Polymer is dissolved in an organic solvent immiscible with water such as dichloromethane, or chloroform. The hydrophobic anticancer drug is dissolved or dispersed into the preformed polymer solution, and the resulting mixture is added into an aqueous solution with emulsification by high-speed homogenization or ultrasonication, to make an oil-in-water emulsion with the aid of an amphiphilic emulsifier (single emulsification). If the anticancer drug is hydrophilic, the technique is slightly modified to form a water-in-oil-in-water emulsion (double emulsification). After the formation of a stable emulsion, the organic solvent is evaporated by continuous stirring in an increased temperature or a reduced pressure (vacuum) environment, with or without the aid of an inertial gas flow. The high output energy disperses the oil phase to small and uniform oil droplets. After the coating of emulsifiers, stable dispersion will be formed. Particles will solidify after the evaporation of organic solvents. Centrifugation or ultrafiltration is applied to collect the formed particles, which can then be freeze-dried to form dry powders for storage. A brief discussion for the effect of process variables on the properties of nanoparticles can be found in the paper published by Scholes et al. (1993). The simple technique is fast to operate with high particle yield, but producing monodispersed particles is not that easy. Since the solvent extraction/evaporation technique is good only for a laboratory-scale operation, other nanoparticle technologies such as spray-dry and spray-freeze-dry have also been developed for a large-scale pilot production of drug-loaded particles. The challenges for spray-drying include how to produce particles with

sufficiently small size and how to increase the drug encapsulation efficiency. Other alternative techniques employing low-energy emulsification are required. One choice is the spontaneous emulsification-diffusion technique, in which a water-miscible solvent such as acetone or methanol and a water-immiscible organic solvent such as dichloromethane or chloroform are used. Due to the spontaneous diffusion of the water-soluble solvent, an interfacial turbulent flow is created between the two phases, leading to the formation of nanoparticles. An alternative is the so-called salting out method. The detailed mechanism and the factors affecting the products have been thoroughly compared by Galindo-Rodriguez et al. (2004).

Nanoprecipitation is another good technique by diffusion of water-miscible solvents containing polymers into aqueous phase by which nanoparticles with small size and narrow size distribution can be produced. The method was firstly reported in 1989 though the term was not clearly stated at that moment (Fessi et al., 1989). Although the yield of nanoparticles and encapsulation efficiency of hydrophobic drugs are sometimes a little lower, instant fabrication and prospective scale-up possibility are the obvious advantages. Especially, by using this method, particles with size less than 100 nm are able to be easily produced. Nanoprecipitation method differs from the emulsification-diffusion and salting-out methods in that formally no precursor emulsion is formed during NP preparation. Basically, NP formation is explained in terms of the interfacial turbulence and the “diffusion-stranding” processes between two unequilibrated liquid phases (Miller, 1988). Typically, the organic phase containing the polymer in water-miscible solvent is poured into the aqueous phase with or without surfactant under slight magnetic stirring. When both phases are in contact, solvent rapidly diffuses from the organic phase into the water and afterwards, the polymer

chains entangle with each other and further aggregate to form solidified particles. In experiments, three major factors affect the properties of the final polymeric particles, which are the polymer concentration in organic solvents, the type of solvent in the organic phase, i.e. the miscibility with water, and volume ratio of organic phase to aqueous phase. Besides, other factors such as polymer type, phase mixing rate, stirring speed, temperature, drug loading, presence of surfactants, etc also have influence. Normally, increasing the polymer concentration, or using solvents with lower miscibility, or enlarging the oil to water ratio leads to larger particle size and size distribution. Detailed comparison and explanations have been extensively reported in the past a few years (Beletsi et al., 2008; Fonseca et al., 2002; Bilati et al., 2005; Govender et al., 1999; Cheng et al., 2007). Dialysis method holds similar mechanism of nanoprecipitation. But precise control of nanoparticle forming should only be guided by previous diffusion study, which is specific for different systems. Also, it is time wasting and low efficient. From the environmental-friendly point of view, production of polymeric nanoparticles by supercritical fluid spraying is an emerging technique without the need of using any toxic organic solvent and surfactant. Hydrophilic polymers like chitosan can be prepared by ionic gelation technique, which involves a mixture of two aqueous phases with different charges.

2.11 Surface coating for producing polymeric nanoparticles

Generally, extra materials are indispensible when fabricating polymeric nanoparticles coating on the surface to provide sufficient colloidal stability, desirable surface properties and functions, and sometimes higher therapeutic effect. Emulsifiers are one

of the most important components in solvent extraction /evaporation method to stabilize the dispersive phase in continuous phase as well as the origin of surface coating on fabricated nanoparticles. The often-used emulsifiers, PVA has the disadvantages of low emulsification efficiency, low drug encapsulation ability, difficulty to clean-up, and possible harms to the body (Feng and Chien, 2003). Other better and more efficient emulsifiers, such as gelatin, Tween-80, F-127, F-68 are thus preferred. But the potential side effects to human bodies are still not fully clear. Moreover, these synthetic macromolecules are not easily washed out of the particles (Feng and Huang, 2001). As a result, they may cause troubles in purification of products and thus influence the properties of the formed nanoparticles. Therefore, natural amphiphilic molecules are better to be emulsifiers for fabricating nanoparticulate carriers. Among various natural emulsifiers, TPGS1k is a rising star as emulsifier due to the natural origin, biocompatibility, high emulsification effect, high encapsulation efficiency of drugs, prolonged circulation time in blood, ability of escape from the recognition of mononuclear phagecytic system and interaction with lipoproteins as passive targeting. TPGS is a water-soluble derivative of natural vitamin E, i.e. a PEGylated Vitamin E, which has amphiphilic structure comprising lipophilic alkyl tail and hydrophilic polar portion (Figure 2.10). Its bulky structure and large surface area makes it an excellent emulsifier, solubilizer, and bioavailability enhancer of hydrophobic drugs. It has also been found that TPGS could inhibit P-gp mediated multidrug resistance and thus greatly enhance oral drug delivery (Lukyanov et al., 2004; Mu et al., 2005; Zhao et al., 2009). Our group has recently shown that TPGS1k can result in promising nanoparticles with the features such as drug encapsulation efficiency as high as 100%, higher cellular uptake and sustainable chemotherapy effect

in vivo, etc (Mu et al., 2004; Win and Feng, 2006; Feng et al., 2007; Lee et al., 2007; Zhang and Feng, 2006; Zhang and Feng, 2006a; Zhang et al., 2007; Pan and Feng, 2008; Gan et al., 2010).

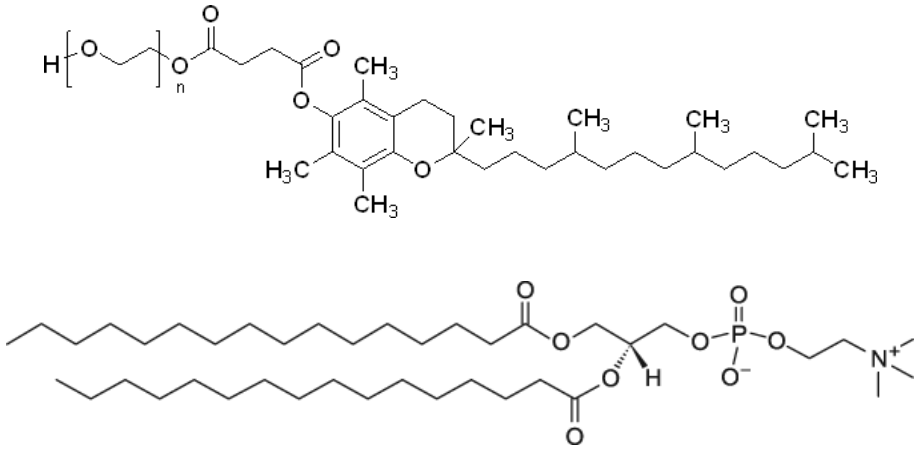

Figure 2.10 Chemical structure of TPGS1k (top) and DPPC (bottom).

Phospholipids are another ideal candidate. They have been widely used as emulsifying agents and for other purposes in industry (Feng and Huang, 2001). The products in which phospholipids are used as emulsifiers include food industry like animal feeds, baking products and mixes, chocolate, light industry like cosmetics and soaps, manufacturing like insecticides, dyes, paints, and plastics. For example, in foods, they promote the suspension of one liquid in another as in the mixture of oil and water in margarine, shortening, ice cream, and salad dressing. Phospholipids are also used in the skin care area such as preparation of cosmetics, lotions, and certain pharmaceuticals, where they prevent separation of ingredients and extend storage life. However, their application as emulsifiers in the solvent extraction/evaporation technique to fabricate polymeric nanoparticles as drug delivery systems has rarely been reported. Only a few publications suggested that the use of DPPC as an additive may

be able to improve the performance of the produced PLGA microspheres in blood flow (Garti, 1999), enhance the pulmonary absorption of peptides and proteins (Zhen et al., 1995) and reduce phagocytic uptake of the microspheres (Evora et al., 1998). All these facts hint at the potential application of phospholipids as natural emulsifiers for polymeric nanoparticle fabrication to load anticancer drugs.

Moreover, phospholipids are essential biomolecules in the structure and function of living matter, besides water, and along with proteins, nucleic acids and carbonhydrates. The most abundant lipids are fats, or triglycerids, and waxes which are oily or greasy nonpolar substances, insoluble in water. For the emulsifiers, only polar lipids are interested, which have amphiphlic properties and are building blocks of cell membranes. Generally a polar lipid molecule consists of three parts in its chemical structure: a polar head group, carbon chain tail(s) and a phosphorous backbone to which the carbon chains and polar head moieties are attached. Polar heads groups vary, constructing the so called phosphatidyl choline, phosphatidyl ethanolamine, phosphatidyl serine, phosphatidyl glycerol, phosphatidyl acid, and phosphatidyl inostiol (New et al., 1990). The water insoluble part consists normally of one or two acyl or alkyl (fatty acid) chains. Chain lengths in these synthetic diacyl lipids range from 8 carbon atoms to 24, mostly from 14 to 18, and they can be fully saturated or unsaturated with 1 to 4 double bonds. The most frequently occurring saturated fatty acids in the natural cell membranes are palmitic, stearic, and miristic, which possesses 16, 18, and 14 carbon atoms, respectively. From the unsaturated fatty acids the oleic, which is a stearic acid with one double bond in the middle of the chain with a cis-configuration is the most important. Saturated fatty acid chains are very flexible and when in a non-frozen state they can exhibit a large number of conformations because

each single bond has complete freedom of rotation. In contrast, unsaturated fatty acids show one or more rigid kinks due to double bond which are non-rotating. Single-chain lipids can have the polar head attached directly to the hydrocarbon chain while natural double-chain lipids contain a molecule which serves as a linker between the three groups. The backbone of lipid is normally either glycerol or sphingosine. Generally, semisynthetic lipids, which can be made by complete organic synthesis or by de- and re-acylation of natural lipids, are widely used in research because their phase behavior and thermodynamic parameters are much better defined as compared to natural analogues with polydisperse hydrocarbon chain populations (Lasic et al., 1993). In contrast to the natural ones, such as lecithins prepared from egg yolk or soy beans, the physical properties like the phase transition temperature (from solid gel phase to liquid crystal phase), enthalpy and entropy value, are more clearly defined and do not vary from source to source. Those parameters might be important to the judge of experimental conditions to fabricate nanoparticles. Therefore, proper selection of phospholipids as emulsifiers should consider the following factors: carbon chain tilt, including chain length, degree of saturation (rigidity of the chains); phase transition temperature; charge and bulky of head group; and solubility in common solvents (since emulsifiers can play better effect in solution). DLPC is a kind of commonly used phospholipid because of its normal chain length, saturation, positively charged headgroup, proper space volume of the head, phase transition temperature (-1 ℃) which is lower than room temperature, easy producing, and relatively high stability.

2.12 Herceptin

Monoclonal antibody accounts for significant portion for targeted nanomedicine as a molecular targeting ligand. Trastuzumab ($C_{6470}H_{10012}N_{1726}O_{2013}S_{42}$) (Herceptin®) is one of the most attractive antibodies since it is the first humanized antibody approved by the FDA for the treatment of HER2-positive MBC (Smith, 2001; Vogel et al., 2002).

The progress of cancerous tumor is often accompanied by the over expression of special proteins called tumor antigens, which can be used as biomarkers to differentiate the cancer cells from the healthy cells for development of targeting strategies. The crucial step is to identify the ideal ligand for targeting (Ross et al., 2004; Longo et al., 2007). The EGFR is a receptor tyrosine kinase overexpressed on many human cancer cells. It is regarded as a key receptor for targeted tumor therapy. The human epidermal growth factor family includes the EGF receptors (EGFR, HER1), HER2/neu, neuregulin/heregulin receptors HER3 and HER4 (Figure 2.11). Under healthy conditions, they regulate the cell-to-cell and cell-to-stroma communication through the signal transduction system, and consequently, affect cell survival and proliferation, angiogenesis, motility and adhesion (Ross et al., 2004). These proteins are composed of three membrane portions: the internal tyrosine kinase responsible for signal transduction; a short transmembrane part, and the extracellular receptor domain. The binding of ligands to EGFR, HER3 and HER4 results in the formation of homodimeric or heterodimeric receptor complexes, and HER2 acts as a co-receptor facilitating the signal transduction (Longo et al., 2007).

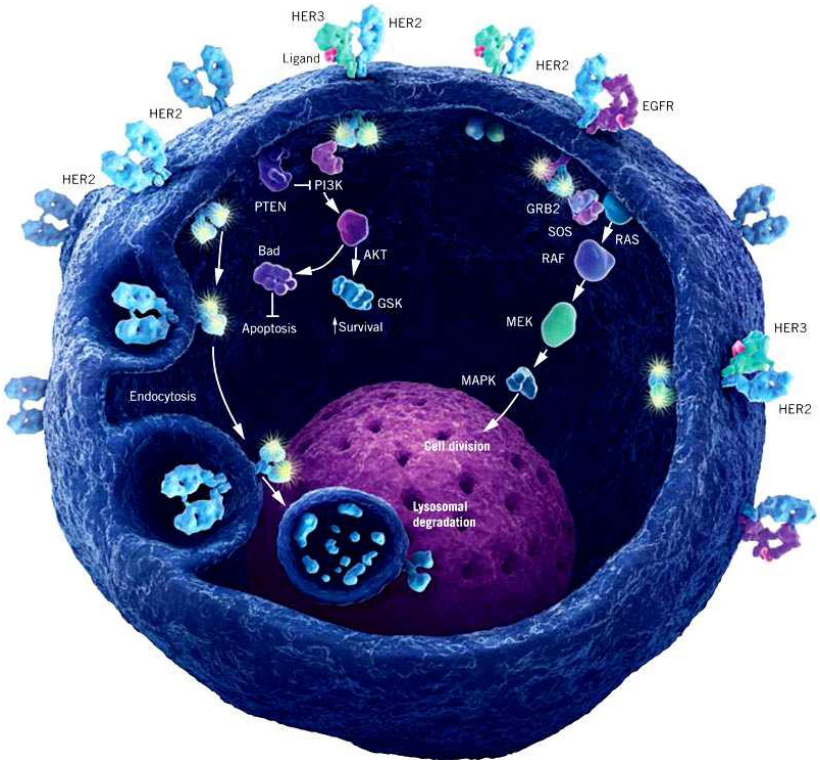

Figure 2.11 The human epidermal growth factor family (adapted from http://www.biooncology.com/).

The MBC is a stage IV breast cancer that HER2 (or HER2/neu or ErbB-2), one of the transmembrane tyrosine kinase receptors with partial homology that normally regulate cellular responses, overexpresses on the cancerous cell membranes (Yarden, 2001). 20-30% of breast cancer tumors are found to have overexpressed HER2 gene. The advanced cancer highly challenges the common therapies in that patients with the advanced cancer cells overexpressing this receptor have decreased overall survival rate and may have differential responses to a variety of chemotherapeutic agents (Seidman et al., 2001). The overexpressed HER2 gene in breast cancer cells is found to result in higher resistance against anticancer drugs such as paclitaxel. Therefore it is of paramount importance to invent new strategies to treat MBC. Particularly, HER2 is an interesting and promising receptor to be targeted for HER2-overexpressing breast

cancer cells (Figure 2.12) (Nahta and Esteva, 2006). Herceptin® (formulated by Genentech from Trastuzumab, simply expressed as herceptin afterwards), a humanized recombinant anti-HER2 monoclonal antibody, is one of the medications which binds to the extracellular juxtamembrane domain of HER2 by its two antigen specific sites and inhibits the proliferation and survival of HER2-dependent tumors (Hudis, 2007).

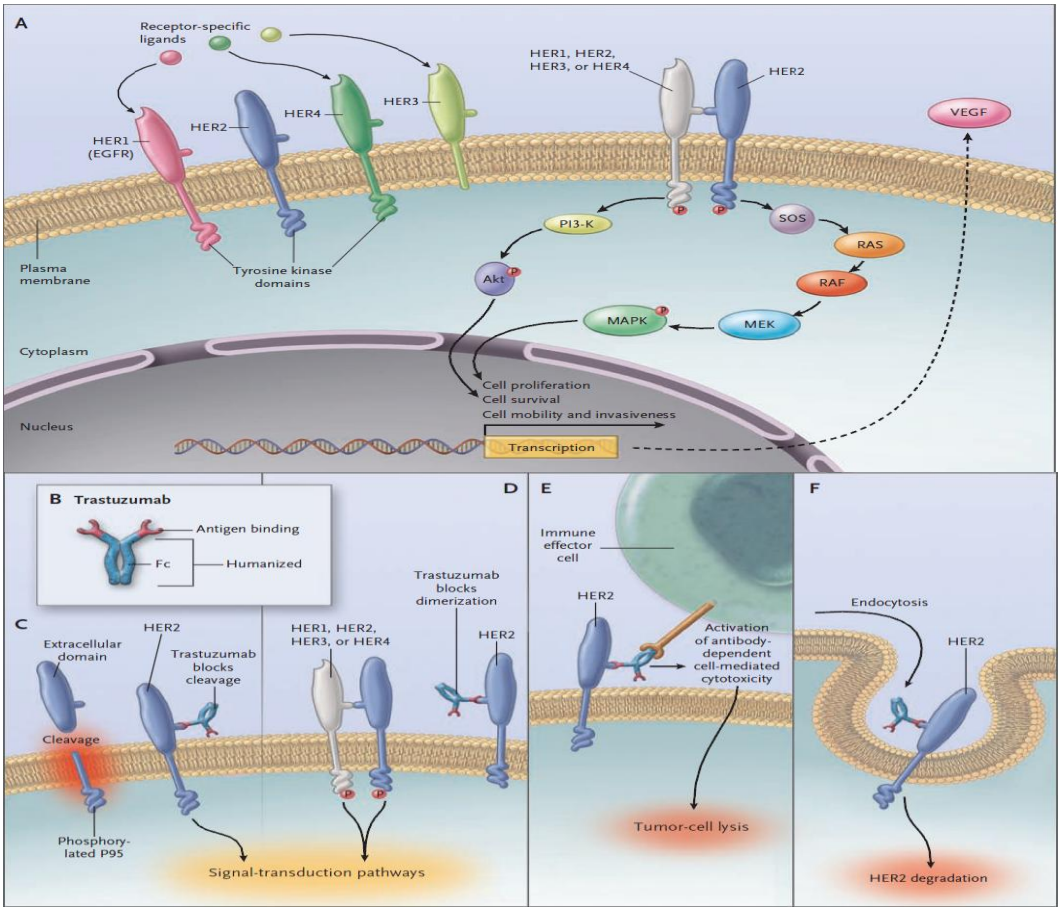

Figure 2.12 Receptor sites for Trastuzumab and mechanism of action of Trastuzumab (Bullock and Blackwell, 2008).

Herceptin's exact mechanism of action is debatable and appears to differ *in vivo* compared to *in vitro*. One of the postulation is that the binding effect prevents the activation of its intracellular tyrosine kinase (Figure 2.13). It may also prevent the

HER2 receptor from dimerization, increase endocytotic destruction of the receptor, and inhibit shedding of the extracellular domain and immune activation (Bullock and Blackwell, 2008). Another proposed mechanism of cancer cell inhibitory by herceptin is that it diminishes signaling from the phosphoinositide 3 kinase and mitogen-activated protein kinase pathways, causing cell cycle arrest at the G1 phase, promoting apoptosis via antibody-dependent cellular cytotoxicity, and inhibiting angiogenesis and DNA repair in tumors (Hudis, 2007).

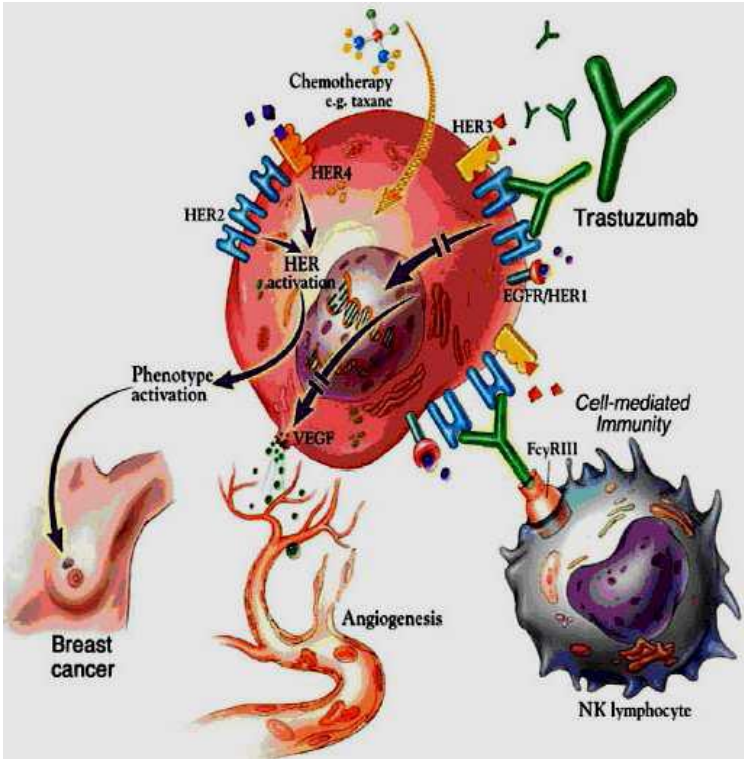

Figure 2.13 Action of Trastuzumab on breast cancer cells (adapted from http://www.salutedomani.com/il_weblog_di_antonio/2010/02/tumore-seno-migliorare-la-sopravvivenza-al-71-trastuzumab.html).

2.13 Precise engineering of polymeric nanoparticles

The properties of nanoparticles have great impact on the performance of nanomedicine. Typically, the size, surface hydrophilicity, surface charge, shape or geometry, and surface coating are regarded as judging factors when investigating the cell-particle interaction and anticancer effect. However, notably, the nature and density of the ligands on the particle surface for targeted drug delivery is as important as other biophysicochemical properties of the drug carrier, and can all impact the circulating half-life of the particles as well as their biodistribution (Farokhzad and Langer, 2009). The presence of targeting ligands can increase the interaction of the drug delivery system with the cells in the target tissue, which can potentially enhance cellular uptake efficiency by receptor-mediated endocytosis. The optimization of the ligand density on the drug carrier surface can facilitate the tissue penetration, cellular uptake, and optimal therapeutic efficacy (Farokhzad and Langer, 2009). Moreover, the surface density of conjugated ligand is an external indicator for the surface chemistry of NPs which is one of the important properties of NPs affecting the safety issues of NPs in biomedical applications (Dusinska et al., 2009). Therefore it is highly valuable to develop the strategy for quantitatively control the ligand density and further precisely engineer the properties of drug carriers.

The most commonly used method to introduce targeting ligands on the carriers is through covalent conjugation which is more easily to be controlled than using physical adsorption method. Yet ligand conjugation is a self-assembly process in which no direct management is available to control successful conjugation between the ligand and the polymeric nanoparticles, which makes it difficult for any quantitative control of the targeting effect to meet the treatment needs to be realized. Recently, in the

literature, there are two strategies developed for quantitative control of the targeting effects by adjusting the ligand density on the nanoparticle surface. The first trial is through conjugation of ligand on the polymers which form the particles later before the nanoparticle formation, which we call the pre-conjugation method. The other is so-called the post-conjugation method, i.e. to conjugate the ligand to the particles after the nanoparticle formation. For the pre-conjugation strategy, one copolymer such as PLGA-PEG of the nanoparticle matrix was firstly conjugated with targeting ligand say A10 aptamer, the NPs was then prepared by the nanoprecipitation method (Gu et al., 2008). The cellular uptake efficiency and biodistribution behavior of the particles with various ligand densities was proved have the relationship with the surface density. This strategy, however, is not desired enough to precisely control the ligand density due to some limitations such as the lost of the ligand in the polymeric matrix and irregular distribution of the ligand among different nanoparticles. For the post-conjugation strategy, instead, the drug loaded nanoparticles were firstly prepared with the two copolymer blend such as functional PLGA-PEG and inert PLGA. The nanoparticles were then functionalized by the ligand such as antibodies. Delie's group produced the thiol-functionalized PLA nanoparticles loading with paclitaxel then conjugated with herceptin to compare the therapeutic effects. The density of the thiol groups on the formed particles was quantified to control the ligand density, which is an illustration of using the post-conjugation strategy (Cirstoiu-Hapca et al., 2007; Cirstoiu-Hapca et al., 2009). The advantages of such a post-conjugation strategy overcome the weakness of the pre-conjugation strategy, which used the ligand much more efficiently and protects its bioactivity, thus resulting higher targeting effects. In this work, post-conjugation strategy would be applied to control the ligand density on nanoparticles and the impact

on anticancer performance of the drug loaded particles with various ligand densities would be investigated.

Chapter 3 : Nanoparticles of Lipid Monolayer Shell and Biodegradable Polymer Core for Anticancer Drug Delivery

The development of a novel anticancer drug delivery system of nanoparticles of lipid monolayer shell and biodegradable polymer core for controlled release of anticancer drugs with paclitaxel as a model drug is reported in this chapter, in which the emphasis is given to the impact of the lipid monolayer shell type and the lipid amount used in the process of nanoparticle preparation on the properties of the nanoparticles. Five different types of phospholipids were investigated with various amounts to find appropriate formulations for delivery of paclitaxel. The drug loaded nanoparticles were characterized by LLS for size and size distribution, zetasizer for surface charge, HPLC for drug encapsulation efficiency, FESEM for surface morphology, and XPS for surface chemistry. The optimal formulation of lipid coated nanoparticles were also compared with PVA emulsified nanoparticles in order to demonstrate the advantages of lipids to formulate drug loaded nanoparticles over the traditional emulsifier in terms of high emulsification efficiency and desired particle characteristics. MCF7 breast cancer cells were employed to evaluate the cellular uptake efficiency and cytotoxicity of the newly formulated nanoparticles. After incubation with MCF7 cells at 0.250 mg/ml NP concentration, the coumarin-6 loaded PLGA NPs of lipid shell showed effective cellular uptake efficiency. The analysis of IC_{50} upon the cytotoxicity analysis demonstrated that the DLPC shell PLGA core NP formulation of paclitaxel could be 5.88-, 5.72-, 7.29×10^3- fold effective than the commercial formulation Taxol® after 24, 48, 72 hr treatment, respectively.

3.1 Introduction

Nanotechnology has been regarded as one of the most promising approaches to deal with cancer, which is still a leading cause of death all over the world (Ferrari, 2005; Jemal et al., 2009; Farokhzad and Langer, 2009). Nonetheless, there are only a few nanotechnology based drug formulations so far which are approved by FDA for clinical application (Duncan, 2006). It is thus of paramount importance to develop smarter and more powerful drug formulations. Liposomes and polymeric nanoparticles are two of the utmost investigated nanocarriers for anticancer drug delivery. Liposomes have been widely used as a drug delivery vehicle due to high biocompatibility, favorable pharmacokinetic profile and ease of surface modification. However, liposomes have disadvantages for drug delivery including insufficient hydrophobic drug loading, fast release of hydrophobic drugs and instability (Rai et al., 2008). Polymeric nanoparticles are another dominant platform for drug delivery. Yet the biocompatibility of NPs formed by most synthetic polymers is not as high as liposomes, especially at the cellular level. It is thus natural to develop novel drug carrier which can combine the advantages and avoid the disadvantages of the liposomes and the nanoparticles of biodegradable polymers.

It has been found that the surface decoration of PLGA NPs by lipids is a promising approach to improve the drug encapsulation efficiency and mediate cellular uptake of the nanoparticles (Feng et al., 2002; Feng et al., 2004). Recently, several researches have been reported regarding the polymer-lipid hybrid nanoparticles, which are nanoparticles of lipid shell and polymer core produced by various methods, which can be summarized in two categories (De Miguel et al., 2000; Wong et al., 2006; Wong et al., 2006a; Thevenot et al., 2007; Wong et al., 2007; Li et al., 2008; Zhang et al.,

2008b; Chan et al., 2009). The first is to prepare the polymeric core firstly and then merge them with liposomes to form the desired lipid shell-polymer core structure. A typical example is the lipoparticles (De Miguel et al., 2000; Wong et al., 2006; Wong et al., 2006a; Thevenot et al., 2007; Wong et al., 2007; Li et al., 2008). The formulation process of such structured nanoparticles usually needs two steps, i.e. formation of polymeric NP core and mixing of the core NPs liposomes, resulting in technical complexity and thus lack of control over the final NP physicochemical properties (Zhang et al., 2008b). The second is to produce the core-shell nanoparticles in a single step which combines the nanoprecipiation and self-assembly method (Zhang et al., 2008b; Chan et al., 2009). Such strategies meet the requirement to develop well-defined and predictable lipid-polymer hybrid NPs and facilitate future scale-up. Consequently, the novel nanocarriers deserve further investigation particularly on the impact of the phospholipid decoration on the performance of NPs. In the previous research of our group, it has been concluded that the lipids of short and saturated chains such as DLPC, which has the HLB index of 13 (calculated from the equation: HLB index = $\sum$ (Hydrophilic groups) + $\sum$ (Lipophilic groups) + 7), could have high emulsification effects for preparation of polymeric particles of the nanoscale size, smooth surface, and desired control release profile of anticancer drugs of high hydrophobicity such as of paclitaxel (Feng and Huang, 2001).

In this research, we continued our earlier work in 2001 to develop a system of biodegradable nanoparticles of various lipid shell and PLGA polymer core for controlled release of paclitaxel which is an excellent antineoplastic agent against a wide spectrum of cancer. The emphasis was given to investigation on the lipid decoration type and optimization of the lipid amount in favor of the particle

characteristics and performance as well as to demonstrate the advantages of the lipid coated NPs over those emulsified by the traditional chemical emulsifier PVA. The NPs were characterized by LLS for size and size distribution, zetasizer for surface charge, HPLC for drug encapsulation efficiency, FESEM for surface morphology, and XPS for surface chemistry. MCF7 human breast cancer cells were employed to evaluate the cellular uptake of the coumarin-6 loaded NPs and the cytotoxicity of the drug formulated in the NPs versus Taxol®.

3.2 Materials and methods

3.2.1 Materials

Paclitaxel (99.8%) was purchased from Dabur Pharma Ltd. (India). Taxol® was provided by National Cancer Center (Singapore). PLGA (75:25, Mw: 90,000-126,000), 1,2-distearoyl-*sn*-glycero-3-phosphocholine (DSPC), 1,2-dipalmitoyl-*sn*-glycero-3-phosphocholine (DPPC), 1,2-dimyristoyl-*sn*-glycero-3-phosphocholine (DMPC), 1,2-dilauroyl-*sn*-glycero-3-phosphocholine (DLPC), 1,2-dicapryl-*sn*-glycero-3-phosphocholine (DCPC), PVA, coumarin-6, PBS (pH 7.4), MTT, and PI were all purchased from Sigma-Aldrich (St. Louise, MO, USA). DMEM, FBS, penicillin-streptomycin solution, and trypsin-EDTA solution were all from Invitrogen Corporation. All solvents used in this study were HPLC grade and offered by Sigma-Aldrich. MCF7 breast cancer cells were provided by American Type Culture Collection. The water used was pretreated with the Milli-Q® Plus System (Millipore Corporation, Bedford, USA).

3.2.2 Preparation of the NPs

Preparation of the drug loaded, lipid shell and PLGA core NPs is based on a modified solvent extraction/evaporation method (Feng et al., 2007). Briefly, weighed amount of PLGA and paclitaxel were dissolved in dichloromethane as the oil phase. The aqueous phase was prepared by dispersing designated amount of lipid (%, w/v as the unit) in ultrapure water by bath sonication. Afterwards, the oil phase was mixed with the aqueous phase under stirring and then the mixture was sonicated by probe ultrasonicator at 20 W output under ice bath for 5 minutes. The produced emulsion was placed on magnetic stirrer to evaporate the solvent with moderate speeding overnight. The particle suspension was centrifuged at 12,000 rpm for 15 minutes to collect the NPs. After washing three times, the particles were resuspended in a fixed volume of water with 3% (w/w) sucrose as cryoprotectant and freeze-dried to obtain the fine powder. The blank NPs and the coumarin-6 loaded NPs were prepared in a similar procedure. The PVA emulsified NPs were produced in a similar manner with 2% (w/v) PVA in water as the aqueous phase.

3.2.3 Characterization of the NPs

For the statistical analysis, data were expressed as the means with 95% confidence intervals. Statistical tests were performed with the Student's *t* test. For all tests, *P* values less than 0.05 were considered to be statistically significant. All statistical tests were two-tailed.

Average particle size and size distribution of the NPs were measured by laser light scattering (90Plus Particle Sizer, Brookhaven Instruments Co. USA). The surface charge of the NPs in water was determined by ZetaPlus zeta potential analyzer (Brookhaven Instruments Co. USA) at room temperature. The amount of paclitaxel

encapsulated in the NPs was measured by high performance liquid chromatography (Agilent LC1100) equipped with a reversed phase Inertsil® ODS-3 column (250×4.6 mm, particle size 5 μm, GL Science Inc., Tokyo, Japan) and 50:50 (v/v) acetonitrile/water solution as mobile phase. Encapsulation efficiency is equal to (amount of drug encapsulated in the yielded NPs) / (amount of drug used in the feed of fabrication). The shape and surface morphology of the NPs were analyzed by field emission scanning electron microscope (JSM-6700F, JEOL, Tokyo, Japan) at an accelerating voltage of 5 kV. The dry particles were coated by platinum coater (JEOL, Tokyo, Japan) for 30 s at 30 mA current. The surface chemistry of the NPs was analyzed by X-ray photoelectron spectroscope (AXIS His-165 Ultra, Kratos Analytical, Shimadzu Corporation, Japan). The data were processed by software provided by the instrument corporation.

3.2.4 *In vitro* evaluation

For the *in vitro* drug release study, the drug loaded NPs were dispersed in PBS (0.1 M, pH 7.4) containing 0.1% w/v Tween-80, which can improve the solubility of paclitaxel in PBS. The dispersion was then put in an orbital shaker shaking at 120 rpm with water bath at 37℃. At designated time intervals, the suspension was centrifuged at 11,000 rpm for 30 min. The pellet was resuspended in fresh medium to continue the drug release. The drug released in the supernatant was extracted by dichloromethane and transferred in the same mobile phase as abovementioned. After the evaporation of the solvent, paclitaxel quantity was determined by the same HPLC procedure aforementioned. The error bars were obtained from triplicate samples.

DMEM medium supplemented with 10% FBS and 1% penicillin-streptomycin was utilized as cell culture medium. Cells were cultivated in this medium at 37℃ in humidified environment with 5% CO_2. For cellular uptake study, MCF7 cells were seeded into 96-well black plates (Costar, IL, USA) at 5×10^3 cells/well (0.1 ml) and after the cells reached 80% confluence, the medium was changed to the suspension of coumarin-6 loaded NPs at a NP concentration of 0.250 mg/ml for 0.5 and 2 hr, respectively. After incubation, the NP suspension in the testing wells was removed and the wells were washed with 0.1 ml PBS three times to remove the NPs outside the cells. 50 μl of 0.5% Triton X-100 in 0.2 N NaOH solution was subsequently added to lyse the cells. The fluorescence intensity presented in each well was then measured by microplate reader (Genios, Tecan, Switzerland) with excitation wavelength at 430 nm and emission wavelength at 485 nm. For confocal microscopy study, MCF7 cells were cultivated in the 8-well coverglass chamber (LAB-TEK®, Nagle Nunc, IL) till 70% confluence. The courmarin-6 loaded NPs dispersed in the cell culture medium at concentration of 0.250 mg/ml were added into the wells. Cells were washed three times after incubation for 0.5 and 2 hr and then fixed by 70% ethanol for 20 min. The cells were further washed twice by PBS and the nuclei were then counterstained by PI for 45 min. The cell monolayer was finally washed thrice by PBS and observed by confocal laser scanning microscope (Olympus Fluoview FV1000).

For the cytotoxicity study, MCF7 cells were incubated in 96-well transparent plates (Costar, IL, USA) at 5×10^3 cells/well (0.1 ml) and after 12 hr, the old medium was removed and the cells were incubated for 24, 48 and 72 hr in the media containing Taxol® or paclitaxel loaded NPs suspension at an equivalent paclitaxel concentration of 25, 10, 2.5, 0.25 μg/ml. The NPs were sterilized with UV irradiation for 1 day prior

to use. At given time intervals, the cultured cells were assayed for cell viability with MTT. The wells were washed twice with PBS and 10 μl of MTT supplemented with 90 μl culture medium was added. After 3 hr incubation, the medium was removed and the precipitate was dissolved in DMSO. The absorbance of the wells was measured by the microplate reader (Genios, Tecan, Switzerland) with wavelength at 570 nm and reference wavelength at 620 nm. Cell viability was calculated by the following equation: cell viability = Int_s / $Int_{control}$ × 100%, where Int_s is the absorbance of the wells containing the cells incubated with the NP suspension and $Int_{control}$ is the absorbance of the wells containing the cells incubated with the culture medium only (positive control).

3.3 Results and discussion

3.3.1 Preparation and structure of the NPs

The schematic structure of the paclitaxel loaded, lipid shell and PLGA core NPs developed in this work is represented in Figure 3.1. The NPs were produced by the oil-in-water (O/W) single emulsion solvent extraction/evaporation method with phospholipid as emulsifier. After emulsification of the oil phase in the aqueous phase by applying ultrasonication, the amphiphilic lipids were adsorbed onto the surface of the oil droplets containing PLGA and paclitaxel by hydrophobic interaction. Followed by the evaporation of DCM under continuous magnetic stirring, the drug loaded NPs were then solidified and formed. Phospholipid was introduced as the amphiphilic molecule to decrease the interfacial tension between oil-water phase and thus attach on the surface of polymer matrix to facilitate stable formation of the solid PLGA cores.

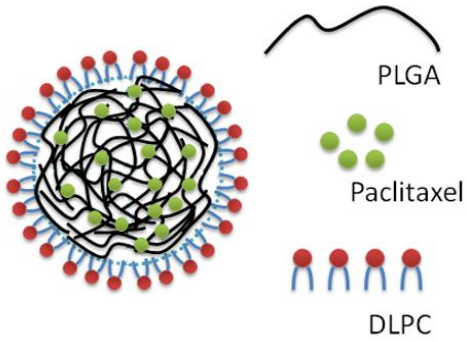

Figure 3.1 Schematic illustration of the structure of the paclitaxel loaded lipid shell (for instance, DLPC) PLGA core NPs.

3.3.2 The influence of lipid type on the characteristics of the NPs

Served as emulsifier in the nano-emulsification process to produce lipid shell polymer core NPs, the type of lipids has distinctive impact on the characteristics of the NPs resulting from the flexibility depended on the satruation of their carbon chains as well as the HLB determined by the length of their carbon chains (Feng and Huang, 2001). Table 3.1 illustrates the size, size distribution, surface charge and drug encapsulation efficiency of the paclitaxel loaded NPs of various saturated lipid shell and PLGA core with lipid amount of 0.05% (w/v). Overally, in terms of the size and polydispersity property, DLPC shell NPs showed smallest hydrodynamic diameter and most narrow size distribution. Additionally, the surface charge of such formulation was shown to be the lowest, which indicates the highest colloidal stability. For the EE results, all of the lipids except DSPC displayed acceptable drug loading capability. It can be concluded that shorter chain lipids, such as DLPC and DCPC could be better candidates to be employed as the agents to produce lipid shell polymer core NPs due to their higher HLB value (13 and 15, respectively).

Table 3.1 Characteristics of the paclitaxel loaded lipid shell and PLGA core NPs of various lipid used with 0.05% (w/v) as concentration in the nano-emulsification process: particle size, size distribution, zeta-potential and encapsulation efficiency. Data represent mean ± SE, n=6 (For EE results, n=3).

lipid shell	Particle Size (nm)	Polydispersity	zeta-potential (mV)	Encapsulation Efficiency (%)
DSPC	> 1000	> 0.3	N.A.	N.A.
DPPC	578.3 ± 14.4	0.220 ± 0.030	-28.11 ± 2.25	45.5 ± 1.44
DMPC	310.0 ± 7.3	0.269 ± 0.028	-34.85 ± 3.76	38.7 ± 0.20
DLPC	243.0 ± 4.2	0.138 ± 0.043	-36.88 ± 1.30	43.8 ± 0.06
DCPC	275.1 ± 8.9	0.153 ± 0.009	-29.95 ± 3.12	48.8 ± 1.90

3.3.3 The influence of lipid quantity on the characteristics of the NPs

We next used DPPC, DMPC, DLPC to formulate NPs and investigate the impact of lipid quantity on the NPs properties since DSPC failed to produce nanoscaled particles due to its low HLB value and DCPC is not stable at room temperature. Table 3.2 to 3.4 summarize the properties of the paclitaxel loaded NPs of DPPC, DMPC, DLPC shell and PLGA core with various lipid amount, respectively. The trend of the size change with lipid quantity was shown to be that increase of lipid quantity would result in smaller NPs. Especially, when increasing the quantity of DPPC to 0.10% (w/v), particles with size smaller than 300 nm was able to be produced. This is understandable since the role of the emulsifier is to stay in the oil-water interface to lower the surface tension to facilitate the nanoparticle formulation. Too little amount of

lipid would not be enough to cover the entire surface of the NPs of small size (large surface area) to stabilize the oil droplets in the O/W emulsion, thus leading to particles of large size. Too much amount of lipid, however, would cause particle adhesion in the aqueous phase. The zeta potential values also showed to be dependent on the lipid quantity. The more lipid used in the preparation process, the larger absolute value of the negative charge would be resulted. The negative charge of the NPs could be due to both of the polymer and the lipid. As for the drug EE of the NPs, it can be seen that the lipid amount is a decisive factor for EE. Too less lipid used could be failed to produce sufficient NPs, which results in less drug encapsulated. Rather, too much lipids used could also decrease EE in that the excess lipids would form free aggregators to compete with polymer matrix to engulf drugs. The optimized amount of lipids was thus able to be confirmed after the two abovementioned investigation (listed in Table 3.5).

Table 3.2 Characteristics of the paclitaxel loaded DPPC shell and PLGA core NPs of various DPPC amount used in the nano-emulsification process: particle size, size distribution and encapsulation efficiency. Data represent mean ± SE, n=6 (For EE results, n=3).

DPPC Concentration (%, w/v)	Particle Size (nm)	Polydispersity	zeta-potential (mV)	Encapsulation Efficiency (%)
0.20	271.0 ± 4.2	0.287 ± 0.010	-41.43 ± 0.68	11.3 ± 0.11
0.10	279.1 ± 8.5	0.178 ± 0.040	-38.16 ± 1.25	39.3 ± 0.81
0.05	578.3 ± 14.4	0.220 ± 0.030	-28.11 ± 2.25	45.5 ± 1.44

Table 3.3 Characteristics of the paclitaxel loaded DMPC shell and PLGA core NPs of various DMPC amount used in the nano-emulsification process: particle size, size distribution and encapsulation efficiency. Data represent mean ± SE, n=6 (For EE results, n=3).

DMPC Concentration (%, w/v)	Particle Size (nm)	Polydispersity	zeta-potential (mV)	Encapsulation Efficiency (%)
0.10	239.6 ± 9.1	0.129 ± 0.052	-36.97 ± 2.60	76.8 ± 0.90
0.05	310.0 ± 7.3	0.269 ± 0.028	-34.85 ± 3.76	38.7 ± 0.20
0.03	401.5 ± 3.3	0.038 ± 0.033	-32.35 ± 0.90	54.2 ± 0.30

Table 3.4 Characteristics of the paclitaxel loaded DLPC shell and PLGA core NPs of various DLPC amount used in the nano-emulsification process: particle size, size distribution and encapsulation efficiency. Data represent mean ± SE, n=6 (For EE results, n=3).

DLPC Concentration (%, w/v)	Particle Size (nm)	Polydispersity	zeta-potential (mV)	Encapsulation Efficiency (%)
0.10	238.7 ± 4.1	0.239 ± 0.037	-44.75 ± 1.39	41.8 ± 0.07
0.05	242.5 ± 4.2	0.138 ± 0.043	-36.88 ± 1.30	43.8 ± 0.06
0.01	434.7 ± 28.5	0.324 ± 0.013	-30.25 ± 1.03	15.1 ± 0.01

Table 3.5 Characteristics of the optimized formulation of paclitaxel loaded lipid shell and PLGA core NPs (highlighted from the above 3 tables). Data represent mean ± SE, n=6 (For EE results, n=3).

lipid % (w/v)	Particle Size (nm)	Polydispersity	zeta-potential (mV)	Encapsulation Efficiency (%)
DPPC 0.10%	279.1 ± 8.5	0.178 ± 0.040	-38.16 ± 1.25	39.3 ± 0.81
DMPC 0.10%	239.6 ± 9.1	0.129 ± 0.052	-36.97 ± 2.60	76.8 ± 0.90
DLPC 0.05%	242.5 ± 4.2	0.138 ± 0.043	-36.88 ± 1.30	43.8 ± 0.06

Next we fixed to use DLPC to formulate the drug loaded, lipid shell and polymer core NPs with a wider range of lipid concentrations, from 0.01 to 0.1% (w/v). The results were summarized in Table 3.6.

Table 3.6 Characteristics of the paclitaxel loaded DLPC shell and PLGA core NPs of various DLPC amount used in the nano-emulsification process: particle size, size distribution, and encapsulation efficiency. Data represent mean ± SE, n=6 (For EE results, n=3).

DLPC Concentration (%, w/v)	Particle Size (nm)	Polydispersity	zeta-potential (mV)	Encapsulation Efficiency (%)
0.1	238.7 ± 4.1	0.239 ± 0.037	-44.75 ± 1.39	41.8 ± 0.07
0.05	242.5 ± 4.2	0.138 ± 0.043	-36.88 ± 1.30	43.8 ± 0.06
0.04	243.6 ± 8.6	0.139 ± 0.035	-36.12 ± 1.18	56.1 ± 0.07
0.02	264.8 ± 4.2	0.174 ± 0.018	-35.07 ± 1.19	36.9 ± 4.17
0.01	434.7 ± 28.5	0.324 ± 0.013	-30.25 ± 1.03	15.1 ± 0.01

The trend of the size and surface charge change with lipid quantity was shown in Figure 3.2, i.e. increase of lipid quantity would result in smaller NPs and lower surface charge. The emulsifier amount used in the nano-emulsification process can be used to quantitatively control the nanoparticles size, which is a dominant factor to determine the key characters of the drug loaded nanoparticles. The surface charge test demonstrated that the more DLPC used in the preparation process, the larger absolute value of the negative charge would be resulted. The negative charge of the NPs could be due to both of the polymer and the emulsifier. Although DLPC is neutral, the DLPC coated NPs could still exhibit non-zero mobilities in an external electric field that may result in higher negative charge since some anions could bind to the neutral lipids, making the surface more negatively charged (Makino et al. 1991). We thus pursued an optimization by using 0.04% (w/v) DLPC in the nano-emulsification process in terms of the combined outstanding particle size, stability and encapsulation efficiency.

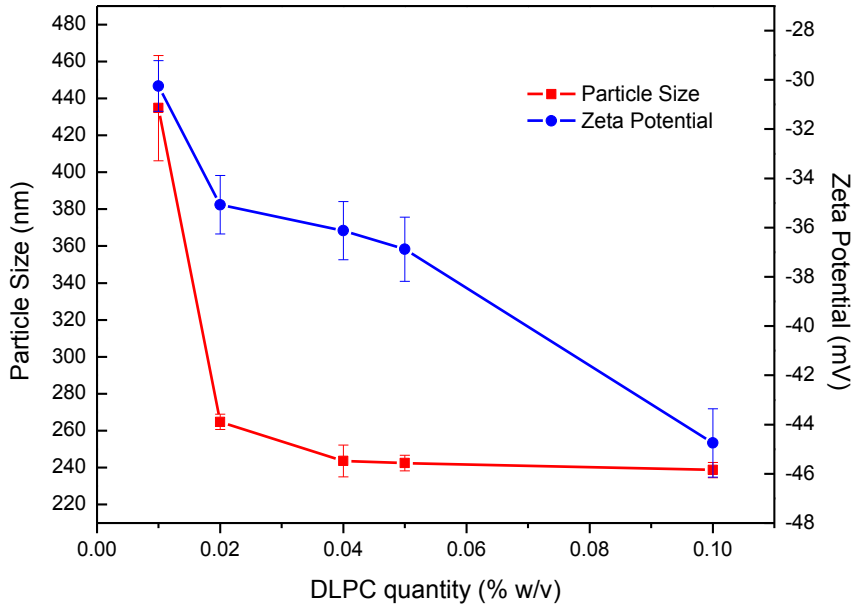

Figure 3.2 Effect of the DLPC amount on the NP size and zeta potential.

To demonstrate the advantages of using phospholipids to formulate NPs, we shows a comparison of the characteristics of DLPC-emulsified and PVA-emulsified PLGA NPs (Table 3.7) at the same initial drug loading (5%), from which it can be seen that as emulsifier, DLPC has advantages over the traditional PVA (1) DLPC has much higher emulsification efficiency than PVA. To form the same amount NPs, the DLPC needed is only 1/50 of the PVA; (2) DLPC-emulsified NPs would result in higher drug encapsulation efficiency. Moreover, DLPC is a natural product and the PVA is a synthetic one. The former can thus cause fewer side effects than the latter.

Table 3.7 Comparison of the characteristics of DLPC shell PLGA core NPs and PVA coated PLGA NPs under 5% initial drug loading: particle size, size distribution, zeta potential and encapsulation efficiency. Data represent mean ± SE, n=6 (For EE results, n=3).

shell	Concentration (% w/v)	Particle Size (nm)	Polydispersity	Zeta Potential (mV)	Encapsulation Efficiency (%)
DLPC	0.04	243.6 ± 8.6	0.139 ± 0.035	-36.12 ± 1.18	56.1 ± 0.07
PVA	2	293.9 ± 4.8	0.143 ± 0.023	-26.54 ± 1.54	43.1 ± 4.98

3.3.4 Particle morphology

Field emission scanning electron microscope was employed to image the morphology of the particles (Figure 3.3 and 3.4). It is revealed from the images that the lipid coated NPs are generally spherical in shape with narrow size distribution. The rough surface of the NPs might be due to the lipid layers coated on the PLGA cores. The particle size observed from the FESEM image is in good agreement with that determined above by LLS. There are a few larger spheres attached with each other, which might be

attributed to the low solubility of lipids in water, thereby the spare amount of which still surrounds the solid polymeric particles or simultaneously forms large vesicle-like aggregators.

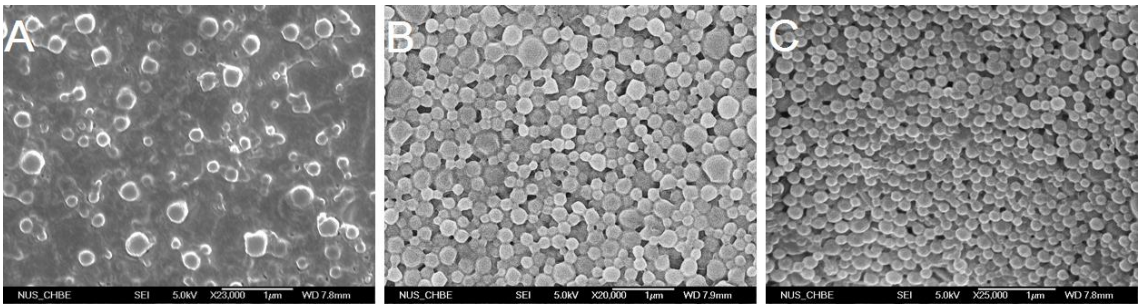

Figure 3.3 FESEM images of the paclitaxel loaded 0.10% (w/v) DPPC shell (A), 0.10% (w/v) DMPC shell (B), and 0.05% (w/v) DLPC shell (C) PLGA core NPs

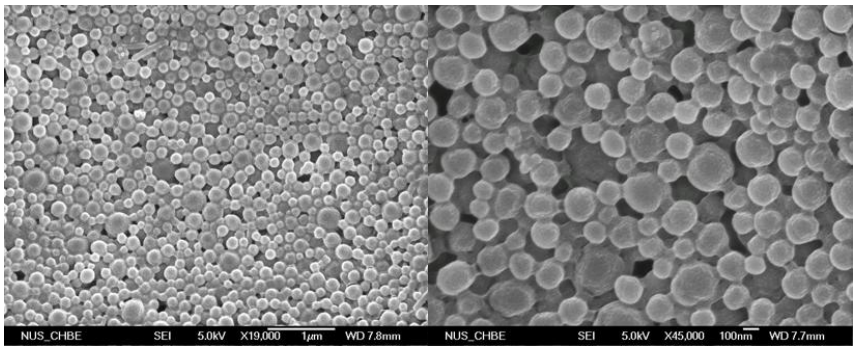

Figure 3.4 FESEM image of the paclitaxel loaded 0.04% w/v DLPC shell and PLGA core NPs (left) and the zoom-in FESEM image of the left one (right).

3.3.5 Surface chemistry

The surface chemistry of the drug loaded NPs was analyzed by XPS. For proving the successful surface coating of lipids on PLGA cores, phosphorous was specifically scanned in that this element only exists in lipid molecules. From Figure 3.5, the distinct peak of signals from 2p orbital of phosphorous (P 2p) qualitatively verifies that lipid molecules embrace PLGA cores since only lipid molecules consist of

phosphorous. Therefore, it can be confirmed that the lipid shell has been successfully coated on the PLGA core. Another method could also be applied to visualize the lipid shell on the top of polymer core thus confirm the coating which involves the counterstaining of nitrogen contained in lipid molecules by phosphotungstic acid. Our group is using this method in another study that is still ongoing.

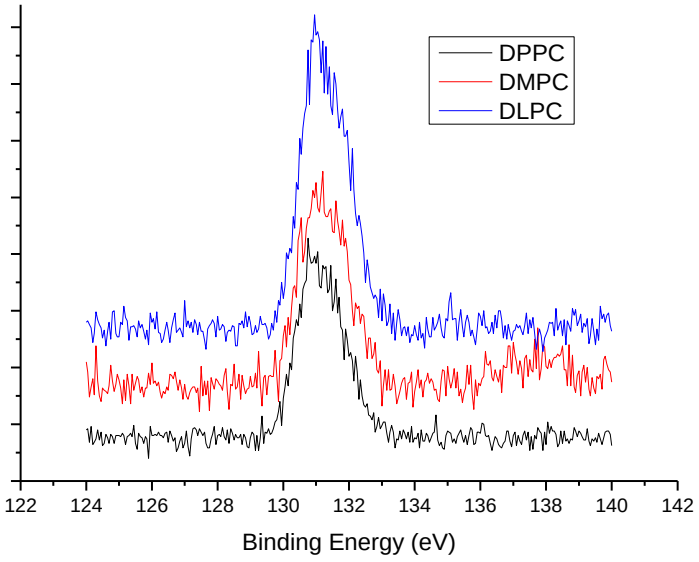

Figure 3.5 XPS spectrum of the paclitaxel loaded lipid shell PLGA core NPs with 0.10% (w/v) DPPC shell (lower curve), 0.10% (w/v) DMPC shell (middle curve), and 0.04% (w/v) DLPC shell (upper curve): P 2p spectrum

3.3.6 *In vitro* drug release

The in vitro drug release profile of the paclitaxel loaded DLPC shell PLGA NPs in 168 hours was shown in Figure 3.6, from which it can be seen that there is an initial burst of 32.48% in the first 12 hours. Such a fast drug release may be due to the drug molecules on and near the surface of the NPs. The initial burst could be helpful to suppress the growth of cancer cells in short time. In the following 72 hours, the cumulative release percent reached 75.83%, and the release presents a sustained

manner, which provides the possibility to continually fight against cancer cells, resulting in the decreased cancer cell viability as shown in the section of in vitro cytotoxicity below. The cumulative release percent almost achieved 100% after 7 days, showing a full release ability of the NP formulation. The generally sustained and controlled release profile of paclitaxel facilitates the application of the NPs for the delivery of anticancer drugs. Rather, it can also be seen that the release rate of paclitaxel from PVA-emulsified PLGA NPs was much slower. The possible reason can be attributed to the much higher molecular weight of PVA (30,000-75,000) than DLPC resulting in denser coating on the PLGA core and thus slower diffusion of the drugs into water in the same time.

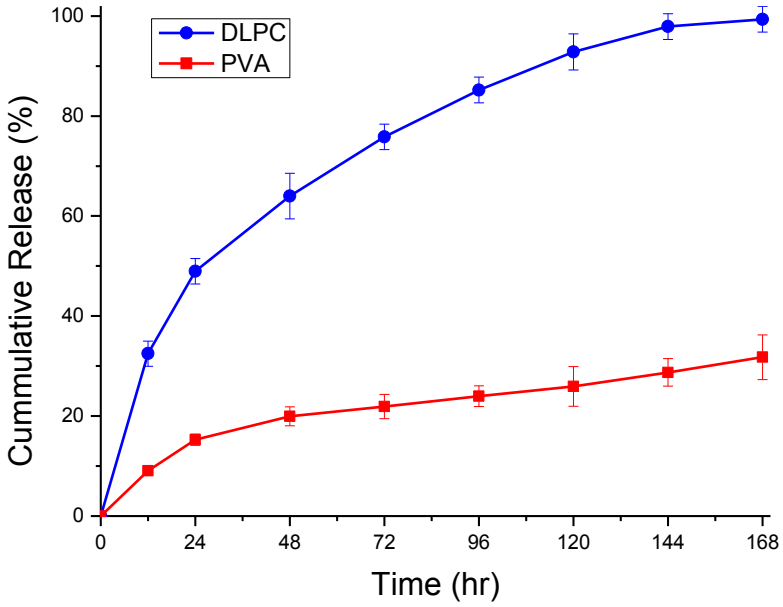

Figure 3.6 *In vitro* paclitaxel release profile from the PVA-emulsified PLGA NPs (square dot curve) and the paclitaxel loaded DLPC shell PLGA core NPs with 0.04% (w/v) DLPC (round dot curve). Data represent mean ± SE, n=3.

3.3.7 *In vitro* cellular uptake

The cellular uptake of the coumarin-6 loaded NPs was examined qualitatively to visualize the internalization in the cells. The Figure 3.7 shows the CLSM images of the MCF7 human adenocarcinoma cells after 0.5 hr (row 1 and 2) and 2 hr (row 3 and 4) incubation with the coumarin-6 loaded 0.10% (w/v) DPPC shell (row 1 and 3) and 0.04% (w/v) DLPC shell (row 2 and 4) PLGA NPs. The pictures in the left column show the green fluorescence in FTIC channel from the coumarin-6 loaded NPs which have been internalized in the MCF7 cells. The pictures in the middle column show the red fluorescence from the cell nuclei stained by PI. The pictures in the right column are the merged images of the corresponding left and middle pictures. It can be seen from this figure that the red fluorescence representing the nucleus stained by PI is circumvented by green fluorescence representing the coumarin-6 loaded NPs internalized in the cytoplasm. In addition, after incubating 2 hr, the fluorescent NPs taken up by the cells are more than those incubated for 0.5 hr, which was confirmed by the higher distribution of green fluorescence in cytoplasm of the cells with 2 hr incubation under the same exciting laser intensity. A quantitative investigation has also been conducted by measuring the fluorescence intensity of the CLSM images to demonstrate the possible advantages of the DLPC shell PLGA NPs versus the PVA-emulsified PLGA NPs. The same concentration of well dispersed coumarin-6 loaded DLPC shell or PVA-emulsified PLGA NPs (250 μg/ml) was used for all four cases of the MCF7 cells after 0.5, 1, 2, 4 hour incubation at 37 ℃, respectively. We can see from the Figure 3.8 that the fluorescence intensity (a.u.) from the DLPC shell PLGA NPs taken up by the cells was 9726 ± 424, 12478 ± 437, 21081 ± 1148, and 27340 ± 1729 in comparison with 7712 ± 365, 9958 ± 354, 12529 ± 569, and 16404 ± 1643 for the PVA-emulsified PLGA NPs, respectively (student's *t* test, $P < 0.05$). This means

that the former is 26.1%, 25.3%, 68.2%, and 66.7% more effective than the latter after 0.5, 1, 2, and 4 hr incubation with the MCF7 cells, respectively, revealing the possibility of such nanoparticulate formulations to deliver anticancer drugs into cancerous cells.

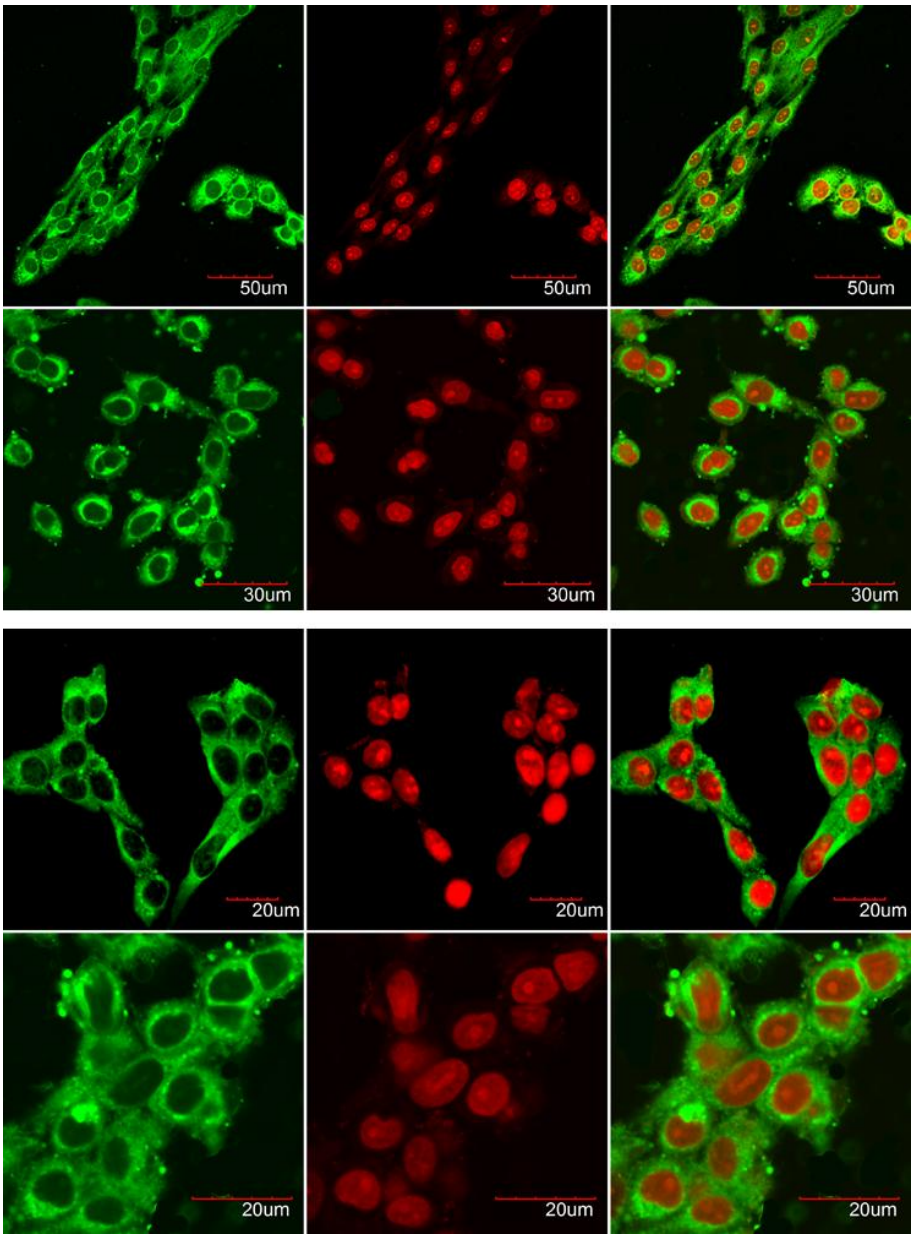

Figure 3.7 The confocal laser scanning microscopy images of MCF7 cancer cells incubated with the NPs, showing the internalization of the NPs in the cells.

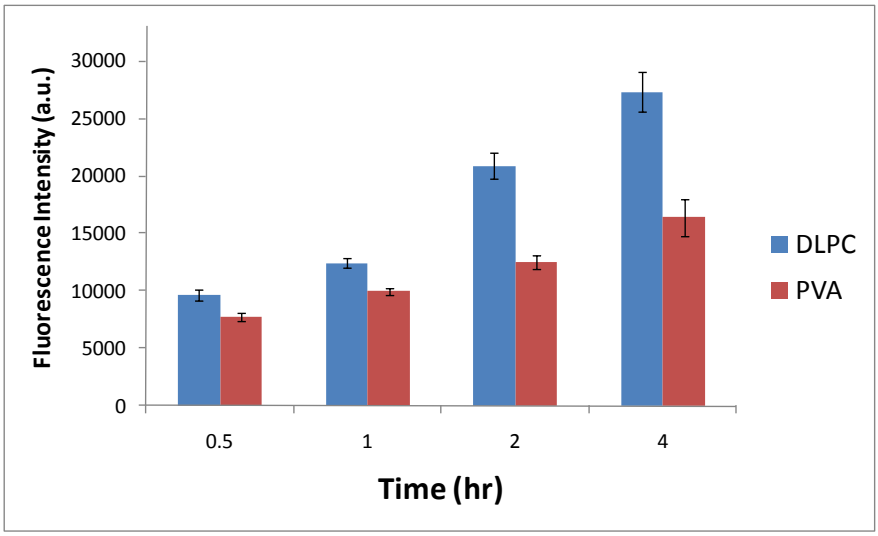

Figure 3.8 Cellular uptake efficiency of the coumarin-6 loaded DLPC- or PVA-emulsified PLGA NPs by MCF7 cells after 0.5, 1, 2, 4 hr incubation at 250 μg/ml NP concentration, respectively. Data represent mean ± SE, n=6.

3.3.8 *In vitro* cell cytotoxicity

Due to the overally distinctive characteristics of 0.04% (w/v) DLPC shell PLGA NPs, it was used to further evaluate the cytotoxicity performance. Figure 3.9 shows the *in vitro* cell viability of MCF7 cancer cells after 24, 48, 72 hour incubation with Taxol® or the paclitaxel loaded DLPC shell PLGA NPs at the equivalent paclitaxel dose of 25, 10, 2.5, 0.25 μg/ml, respectively (In all cases, $P < 0.05$ under the two-tailed student's *t* test). T25, T10, T2.5, T0.25 and NP25, NP10, NP2.5, NP0.25 denote the cases of Taxol® and the NP formulation at 25 μg/ml, 10 μg/ml, 2.5 μg/ml, and 0.25 μg/ml dose respectively. From this figure, the effects of the drug dose and the incubation time can be clearly observed. It is straightforward to notice that the lower cell viability corresponds to the higher concentration of drugs and longer treating time. As for the NP formulation, the cell viability obviously decreased with the increase of drug concentration and the exposure time. It can be concluded from this finding that the NP

formulation presented controlled and sustained release property. Rather for Taxol®, although less living cells were counted at 48 and 72 hr time points, the concentration dependence of cell viability was virtually disappeared, which could be attributed to the toxic effect of the commercial drug formulation. Moreover, 25μg/ml far exceeds the toxic level of paclitaxel (8.540 μg/ml) (Zhang et al., 2008), resulting severe side effects to normal cells. A quantitative evaluation of the *in vitro* therapeutic effect of a dosage form is IC_{50}, which is defined as the drug concentration needed to kill 50% of the incubated cells in a designated time period. It can be calculated from the above *in vitro* cell viability data that the IC_{50} for 24, 48, 72 hour treatment was 5.06, 0.0163, 0.00897 μg/ml for Taxol® and 0.86, 0.00285, 1.23×10^{-6} μg/ml, for the NP formulation, respectively. This means that the DLPC shell PLGA core NP formulation of paclitaxel could be 5.88-, 5.72-, 7.29×10^{3}- fold effective than the commercial formulation Taxol® after 24, 48, 72 hr treatment, respectively.

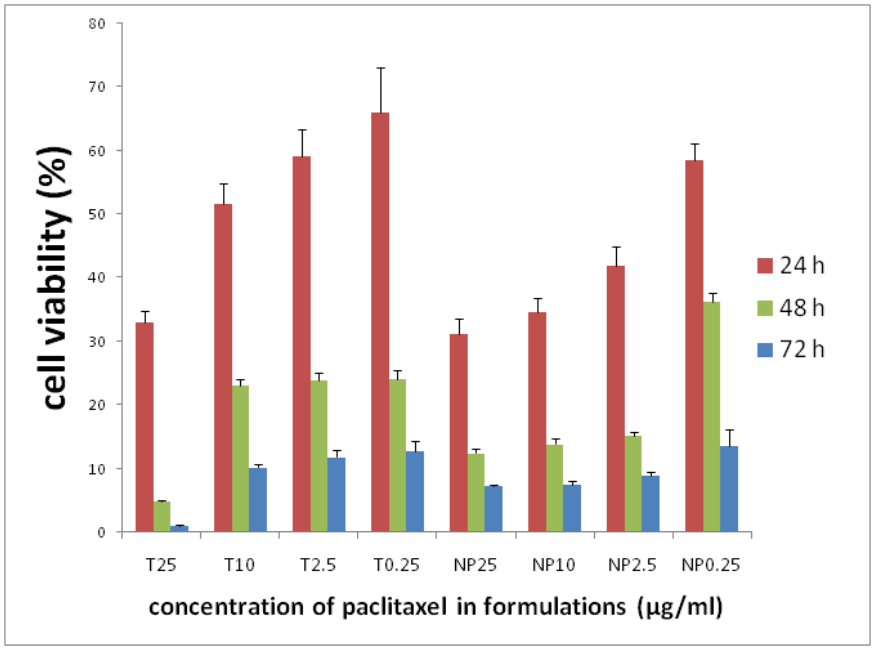

Figure 3.9 *In vitro* cell viability of MCF7 cancer cells after 24, 48, 72 hour incubation with Taxol® or the paclitaxel loaded DLPC shell PLGA core NPs at the equivalent

paclitaxel dose of 25, 10, 2.5, and 0.25 μg/ml. T25, T10, T2.5, T0.25 and NP25, NP10, NP2.5, NP0.25 denote the cases of Taxol® and the NP formulation at 25 μg/ml, 10 μg/ml, 2.5 μg/ml, and 0.25 μg/ml dose, respectively. Data represent mean ± SE, n=6.

3.4 Conclusions

We have successfully developed a system of nanoparticles of lipid shell and PLGA core for sustained and controlled release of anticancer drugs with paclitaxel as a model drug. We continued our earlier work of using phospholipids as emulsifier in the nanoparticle formulation with the focus that the type and amount of lipids used in the nano-emulsification process would play a key role to determine the physicochemical properties and *in vitro* performance of the drug loaded NPs. Five types of phospholipids were selected to produce the nanoparticles and the properties were compared. Selective formulations with various lipids were completely characterized to demonstrate the possibility of being employed as drug delivery systems. We also presented great advantages of phospholipid versus traditional PVA as emulsifier with higher emulsification efficiency, higher drug encapsulation efficiency and better *in vitro* performance. We demonstrated that after incubation with MCF7 cells at 0.250 mg/ml NP concentration, the coumarin-6 loaded PLGA NPs of DLPC shell showed effective *in vitro* cellular uptake performance. The analysis of IC_{50} based on *in vitro* cytotoxicity evaluation demonstrated that the DLPC shell PLGA core NP formulation of paclitaxel could be 5.88-, 5.72-, 7.29×10^{3}- fold effective than the commercial formulation Taxol® after 24, 48, 72 hr treatment, respectively. Consistent evaluation and analysis on the novel formulations evolve a fascinating opportunity and promising prospect to develop these new drug delivery systems.

Chapter 4 : Folic Acid Conjugated Nanoparticles of Mixed Lipid Monolayer Shell and Biodegradable Polymer Core for Targeted Delivery of Docetaxel

A system of nanoparticles of mixed lipid monolayer shell and biodegradable polymer core was developed for targeted delivery of anticancer drugs with docetaxel as a model drug, which provides targeting versatility with a quantitative control of the targeting effect by adjusting the lipid component ratio of the mixed lipid monolayer, and combine the advantages and avoid disadvantages of polymeric nanoparticles and liposomes in drug delivery. X-ray photoelectron spectroscopy confirmed the coating of the mixed lipid monolayer on the polymeric core. Fluorescent microscopy proved the targeting efficacy of the folic acid conjugated on the mixed lipid monolayer for the cancer cells of over expression of folate receptors. The folic acid conjugated nanoparticles of mixed lipid monolayer shell and biodegradable polymer core were proved to possess sustainable, controlled and targeted delivery of anticancer drugs with docetaxel as a model drug, which may provide a novel drug delivery system of precise control of the targeting effect.

4.1 Introduction

Nanotechnology has been extensively exploited to improve conventional cancer therapy in the recent years (Ferrari, 2005; Sinha et al., 2006; Farokhzad and Langer, 2006; Farokhzad and Langer, 2009; Zhang et al., 2008a). The designed nanocarriers for achieving precise drug delivery to cancer cells are expected to be non-toxic,

efficiently load the drugs, enhance the circulation time in bloodstream, and actively target the cancer cells (Cho et al., 2008). The nanocarries currently under intensive investigation can be divided into two categories in general, i.e. the lipid-based and the polymer-based with liposomes and polymeric nanoparticle as their typical representative, respectively. Liposomes have been widely used due to their high biocompatibility, favorable pharmacokinetic profile, high delivery efficiency and ease of surface modification. Limitations of liposomal drug delivery, however, include insufficient drug loading, fast drug release, and instability in storage (Rai et al., 2008). Nanoparticles of biodegradable polymers, featured by their small size, acceptable biocompatibility, high drug encapsulation efficiency especially for hydrophobic drugs, controlled drug release manner, high cellular internalization, desired pharmacokinetics and long circulation half-life, are another prospective platform for drug delivery (Zhang et al., 2008a; Cho et al., 2008; Tong and Cheng, 2007). It is thus ideal if any technology could be developed to combine the advantages and overcome the disadvantages of the two types of drug nanocarriers. One possibility is to synthesize lipid-shell and polymer-core nanoparticles (LPNPs) as a novel drug delivery system. The pioneering work of such a design can be back to 2001, when phospholipids were used as effective emulsifier, which stays between the oil-water interface to lower the interfacial tension and thus facilitate the formulation of colloidal nanoparticles (Feng and Huang, 2001). The LPNPs can be formulated via a single step, which combines the nanoprecipiation method and the self-assembly technique to produce the desired structured NPs of lipid shell and polymer core (Zhang et al., 2008b; Chan et al., 2009). The strategy meets the requirement to develop well-defined LPNPs with predictable

physicochemical and pharmaceutical properties as well as facilitates future scale-up, which thus deserves further development.

Active targeting can then be further realized by conjugating molecular probes onto the LPNPs surface, which provides a promising approach for the drug delivery system to reach and penetrate into the malignant cells with overexpression of the corresponding receptors on their surface, and then release the encapsulated therapeutics in a controlled and sustained manner (Cho et al., 2008; Wang et al., 2008). Phospholipid molecules can provide their end functional groups to facilitate conjugation of the molecular probes, i.e. the targeting ligands on the LPNPs surface. For instance, the carboxylic group linked to the ligand can be employed to conjugate the active primary amine group of phosphoethanolamine or amino PEG attached with phosphoethanolamine (Torchilin, 2005; Allen et al., 1996; Yang et al., 2007). The targeted drug delivery by nanoparticles can thus be made feasible and the conjugation technology can be not as complicated.

In this work, we synthesized a novel kind of nanoparticles of mixed lipid monolayer shell and biodegradable polymer core to provide targeting versatility with a quantitative control of the targeting effect by controlling the lipid component ratio of the mixed lipid monolayer shell. Docetaxel is used as a model hydrophobic anticancer drug, which is a potent anticancer drug effective to a wide spectrum of cancers (Engels et al., 2007). Folic acid is selected as the model molecular probe for targeted delivery of the drug to the cancer cells of folate overexpression such as certain breast cancer and ovarian cancer cells. PLGA, one of the most popular FDA approved polymers, is used to form the polymer core matrix, which is wrapped by the mixed lipid monolayer shells of three distinct functional components: (i) 1,2-dilauroylphosphatidylocholine

(DLPC), a phospholipid of an appropriate HLB value which is employed to stabilize the NPs in the aqueous phase; (ii) 1,2-distearoyl-*sn*-glycero-3-phosphoethanolamine-N-[methoxy(polyethylene glycol)-2000] (DSPE-PEG_{2k}), a PEGlyated DSPE to facilitate stealth NPs formulation to escaped from recognition by the RES and thus increase the systemic circulation time of the LPNPs (Yamamoto et al., 2001); and (iii) 1,2-distearoyl-*sn*-glycero-3-phosphoethanolamine-N-[folate(polyethylene glycol)-5000] (DSPE-PEG_{5k}-FOL), a PEGylated DSPE of longer PEG chains for the LPNPs to be functionalized by folic acid conjugation for targeted delivery purpose. From now on we use LPNPs to denote the docetaxel loaded nanoparticles of the mixed DLPC and DSPE-PEG_{2k} shell and PLGA core, which have no targeting function, and TLPNPs to denote the docetaxel loaded nanoparticles of the mixed DLPC, DSPE-PEG_{2k} and DSPE-PEG_{5k}-FOL shell and PLGA core, which have targeting function to the cancer cells of folate receptors overexpression. Such kind of ligand conjugated nanoparticles of mixed lipid monolayer shell and biodegradable polymer core are expected to combine the desirable characteristics of liposomes and polymeric NPs while exclude some of their intrinsic limitations as well as to precisely control the targeting effect by adjusting the component lipid ratio, and thus to evolve a fascinating opportunity to develop new drug delivery systems.

4.2 Materials and methods

4.2.1 Materials

Docetaxel (anhydrous, 99.56%) was purchased from Shanghai Jinhe Bio-Technology Co. Ltd, China. Taxotere® was provided by National Cancer Center (Singapore).

PLGA (75:25, Mw: 90,000-126,000), 1,2-didodecanoyl-*sn*-glycero-3-phosphocholine (synonyms: 1,2-dilauroyl-*sn*-glycero-3-phosphocholine or DLPC, $C_{32}H_{64}NO_8P$), folic acid, sucrose, methanol, ethanol, DCM, ACN, DMSO, coumarin-6, PBS (pH 7.4), MTT, trypsin-EDTA solution and PI were all purchased from Sigma-Aldrich (St. Louise, MO, USA). DSPE-PEG_{2k} was provided by Lipoid GmbH (Ludwigshafen, Germany). Poly [ethylene glycol]-5000 bis-amine (PEG_{5k} bis-amine) was offered by Laysan Bio (Arab, AL, USA). DSPE-PEG_{5k}-FOL was synthesized by carbodiimide chemistry as previously reported (Lee and Low, 1995; Wu et al., 2006). Tween-80 was from ICN Biomedicals, Inc. (OH, USA). Triton X-100 was provided by USB Corporation (OH, USA). FBS was purchased from Gibco Life Technologies (AG, Switzerland). Penicillin-streptomycin solution was from Invitrogen. DMEM was from Sigma. All solvents used in this study were HPLC grade. MCF7 breast cancer cells and NIH/3T3 fibroblast cells were provided by American Type Culture Collection. The water used was pretreated with the Milli-Q® Plus System (Millipore Corporation, Bedford, USA).

4.2.2 Preparation of the NPs

Weighed amount of PLGA and docetaxel were dissolved in DCM to form the oil phase. For TLPNPs, weighed amount of DLPC, DSPE-PEG_{2k}, and DSPE-PEG_{5k}-FOL (molar ratio = 85:10:5) were dispersed in ultrapure water by sonication to form the aqueous phase. For LPNPs, the aqueous phase consists of DLPC and DSPE-PEG_{2k} as molar ratio of 85:15. The oil phase was then poured into the water phase and the mixture was sonicated by probe ultrasonicator under ice bath. DCM was evaporated from the emulsion by magnetic stirring. The suspension was centrifuged at 12,000 rpm for 15 minutes at 4 °C to collect the nanoparticles. After washing three times, the

nanoparticles were resuspended in the water of designated volume with 3% w/w sucrose as cryoprotectant and freeze-dried to obtain the fine powder. The fluorescent LPNPs and TLPNPs were fabricated in a same way with drug replaced by coumarin-6.

4.2.3 Characterization of the NPs

Data were expressed as the means with 95% confidence intervals. Statistical tests were performed with the Student's *t* test. For all tests, *P* values less than 0.05 were considered to be statistically significant. All statistical tests were two-tailed.

The particle size and size distribution of the drug loaded NPs were measured by dynamic light scattering (90Plus, Brookhaven Instruments Co. USA). The dispersion of NPs was diluted by ultrapure water according to the mass concentration and completely sonicated before measurement.

The amount of docetaxel encapsulated in the NPs was measured by high performance liquid chromatography (Agilent LC1100). A reversed phase Inertsil® ODS-3 column (250×4.6 mm, particle size 5 μm, GL Science Inc., Tokyo, Japan) was used. 3 mg freeze-dried NPs were dissolved in 1 ml DCM. After evaporating DCM, 3 ml mobile phase (50:50 v/v acetonitrile/water solution) was added to dissolve the drugs. The solution was then filtered by 0.45 μm PVDF syringe filter for HPLC analysis. The column effluent was detected at 230 nm with a UV/VIS detector. The EE is calculated as (actual amount of drug encapsulated in NPs) / (initial amount of drug used in the fabrication of NPs) × 100%.

The surface charge of the the drug loaded NPs was determined by ZetaPlus zeta potential analyzer (Brookhaven Instruments Co. USA) at room temperature in water.

The suspension of NPs was diluted by ultrapure water. The pH value and concentration of the NPs dispersion were fixed before measurement.

The shape and surface morphology of the NPs were investigated by field emission scanning electron microscope (JSM-6700F, JEOL, Japan). The layer of the NP powder was obtained on copper tape for FESEM under reduced pressure from the particle dispersion. The dried particles were then coated by platinum carried out by the Auto Fine Coater (JEOL, Tokyo, Japan).

The surface chemistry of the NPs was studied by X-ray photoelectron spectroscopy (AXIS His-165 Ultra, Kratos Analytical, Shimadzu Corporation, Japan) to confirm the existence of lipid coating on the surface of the NPs. The elements on the NP surface were identified according to the specific binding energy (eV), which was recorded from 0 to 1200 eV with pass energy of 80 eV under the fixed transmission mode. The data were processed by specific XPS softwares.

4.2.4 *In vitro* evaluation

For the controlled release study, the drug loaded NPs were dispersed in PBS (0.1 M, pH 7.4) containing 0.1% w/v Tween-80, which can improve the solubility of docetaxel in PBS. The dispersion was then put in an orbital shaker shaking at 120 rpm with water bath at 37 ℃. At designated time intervals, the suspension was centrifuged at 12,000 rpm for 30 min. The pellet was resuspended in fresh medium to continue the release. The drug released in the supernatant was extracted by DCM and transferred in the same mobile phase. After the evaporation of DCM, docetaxel quantity was determined by the same HPLC procedure as mentioned above. The error bars were obtained from triplicate samples.

MCF7 breast cancer cells, which are of folate overexpression, and NIH/3T3 fibroblast cells, which lack folate overexpression, were employed in this work. The DMEM supplemented with 10% FBS and 1% penicillin-streptomycin was utilized as the cell culture medium. Cells were cultivated in humidified environment at 37℃ with 5% CO_2. Before experiment, the cells were pre-cultured until confluence was reached to 75%.

For quantitative cellular uptake analysis, MCF7 cells were seeded into 96-well black plates (Costar, IL, USA) at 5×10^3 cells/well (0.1 ml) and after the cells reached 80% confluence, the medium was changed to the suspension of coumarin-6 loaded NPs at a NP concentration of 0.250 mg/ml for 0.5 and 2.0 h, respectively. After incubation, the NP suspension in the testing wells was removed and the wells were washed with 0.1 ml PBS three times to remove the NPs outside the cells. After that, 50 μl of 0.5% Triton X-100 in 0.2 N NaOH solution was added to lyse the cells. Microplate reader (Genios, Tecan, Switzerland) was used to measure the fluorescence intensity from coumarin 6 loaded NPs in the desired wells with excitation wavelength at 430 nm and emission wavelength at 485 nm. The cellular uptake efficiency was expressed as the percentage of the fluorescence of the testing wells over that of the positive control wells.

For fluorescent microscope study, MCF7 and NIH/3T3 cells were cultivated in the 8-well coverglass chamber (LAB-TEK®, Nagle Nunc, IL) till 70% confluence. The fluorescent NPs dispersed in the cell culture medium at concentration of 0.250 mg/ml were added into the wells. Cells were washed three times after incubation for 0.5 and 2 h and then fixed by 70% ethanol for 20 mins. The cells were further washed thrice by PBS and the nuclei were then counterstained by PI for 45 mins. The fixed cell

monolayer was finally washed thrice by PBS and observed by confocal laser scanning microscope (Olympus Fluoview FV1000).

For cytotoxicity measurement, MCF7 cells were incubated in 96-well transparent plates (Costar, IL, USA) at 5×10^3 cells/well (0.1 ml) and after 12 h, the old medium was removed and the cells were incubated for 24, 48 h and 72 h in the media containing Taxotere® or docetaxel loaded NPs at the equivalent drug concentration of 25, 10, 2.5, 0.25 μg/ml. The NPs were sterilized with UV irradiation for 1 day prior to use. MTT assay was used to measure the cell viability at given time intervals. The absorbance of the wells was measured by the microplate reader with wavelength at 570 nm and reference wavelength at 620 nm. Cell viability is defined as the percentage of the absorbance of the wells containing the cells incubated with the drug contained dosage over that of the cells only.

4.3 Results and discussion

4.3.1 Fabrication of the NPs

The schematic structure of such kind of LPNPs is represented in Figure 4.1. The LPNPs were produced by the oil-in-water single emulsion and solvent evaporation method with the mixed lipids as emulsifiers (Feng et al., 2007). After emulsification of the oil phase in the aqueous phase by applying ultrasonication, the amphiphilic lipids were adsorbed on the surface of oil droplets containing PLGA and docetaxel by hydrophobic interaction. Followed by the evaporation of DCM under continuous magnetic stirring, the drug loaded NPs can be collected. DLPC was introduced as the major stabilizer to facilitate formation of the solid PLGA cores. The HLB of DLPC is

calculated as around 13 by the equation: HLB value=∑ (Hydrophilic groups) + ∑ (Lipophilic groups) + 7, which is appropriate to stabilize oil-in-water emulsions, thus promoting to form solid polymeric cores. DSPE-PEG_{2k}, the PEGlyated DSPE, was selected to facilitate stealth NPs formulation to be escaped from the recognition by the RES and thus increase the systemic circulation time of the LPNPs. DSPE-PEG_{5k}-FOL, a PEGylated DSPE of longer PEG chains functionalized by folic acid conjugation was employed for providing the LPNPs for targeted delivery capability. PEG_{5k}, the space linker with longer chain length was selected since it could ensure better recognition of the targeting moiety on the NPs surface by the receptors (Shiokawa et al., 2005).

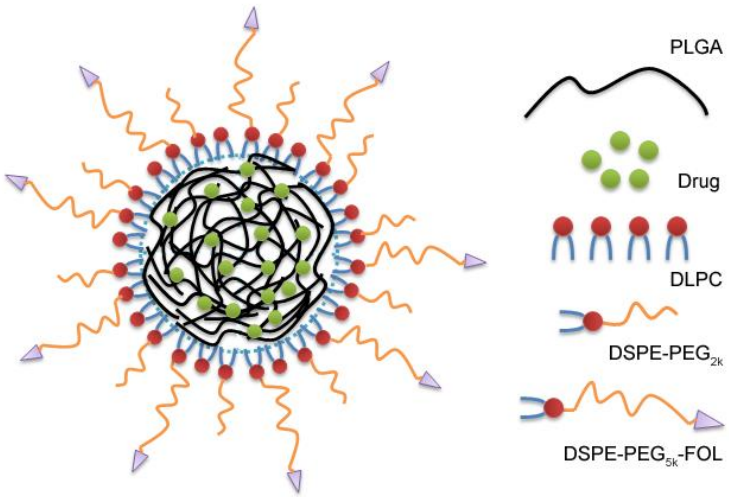

Figure 4.1 Schematic illustration of the formulation of TLPNPs. The NPs comprise a PLGA core, an amphiphilic lipid monolayer shell on the surface of the core, a stealth lipid shell, and a targeted lipid corona.

4.3.2 Characterization of the NPs

Table 4.1 illustrates the characteristics of the drug loaded LPNPs and TLPNPs. The general sizes of the two formulations measured by DLS are in the range of 200 to 300

nm with polydispersity of 0.130 to 0.160, which is not wide size distribution. It can be shown that the DLPC is helpful in stabilizing polymeric NPs in the aqueous phase. Including the DSPE-PEG_{5k}-FOL in the lipid monolayer shell increased the hydrodynamic diameter of the LPNPs in that the longer chain length of PEG_{5k} had more significant effect on the nanoparticle size than that of the PEG_{2k} in DSPE-$PEG_{2k.}$

The drug encapsulation efficiency of the NPs is crucial to justify their clinical applications. Table 4.1 shows the EE of the two types of NP formulations. It can be attributed that the EE not as high as 100% to the interaction between the lipids and docetaxel (Feng and Huang, 2001). The excess lipids might either form lipid vesicles that entrap certain amount of drugs or absorb drugs via hydrogen bonding or hydrophobic-hydrophobic interaction. Subsequently, the vesicles or the complex of excess lipid molecules and drug molecules will be washed away in the washing process. However, after all, the reasonable EE values prove the effectiveness of the NPs of lipid monolayer shell and polymer core to load anticancer drugs. Obviously, such a novel formulation demonstrates the prospect for a practically useful drug delivery carrier with appropriate size, stability and drug loading capacity.

Surface charge is an important indication for the stability of a colloidal system in medium. The repulsion among the nanoparticles with the same type of surface charge provides extra stability. The zeta-potential of the drug loaded LPNPs and TLPNPs also shown in Table 4.1 indicates the negative charges on the nanoparticle surface. It is due to the overall negative charges of the lipids and PLGA. The lower absolute value of the zeta potential of TLPNPs than that of the LPNPs results by the shield of longer PEG chains on DSPE-PEG_{5k}-FOL.

Table 4.1 Characteristics of docetaxel loaded LPNPs and TLPNPs: particle size, size distribution, zeta-potential and drug encapsulation efficiency. Data represent mean ± SD, n=6 (For EE results, n=3).

	Particle Size (nm)	Polydispersity (size distribution)	Zeta-potential (mV)	Encapsulation Efficiency (%)
LPNPs	203.8 ± 7.5	0.130 ± 0.030	-26.12 ± 1.16	60.46 ± 0.25
TLPNPs	263.6 ± 8.7	0.160 ± 0.032	-20.74 ± 1.21	66.88 ± 0.67

4.3.3 Surface morphology

FESEM was used to image the morphology of the LPNPs and TLPNPs (Figure 4.2). It is revealed in FESEM image that the NPs are generally spherical in shape with narrow size distribution. The particle sizes observed from the FESEM image are in good agreement with that determined by the DLS. However, few larger spheres attached with each other might be attributed to the low solubility of DLPC in water, thereby the little excess amount of which still surrounds the solid polymeric particles or simultaneously forms large vesicle-like aggregators.

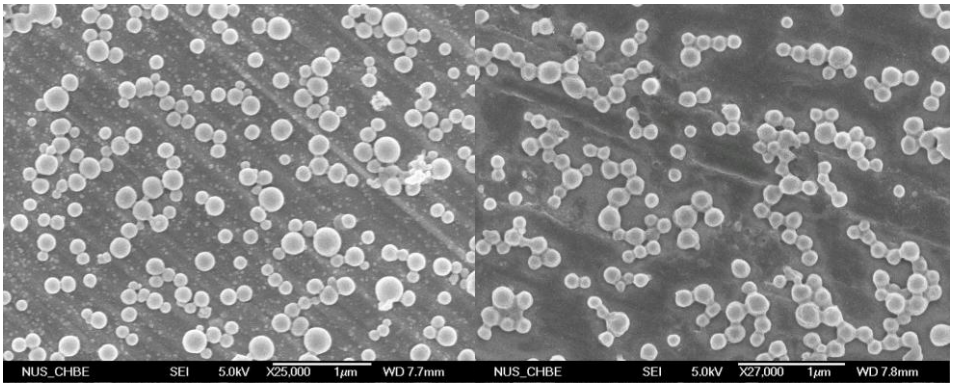

Figure 4.2 FESEM image of the docetaxel loaded LPNPs (left) and TLPNPs (right).

4.3.4 Surface chemistry

The existence of elements on the surface of samples was presented by specific binding energy (eV) on XPS spectrum. The elements on the NP surface were identified according to the specific binding energy (eV), which was recorded from 0 to 1200 eV with pass energy of 80 eV under the fixed transmission mode. The data were processed by specific XPS softwares. For proving the successful surface coating of lipids on PLGA cores, phosphorous was specifically scanned in that phosphorous only exists in lipid molecules. From Figure 4.3, the distinct peak of signals from 2p orbital of phosphorous (P 2p) qualitatively verifies that lipid molecules embrace PLGA cores since only lipid molecules consist of phosphorous. Meanwhile, the conjugation of folic acid on the NPs surface was proved via N 1s signals. Two peaks (left: folic acid, right: lipids) were detected from the TLPNPs, while only one peak was detected from the LPNPs. Therefore, it can be confirmed that lipid molecules coat polymer matrix as well as certain amount of folic acid conjugated lipids stay on the surface of TLPNPs, which could be assumed that the targeting ligands can be detected by corresponding receptors on cell membranes.

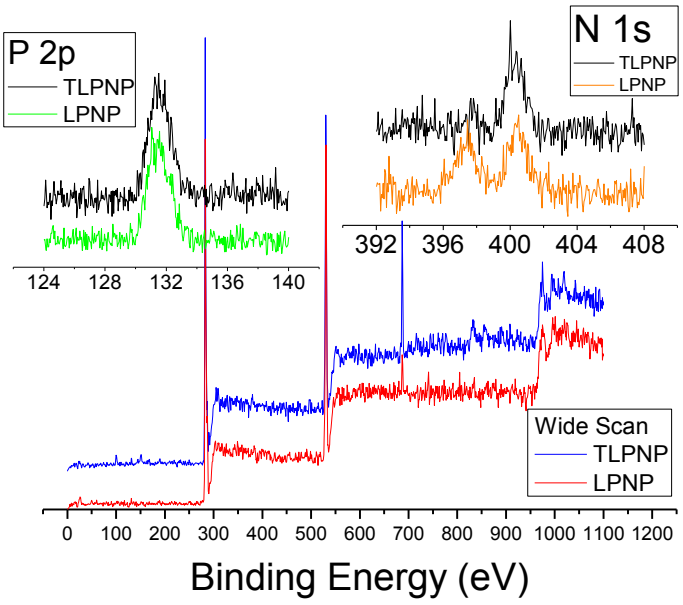

Figure 4.3 XPS peaks of the NPs. Wide scan spectra (bottom), P 2p signal spectra (left inset) and N 1s signal spectra (right inset) were shown in the figure.

4.3.5 *In vitro* drug release

The *in vitro* drug release profiles of the docetaxel loaded LPNPs and TLPNPS in 168 hours are shown in Figure 4.4. From the data, for TLPNPs, an initial burst of 18.38% in the first 12 hours can be observed. This relatively speedy release formed by certain amount of docetaxel stayed on the surface of the NPs is helpful to suppress the growth of cancer cells in short time. In the following 72 hours, the cumulative release percent reached 60.94%, and the release presents a sustainably increased manner, which provides the possibility to continually fight against cancer cells, resulting in the decreased cancer cell viability (shown in the section of *in vitro* cytotoxicity below). The cumulative release percent almost achieved almost 90% after 7 days, showing a virtually full released ability of the NP formulation. It is known that in the short period of time, the release of hydrophobic drugs from PLGA NPs is dominantly due to

diffusion. Hence the reason of fast release of docetaxel is possibly due to the strong interaction between lipid molecules and drug molecules, therefore drugs are more likely to diffuse from PLGA matrix to lipid monolayers. Meanwhile, water molecules are attracted by the hydrophilic parts of lipid molecules and permeate into the lipid monolayers, thus leading to the fast diffusion of drugs. Comparatively, the drug release from the LPNPs shows similar behavior to that of TLPNPs apart from the little faster rate. It is highly due to the shorter chain length of PEG_{2k}, resulting in the weaker shielding of lipid monolayers on polymer cores and easier permeation of water into lipid monolayers. All in all, the generally sustained and controlled release profile of docetaxel facilitates the application of the NPs of lipid shell and polymer core for the delivery of anticancer drugs.

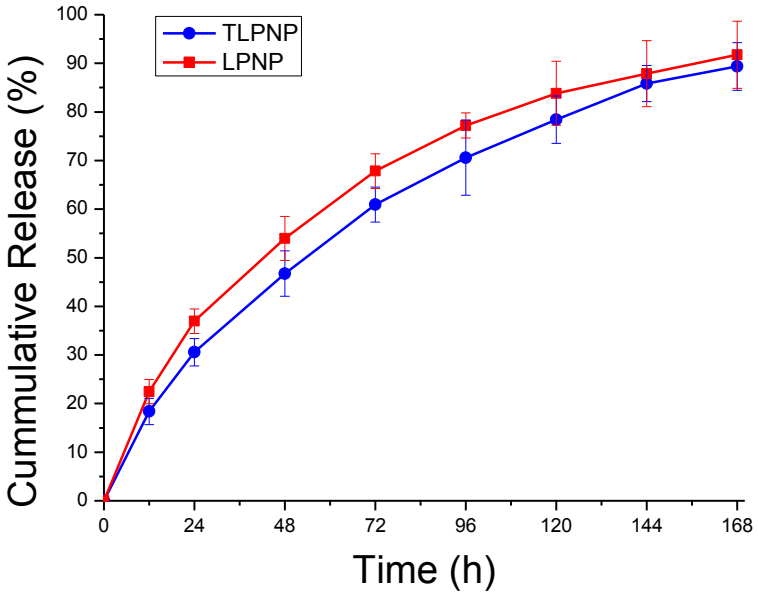

Figure 4.4 *In vitro* docetaxel release profile from the LPNPs (upper curve) and TLPNPs (lower curve). Data represent mean ± SE, n=3.

4.3.6 *In vitro* cellular uptake

The cellular uptake of the LPNPs and the TLPNPs was examined to demonstrate the penetration of the nanoparticles into the cells and the targeting effects of the nanoparticles conjugated with folic acid. The internalization of coumarin-6 loaded NPs incubated for 2 hours was visualized by CLSM. In Figure 4.5, the fluorescence from the NPs internalized in MCF7 human adenocarcinoma cells and NIH/3T3 murine fibroblast cells were shown in Row 1, 2 and 3, 4, respectively. Row 1 and 3 show the images of the cells incubated with the LPNPs of no targeting effect, and Row 2 and 4 show the TLPNPs with targeting effect. The images obtained from the FITC channel which shows the green fluorescence of the coumarin-6 loaded LPNPs are shown in column A; the column B lists the images obtained from the PI channel which show the nuclei in red fluorescence stained by the propidium iodide; and column C lists the images obtained from the merge channels of FITC and PI, from which it can be seen that , the red fluorescence representing the nucleus stained by PI is circumvented by green fluorescence representing the coumarin-6 loaded NPs internalized in the cytoplasm. Hence, the qualitative cellular uptake can be visually verified by the CLSM images. In addition, the folate receptor (FR) targeted behavior of the TLPNPs can also be examined. Folic acid, an oxidized form of folate, is an attractive target ligand due to its high binding affinity for the folate receptors ($K_d \sim 10^{-10}$ M). Folic acid is able to be efficiently internalized into the cells through the receptor-mediated endocytosis even when conjugated with a wide variety of molecules (Leamon and Low, 1991; Yoo and Park, 2004). Folic acid and its conjugate were widely used for selective delivery of anticancer agents to cells with folate receptors. In the condition of the same exciting laser intensity from the same confocal microscope, viewing row 1 and 2, after incubating 2 hours, the fluorescence of TLPNPs in the cytoplasm (row 2) is much

brighter than that of the LPNPs (row 1). It can be explained that RME facilitates and promotes the entry of NPs into cells when folate targeted NPs meet the overexpressed folate receptors (FR (+)) on MCF7 cells (Lee et al., 2003; Decuzzi and Ferrari, 2007). While for NIH/3T3 cells without overexpressed folate receptors (FR (-)) (Pan and Feng, 2009), the fluorescence in cytoplasm does not display distinct difference between the LPNPs and the TLPNPs.

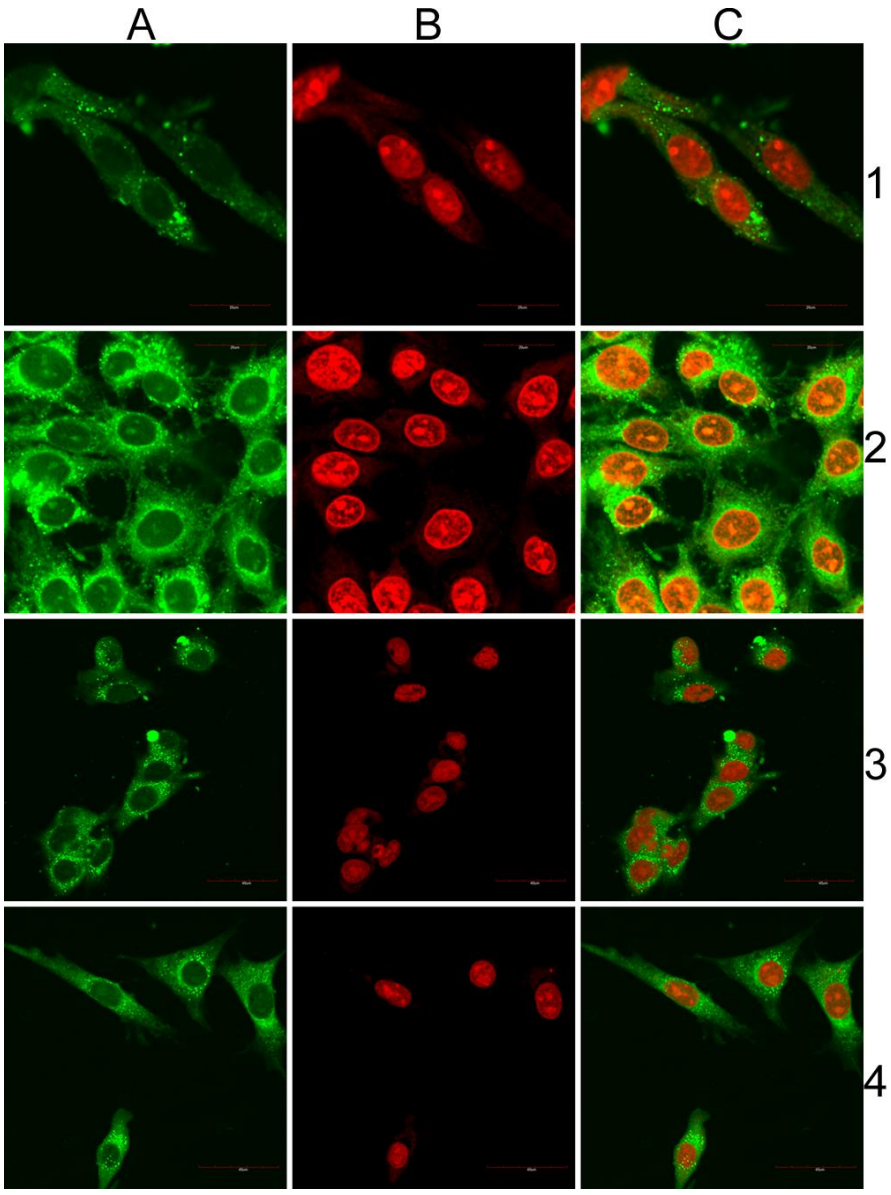

Figure 4.5 CLSM images show the internalization of fluorescent NPs in cells (2 hours incubation). Column A: FITC channels showing the green fluorescence from

coumarin-6 loaded NPs distributed in cytoplasm. Column B: PI channels showing the red fluorescence from propidium iodide stained nuclei. Column C: Merged channels of FITC and PI channels. Row 1 and 2: MCF7 cells were used. Row 3 and 4: NIH/3T3 cells were used. In row 1 and 3, LPNPs were used while in row 2 and 4, TLPNPs were used.

A quantitative analysis of cellular uptake efficiency was conducted by measuring percentage of the NPs used in incubation which have been entrapped in the cells. The same concentration of well dispersed NPs (250 μg/ml) as used in the previous CLSM was applied in this investigation. After 0.5 h and 2 h incubation, the cellular uptake efficiency of the LPNPs was measured to be 18.99 ± 0.75 % and 25.39 ± 0.54%, respectively. Instead, after 0.5h and 2h incubation, the cellular uptake efficiency of the TLPNPs was measured to be 26.24 ± 0.68 % and 39.09 ± 0.64 %, respectively. The targeting effect of folic acid conjugation is thus significant of 38.2% increment for 0.5 h incubation and 54.0% increases for 2 h incubation, respectively (Figure 4.6, two-tailed student's *t* test, $P < 0.05$). The mechanism of the *in vitro* cellular uptake of the LPNPs can be assumed to be the carrier-mediated endocytosis and cell fusion (Ito et al., 1991). Due to the existence of lipids on the NPs' surface, which are similar to the cell membrane conmponent, the uptake of the NPs is facilitated by the mutual interaction between the NPs and the cell membrane. For the TLPNPs, the RME can further facilitates the cellular uptake, resulting in higher uptake efficiency.

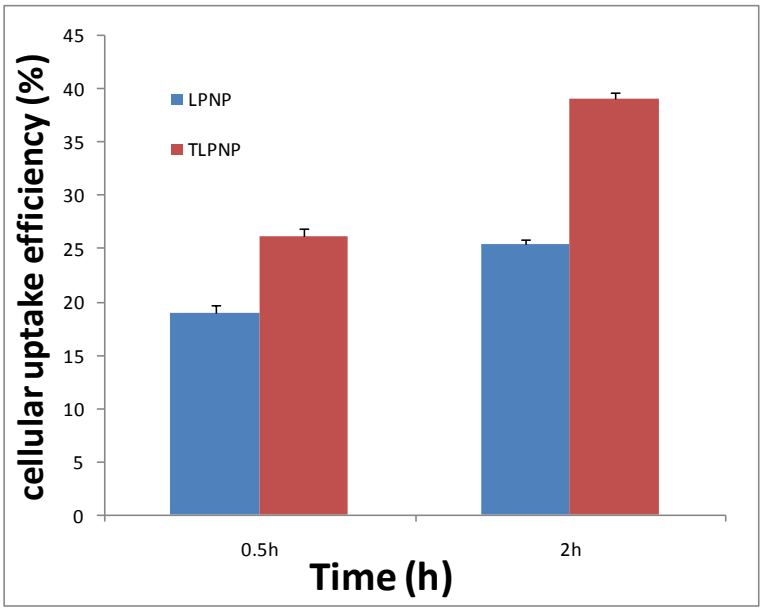

Figure 4.6 The diagram of *in vitro* cellular uptake efficiency at 0.5 h and 2 h incubation. TLPNPs show greater efficiency than LPNPs under the same incubation time. Data represent mean ± SE (shown as plus SE only), n=6.

4.3.7 *In vitro* cytotoxicity

The efficacy of the formulations to defeat cancer cells is reflected by their cytotoxicity. It is shown in Figure 4.7A-C that for the cancer cells incubated with Taxotere® at 25, 10, 2.5, and 0.25 μg/ml drug concentration, the cell viability shows the drug concentration and incubation time dependent trend. For the cytotoxicity of the NP formulations, the same concentration 25, 10, 2.5, and 0.25 μg/ml of the drug, which is encapsulated in the NPs, were applied. The lowest cell viability, i.e. the highest cell mortality, appeared at the highest concentration of the various formulations after treatment for the longest time, which proves the controlled and sustained efficacy of the NP formulation (In all cases, $P < 0.05$ under the two-tailed student's t test). Furthermore, the NP formulations prevent the toxic effect of the drug applied at high concentration of drugs (25 μg/ml) and thus can increase the maximum tolerable dose.

Such a high concentration of drug instantly exposed in blood is presumed to be toxic not only for the cancer cells but also for the normal cells since it has exceeded the suggested maximum tolerable level of docetaxel (2,700 ng/ml) (Feng et al., 2009). It is also clear that the TLPNPs formulation demonstrated higher cytotoxicity than the LPNPs formulation at the same drug concentration and exposure time resulting by the targeting effect, which means that for the same therapeutic effect, the drug needed for the TLPNPs formulation could be much less than that for the LPNPs formation and Taxotere®. The development of the TLPNPs formulation thus can enhance the therapeutic effect as well as to decrease the side effects of docetaxel.

A quantitative evaluation of the *in vitro* therapeutic effect of a dosage form is IC_{50}, which is defined as the drug concentration needed to kill 50% of the incubated cells in a designated time period. It can be calculated from the above *in vitro* cellular viability data that the IC_{50} after 24 h treatment is 0.0509 μg/ml for Taxotere®, 0.00658 μg/ml for the LPNPs formulation and 0.00323 μg/ml for the TLPNPs formulation, which means the TLPNPs formulation to be 50.91% more effective than the LPNPs formulation and 93.65% more effective than Taxotere®, respectively.

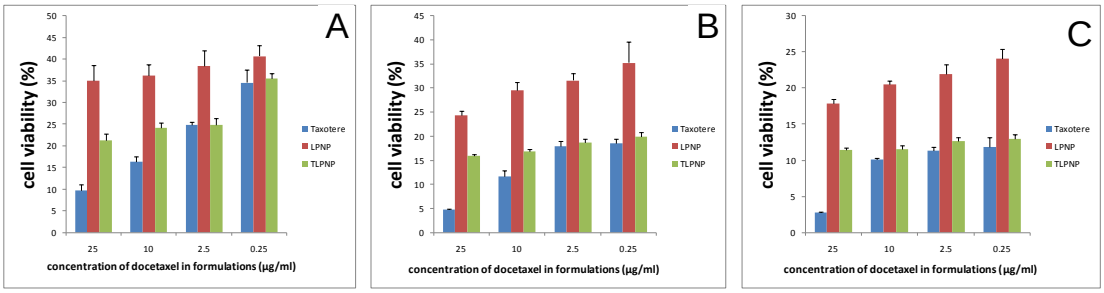

Figure 4.7 The diagrams of cell viability at various concentrations of the drug under 24 h (A), 48 h (B), and 72 h (C) treatment. Compared with LPNPs, TLPNPs show higher cytotoxicity, that is, lower cell viability. Data represent mean ± SE (shown as plus SE only), n=6.

4.4 Conclusions

Two systems of the lipid shell polymer core NPs, i.e. the nanoparticles of mixed lipid monolayer shell and biodegradable polymer core and the ligand-conjugated nanoparticles of mixed lipid monolayer shell and biodegradable polymer core, were successfully developed in this research for sustainable, controlled and targeted delivery of anticancer drugs with docetaxel as a model drug. The mixed lipid monolayer shells provide the nanoparticles with the natural property, high stability, desired surface properties in favor of cellular uptake, stealth feature of long half life in the plasma, and most importantly, quantitative (exact) management of the targeting effect by adjusting the component ratio of the mixed lipid monolayer to provide the moieties for ligand conjugation.

Chapter 5 : Development of New TPGS Surfactants Coated Nanoparticles of Biodegradable Polymers for Targeted Anticancer Drug Delivery

This research focused on engineering biodegradable nanoparticles by a series of new surfactants for new-concept chemotherapy aiming to achieve greater efficacy against cancer over traditional chemotherapy and the nanoparticles constructed by conventional surfactant. Synthesis of the new surfactant materials TPGS2k, TPGS5k and TPGS2kNH_2 was conducted by carbodiimide chemistry. The surfactants were used for the fabrication of docetaxel loaded polymeric nanoparticles. Characterizations and *in vitro* evaluation of the new formulations were carried out to demonstrate the potential for chemotherapy. Analysis of the new nanoparticle formulations was fulfilled by comparison to the conventional surfactant TPGS1k coated particles and also to the particles without surfactant. Characteristics of the new nanoparticles in terms of size, size distribution, surface charge and surface morphology were similar. However, the new formulations were superior in terms of drug loading, cellular uptake efficiency and cytotoxicity. In addition, targeting effect by folic acid conjugation to the new surfactant coated nanoparticles was also evaluated. The targeted formulation to folate receptors was proved to be effective in increasing *in vitro* cellular uptake efficiency and cytotoxicity. Consistent evaluation and analysis on the novel formulations evolve a fascinating opportunity to continuously engineer the new drug delivery systems for new-concept chemotherapy.

5.1 Introduction

Although chemotherapy is a complicated procedure and carries a high risk due to dosage form, drug toxicity, restricted pharmacokinetics and pharmacodynamics, severe side effects and drug resistance at various physiological levels (Feng, 2006), chemotherapy has still played important role in fighting against cancer due to the systemic property. With the emerging of nanotechnology to engineer chemotherapy, the problems could be readily solved by new-generation nanoscaled drug carriers. Among various types of nano-systems, nanoparticles of biodegradable polymers may provide an ideal solution for the problems encountered in current regimen of chemotherapy owing to their unique properties such as the small size, acceptable biocompatibility, high drug encapsulation efficiency especially for hydrophobic drugs, controlled and sustained drug release manner, high cellular uptake efficiency, desired pharmacokinetics, long circulation half-life, and highly tailored functions (Cho et al., 2008; Tong and Cheng, 2007; Zhang et al., 2008a). With the aid of NPs, the problems of traditional chemotherapy, i.e. the dosage form, toxicity, severe side effects, and unfavorable pharmacokinetics could be settled with satisfaction. Furthermore, new-concept chemotherapies can be progressively promoted which may include sustained, controlled and targeted delivery of chemotherapeutic drugs; personalized chemotherapy; delivery of therapeutic agents across physiological drug barriers; and eventually, chemotherapy at home (Feng, 2004).

However, at present, NPs should be appropriately engineered to overcome several fundamental problems and technical barriers for anticancer drug delivery (Nie, 2010), such as escape from the recognition by RES, ability of long enough circulation lifetime, accumulation in the vicinity of solid tumors and targeting the cancerous cells (Dreher

et al., 2006; Minchinton and Tannock, 2006). The effective solution is to engineer NPs by tuning their size, shape, surface area, surface charge, as well as surface chemical property. Among those characteristics of NPs, surface property plays a key role in determining the performance on chemotherapy in the aspects of 1) enhancing the circulation time of the NPs, which results by avoiding the capture by phagocytic system and escaping from the adsorption of proteins in bloodstream; 2) prompting cellular uptake efficiency benefiting from higher interaction of the surface of NPs with the cell membrane; and 3) decorating NPs surface to achieve designed chemotherapy by coating with various functional materials and/or conjugating desired targeting ligands. It is highly anticipated to achieve the desired surface properties through introducing versatile materials to coat on the NPs.

D-α-tocopheryl polyethylene glycol 1000 succinate (TPGS1k) surfactants are amphiphilic macromolecules comprising the hydrophilic PEG segment and hydrophobic tocopherol (vitamin E) segment (Sadoqi et al., 2009). TPGS1k was proved as a favorable material for nanoparticle formation for drug delivery (Win and Feng, 2006; Feng et al., 2007). Moreover, due to its bulky lipophilic segment, TPGS1k was thought to possess properties such as better drug solubilization, high emulsification effect, high drug encapsulation efficiency, high cellular adhesion and adsorption (Feng et al., 2009; Gao et al., 2009; Mu and Seow, 2006). TPGS1k was also proved to be able to effectively block P-glycoprotein efflux pump which is a major component in the multi-drug resistance system expressed on a lot of cancerous cells that removes the drug molecules from the cancerous cells, thus alleviating bioavailability of the drug (Dintaman and Silverman, 1999; Mu and Feng, 2002).

Inhibition of P- glycoprotein allows drugs to be retained within the pathological cells enabling drug concentration to keep effective doses to kill the cells.

Nonetheless, the chain length of PEG in TPGS1k (Mw = 1,000) is not long enough to fulfill the requirement of avoiding RES scavenging and protein adsorption. It is widely believed that, however, only molecular weight of PEG not shorter than 2,000 could achieve those benefits (Kah et al., 2009; Owens and Peppas, 2006). In 2006, researchers synthesized a series of TPGS analogues with a variety of PEG chain length and indicated that the transportation of rhodamine 123 in Caco-2 cells was influenced by the chain length of PEG (Collnot et al., 2006). It is thus inspired that the performance of the materials is related to the types of PEG molecules. Therefore, we would expect to modify the currently used TPGS1k to be better surfactant materials to formulate NPs for chemotherapy by conjugating longer PEG molecules as well as other functional PEG on the hydrophobic segment vitamin E.

In this work, we synthesized a series of TPGS surfactants using various PEG to demonstrate the effectiveness of those new materials as the additives to nanoparticle formation for drug delivery and broaden the application of TPGS molecules to be a family of candidates for engineering NPs. It is expected that the new materials are able to display better performance than the conventional one. Functional TPGS was also produced to provide the possibility of active targeting to folate receptors overexpressed on lots of cancer cells after conjugating with folic acid, the widely applied small molecules of targeting with high affinity with the receptor. PLGA NPs were prepared by the nanoprecipitation method with TPGS as surfactants for sustained and controlled chemotherapy by using docetaxel as a prototype drug, which is one of the best antineoplastic agents aiming to a wide spectrum of cancers. The chemotherapeutic

engineering technology developed in this article devoid of toxic additives by preparing novel TPGS macromolecules coated PLGA NPs, which showed a variety of advantages over the commercial formulation of docetaxel, Taxotere® and supply a lot more choices for engineering versatile NPs by selecting different TPGS molecules in the family.

5.2 Materials and methods

5.2.1 Materials

Docetaxel (anhydrous, 99.56%) was purchased from Shanghai Jinhe Bio-Technology Co. Ltd, China. Taxotere® was provided by National Cancer Center, Singapore. TPGS1k, PLGA (75:25, Mw = 90,000-126,000), monomethoxy PEG (MPEG, Mw = 2,000 and 5,000, from now on, simply MPEG2k and MPEG5k, respectively), tocopherol succinate (or vitamin E succinate, simply, VES), dicyclohexylcarbodiimide (DCC), 4-(Dimethylamino) pyridine (DMAP), *N*-Hydroxysuccinimide (NHS), triethylamine (TEA), *N*-(3-Dimethylaminopropyl)-*N*′-ethylcarbodiimide hydrochloride (EDAC), folic acid, sucrose, methanol, ethanol, dichloromethane, diethyl ether, acetone, acetonitrile, dimethyl sulfoxide, coumarin-6, PBS (pH 7.4), MTT, and PI were purchased from Sigma-Aldrich (St. Louise, MO, USA). Poly [ethylene glycol]-2000 bis-amine (PEG2k bis-amine) was offered by Laysan Bio (Arab, AL, USA). Tween-80 was from ICN Biomedicals, Inc. (OH, USA). Triton X-100 was provided by USB Corporation (OH, USA). FBS, trypsin-EDTA solution and penicillin-streptomycin solution were purchased from Invitrogen. DMEM was from Sigma. All solvents used in this study were HPLC grade. MCF7 breast cancer cells were provided

by American Type Culture Collection. The water used was pretreated with the Milli-Q® Plus System (Millipore Corporation, Bedford, USA).

5.2.2 Synthesis of various surfactants

The surfactants were synthesized by carbodiimide chemistry. Briefly, tocopherol succinate was weighed and dissolved in DCM. MPEG2k or MPEG5k was also weighed and dissolved in DCM. Both the tocopherol succinate and MPEG were then added together with DCC and DMAP with stoichiometric ratio of 1:1:2:0.1 respectively and left to stir overnight in nitrogen environment at dark. The solution was then filtered to remove by-product and precipitated in cold diethyl ether. The precipitate obtained was then washed by diethyl ether again and dissolved in water and dialyzed against water. The milky dispersion was filtered again to remove impurities and the filtrate was collected. D-α-tocopheryl polyethylene glycol 2000 succinate (TPGS2k) and D-α-tocopheryl polyethylene glycol 5000 succinate (TPGS5k) powder was obtained after freeze drying of the filtrate. For amine terminated TPGS, tocopherol succinate, PEG2k bis-amine, DCC and NHS were weighed and dissolved in DCM separately with stoichiometric ratio of 1:1.2:2:2 respectively. The solution was mixed with 20 μl of TEA and left to stir in a nitrogen environment at dark for 2 days. The solution was then filtered to remove by-product and precipitated in cold diethyl ether. The precipitate obtained was then washed by diethyl ether again and dissolved in water and dialyzed against water. The milky dispersion was filtered again to remove impurities and the filtrate was collected. D-α-tocopheryl amino polyethylene glycol 2000 succinate (TPGS2kNH_2) powder was obtained after freeze drying the filtrate. The ^{1}H NMR spectra were collected on a Bruker ACF300 (300MHz) spectrometer using d_6-DMSO as solvent.

5.2.3 Fabrication of surfactant coated PLGA NPs

Nanoparticles were fabricated using the nanoprecipitation method. The aqueous phase was first prepared by dispersing various surfactants in ultrapure water (as concentration of 0.08mg/ml). PLGA was weighed and dissolved in acetone forming a 10mg/ml oil phase. The oil phase was then added dropwise into 10 times of the aqueous phase while continuously stirring. The particle suspension was left to stir until all the solvent was evaporated. The particle suspension was then filtered and centrifuged and washed 3 times at 8,000 rpm for 15 minutes at 4℃. The powder of the NPs was obtained by freeze drying. The docetaxel loaded NPs were fabricated using the same method with the drug contained oil phase. The fluorescent NPs were fabricated as the same procedure except using coumarin-6 contained oil phase. Formulations without surfactant were prepared using the same method but replacing the aqueous phase with only ultrapure water. From now on, PLGA NP, T1k NP, T2k NP, and T5k NP are assigned in abbreviation to PLGA nanoparticles without surfactant, TPGS1k coated PLGA nanoparticles, TPGS2k coated PLGA nanoparticles, and TPGS5k coated PLGA nanoparticles, respectively.

5.2.4 Conjugation of folic acid onto the TPGS2kNH_2 coated PLGA NPs

Post-conjugation strategy to conjugate folic acid to TPGS2kNH_2 coated NPs was applied. Suspended NPs were mixed with folic acid at a molar ratio of 20:1. EDAC and NHS were added in excess and the suspension was stirred overnight before filtering through a filter paper. Filtrate collected was dispersed in ultrapure water and washed three times. The particles were collected and freeze dried. Similarly, T2kN NP

and T2k NP-FOL infer TPGS2kNH_2 coated PLGA nanoparticles and the PLGA nanoparticles coated by TPGS2kNH_2 and further conjugated by folic acid, respectively.

5.2.5 Characterization of the NPs

Data were expressed as the means with 95% confidence intervals. Statistical tests were performed with the Student's *t* test. For all tests, *P* values less than 0.05 were considered to be statistically significant. All statistical tests were two-tailed.

The average particle size and size distribution of the NPs were measured using laser light scattering (90Plus Particle Sizer, Brookhaven Instruments Corporation, Huntsville, NY, USA) at a laser angle of 90° at 25℃. The sample was prepared by diluting the nanoparticle suspension with ultrapure water and sonicating for 1 minute to ensure homogenous dispersion of the particles. The surface charge of the NPs in water was measured using a zeta-potential analyzer (Zeta Plus, Brookhaven Instruments Corporation, Huntsville, NY, USA) at 25℃. The sample was prepared by diluting the nanoparticle suspension with ultrapure water and sonicating for 1 minute to ensure homogenous dispersion of the particles. The zeta potential was measured under certain pH value and concentration of the dispersion. The drug loading efficiency of the NPs was determined in triplicates by high performance liquid chromatography (Agilent LC 1100 series, USA). A reversed phase Inertsil® ODS-3 column (250×4.6 mm, particle size 5 μm, GL Science Inc., Tokyo, Japan) was used. 3 ml of nanoparticle suspension with known amount of NPs was freeze dried, re-dissolved in 1ml of DCM and left overnight to evaporate. 4 ml of mobile phase (50:50, v/v acetonitrile/water solution) was added and the solution was filtered using a 0.45 μm PVDF syringe filter before being transferred to a HPLC vial. The effluent was

detected at 230nm with a UV-VIS detector. The drug loading is defined as the ratio between the mass of drug encapsulated in the NPs and the mass of the drug loaded NPs presented.

The surface morphology of the NPs was visualized using field-emission scanning electron microscope (JSM-6700F, JEOL, Japan) at an accelerating voltage of 5 kV. The samples were prepared by placing a drop of the nanoparticle suspension on copper tape placed on top of a sample stub and left under reduced pressure to dry. The sample was then coated with a platinum layer using Auto Fine Coater (JEOL, Tokyo, Japan) for 30s at 30 mA current.

The surface composition of the NPs was analyzed using X-Ray photoelectron spectroscopy (AXIS His-165 Ultra, Kratos Analytical, Shimadzu Corporation, Japan). The samples were analyzed using a fixed transmission mode covering a range of binding energy from 0 to 1100 eV with pass energy of 80 eV. Spectrum generation was performed using software provided by the instrument manufacturer.

5.2.6 *In vitro* evaluation

Cell line experiments were carried out using MCF7 human breast adenocarcinoma cells cultured in DMEM supplemented with 10% FBS and 1% penicillin-streptomycin as the antibiotics in humidified environment of 5% CO_2 at 37 ℃. Growth medium was replenished every other day and subculture was performed when cells reached 80% confluence.

For quantitative cellular uptake study, MCF7 cells were seeded into 96-well black plates (Costar, IL, USA) at 5×10^3 cells/well (0.1ml) and after the cells reached 80% confluence, the medium was changed to the suspension of coumarin-6 loaded NPs at a

NP concentration of 0.125 mg/ml for 2 h. After incubation, the NP suspension in the testing wells was removed and the wells were washed with 0.1 ml PBS three times to remove the NPs outside the cells. After that, 50 µl of 0.5% Triton X-100 in 0.2N NaOH solution was added to lyse the cells. The fluorescence intensity present in each well was then measured by microplate reader (Genios, Tecan, Switzerland) with excitation wavelength at 430 nm and emission wavelength at 485 nm.

For qualitative cellular uptake studies, MCF7 cells were seeded in a chambered cover glass system (LAB-TEK®, Nagle Nunc International, Naperville, IL, USA) in humidified environment of 5% CO_2 at 37 ℃. After incubation of 24 h, the medium was replaced by coumarin-6 loaded nanoparticle suspension at a concentration of 0.125 mg/ml. Cells were incubated again for 2 h and washed thrice with PBS. Cells were then fixated by addition of 75% ethanol for 20 min. Cells were further washed twice with PBS and nuclei counterstaining was carried out with propidium iodide for 45 min. Washing of the cells was carried out twice with PBS. Finally, the cells were observed using confocal laser scanning microscope (Olympus Fluoview FV1000) using a PI and FITC channel.

For cytotoxicity study, MCF7 cells were seeded in 96-well transparent plates (Costar, IL, USA) at 5×10^3 cells/well (0.1 ml) and after 12 h, the old medium was removed and the cells were incubated for 24, 48 and 72 h in the medium containing Taxotere® or docetaxel loaded nanoparticle suspension at an equivalent drug concentration of 0.5, 0.25, 0.1 and 0.025 µg/ml. The NPs were sterilized with UV irradiation for 1 day prior to use. At given time intervals, the cultured cells were assayed for cell viability with MTT. The wells were washed twice with PBS and 10 µl of MTT supplemented with 90 µl culture medium was added. After 3 hr incubation, the medium was removed and

the precipitate was dissolved in DMSO. The absorbance of the wells was measured by the microplate reader (Genios, Tecan, Switzerland) with wavelength at 570 nm and reference wavelength at 620 nm. Cell viability was calculated by the following equation: cell viability = Abs_s / $Abs_{control}$ × 100%, where Abs_s is the absorbance of the wells containing the cells incubated with the nanoparticle suspension and $Abs_{control}$ is the absorbance of the wells containing the cells incubated with the culture medium only (positive control).

5.3 Results and discussion

5.3.1 Synthesis of various surfactants

The class of TPGS surfactants was synthesized using the carbodiimide reaction. ^1H NMR was applied to confirm the successful conjugation of PEG molecules with VES. Typically, the results of TPGS2k from the NMR analysis were shown in the Figure 5.1. This figure showed a comparison between MPEG2k, VES and the product of the reaction. Most peaks that occur in the spectrum of MPEG2k and VES also occur in the spectrum of the product, albeit slightly shifted, showing a strong resemblance between the structures of the basic compounds and the product as well as the change of chemical environment in the product. TPGS5k was synthesized similarly except using MPEG5k instead of MPEG2k. The functionalized material, TPGS2kNH_2 was also synthesized using the carbodiimide reaction in the presence of NHS. The reaction resulted in the formation of a yellowish solid. Figure 5.2 showed a comparison between PEG2k bis-amine, VES and the product. All peaks that occur in the spectrum

of PEG and VES also occur in the spectrum of the product with slight shift, pointing to a successful synthesis of TPGS2kNH_2.

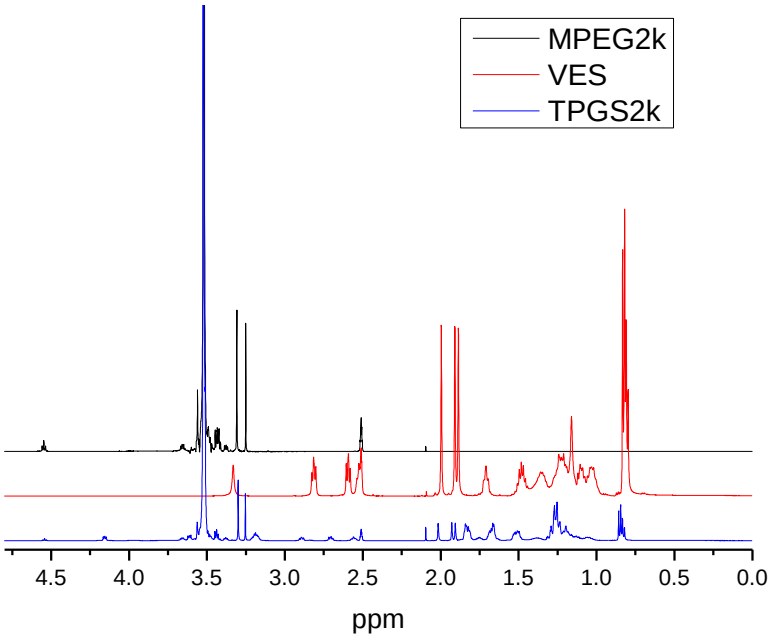

Figure 5.1 ^{1}H NMR Spectra of MPEG2k, VES and TPGS2k.

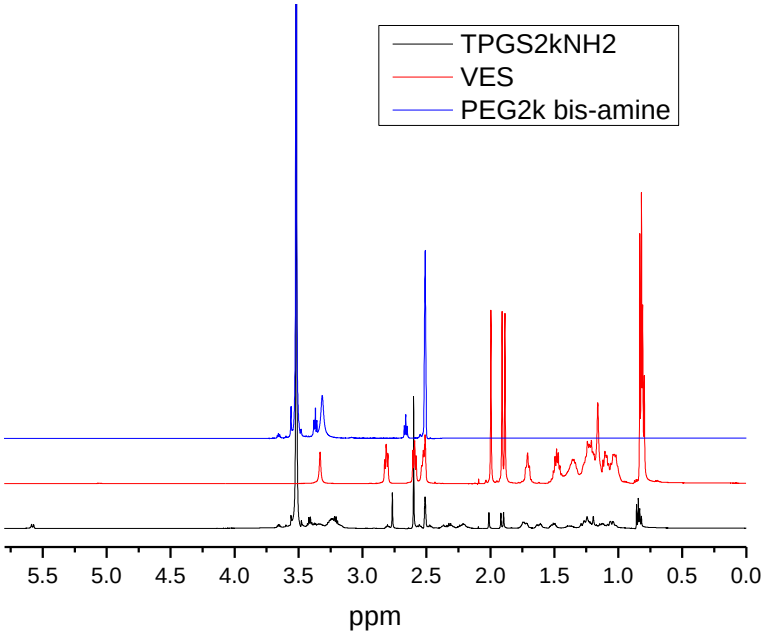

Figure 5.2 ^{1}H NMR Spectra of PEG2k bis-amine, VES and TPGS2kNH_2.

5.3.2 Fabrication of the NPs and conjugation of folic acid to the NPs

The NPs were fabricated using the nanoprecipitation method. The surfactants dispersed in aqueous phase were subsequently adsorbed onto the surface of the nanoparticles due to hydrophobic interaction. Surface coating of nanoparticles was thus able to be achieved by using various desired surfactants. The surfactants used during the fabrication included TPGS1k, TPGS2k, and TPGS5k. TPGS1k is the conventional surfactant currently used which was used as a comparison to benchmark the effectiveness of the new surfactants introduced.

The conjugation was proposed to fulfill the targeted delivery purpose aiming to target folate receptors overexpressed on cancerous cells by folic acid on the top of the NPs. Post-conjugation strategy was employed which was achieved via the aqueous phase carbodiimide reaction between folic acid and the free amine groups on TPGS2kNH_2 coated NPs using EDAC and NHS. The schematic diagram of the structure of the NPs and the reaction was illustrated in Figure 5.3. The merit of post-conjugation for attaching the targeting ligands onto nanoparticles is that it ensures the ligands to stay on the top of the particles but not buried inside the spheres.

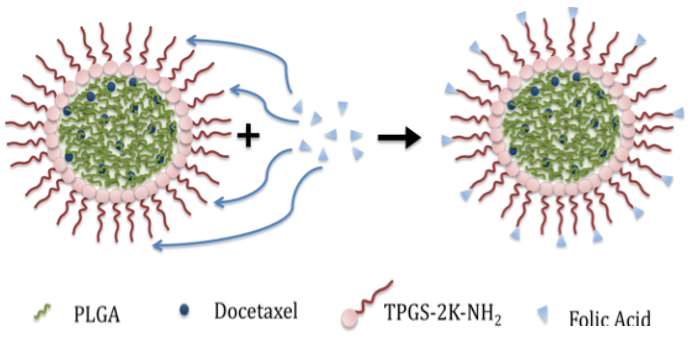

Figure 5.3 Schematic illustration of the structure of the nanoparticles and the post-conjugation of folic acid onto the particles.

5.3.3 Characterization of the NPs

The size and size distribution of the NPs with different surfactants was compared in Table 5.1. It can be seen that the particle size measured using LLS is between 200 to 250 nm. The size of the NPs coated by the new surfactants, namely TPGS2k and TPGS5k falls close to that of TPGS1k coated NPs. The particles conjugated with folic acid are slightly larger in size due to the extra folic acid tail attached to the surface. The size distribution is quite narrow indicating that the NPs are quite uniform in size. A low variation would allow for better control of the properties of the NPs.

The surface charge of the NPs indicates the stability of the particle dispersion. Surface charge that is highly negative or positive points to a stable colloidal suspension due to the high repulsion force between the particles of the same charge. Yet nanoparticles that are too negatively charged are believed to be hindered from crossing the cell membrane due to the negative nature of the membrane which might repel the nanoparticles. The NPs fabricated all have a negative surface charge below -19 mV. The negative surface charge of the NPs could be due to the ionized oxygen contained groups of PLGA. Surfactants stabilized NPs are less negative possibly because of shielding of the negative charge by the surfactants. The formulations with surfactants have a zeta potential close to -20 mV indicating that the NPs are stable in its suspension. Furthermore, the charges of the NPs are not too negative thus allowing the possibility of passage through the cell membrane.

Drug loading is defined as the amount of drug encapsulated in a certain amount of nanoparticles and is represented by the units of μg drug per mg nanoparticles. The

drug loading of T2k NP and T5k NP are higher in comparison to other nanoparticle formulations, which suggests that new surfactants are more effective in ensuring more drugs entrapped within PLGA matrix.

Table 5.1 Characteristics of the docetaxel loaded PLGA NPs with various surfactants: particle size, size distribution, zeta-potential and encapsulation efficiency. Data represent mean ± SE, n=6 (For EE results, n=3).

Nanoparticles	Particle Size (nm)	Polydispersity	Zeta-potential (mV)	Drug loading (μg / mg NP)
NP	206.7 ± 2.9	0.065 ± 0.027	-42.57 ± 0.60	8.23 ± 0.026
T1k NP	215.8 ± 2.7	0.035 ± 0.014	-21.48 ± 1.14	5.60 ± 0.040
T2k NP	202.3 ± 6.1	0.069 ± 0.049	-22.21 ± 0.98	28.48 ± 0.110
T5k NP	249.2 ± 16.6	0.225 ± 0.028	-24.91 ± 0.80	36.90 ± 4.170
T2k NP-FOL	241.5 ± 4.3	0.150 ± 0.023	-19.00 ± 0.82	3.79 ± 0.054

5.3.4 Particle morphology

High-resolution images to study the surface morphology of the NPs were obtained using FESEM (Figure 5.4). Particles with different surfactants were shown to be about 200-300 nm, consistent with the results obtained from LLS. In addition, the particles were revealed to be generally spherical in shape and uniform in size. The particles were also quite similar in visualization under using different surfactants. The surface of the NPs was also revealed to be smooth on the images. However, T2k NP-FOL

formulation was seen to be more adhesive than others which could be attributed to the bulky condition of the surface causing entanglement between particles after drying.

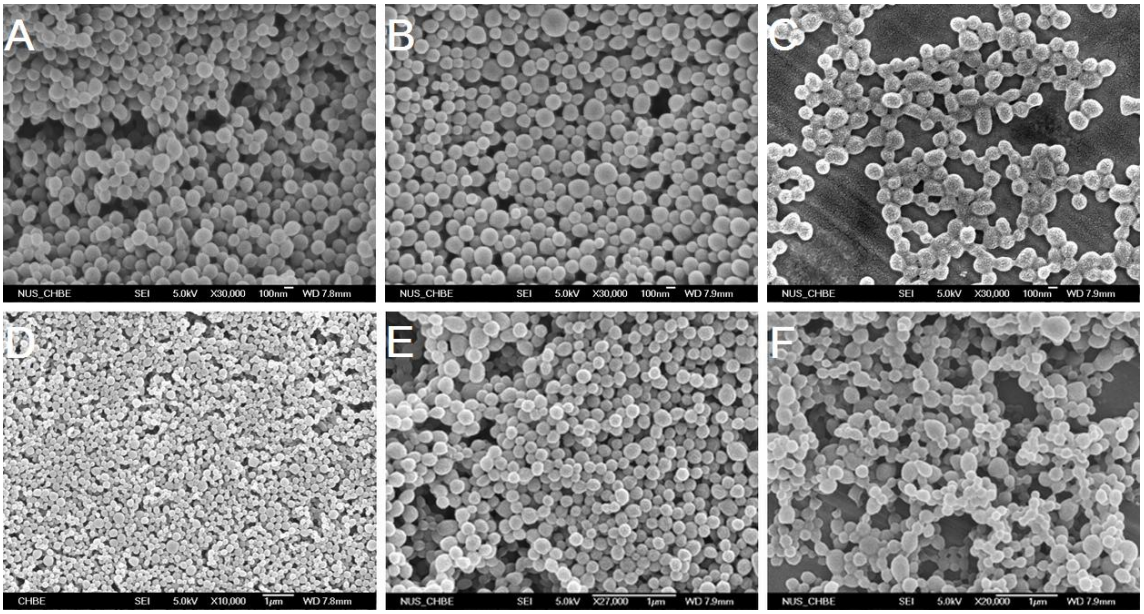

Figure 5.4 FESEM images of (A) PLGA NP, (B) T1k NP, (C) T2k NP, (D) T5k NP, (E) T2kN NP, and (F) T2k NP-FOL.

5.3.5 Surface chemistry

In order to confirm the existence of the primary amine groups as well as the folic acid on the NPs' surface, surface chemical composition of the NPs was elucidated from the specific binding energy on the XPS spectrum. Figure 5.5 showed the wide scan comparison between TPGS2kNH_2, T2kN NP and T2k NP-FOL. To prove the successful synthesis of TPGS2kNH_2, nitrogen was specifically scanned. From the inset of Figure 5.5, a peak for nitrogen at a binding energy of 396 eV was observed in the XPS spectrum, indicating the successful conjugation of amino PEG onto VES resulting in the product. In addition, the nitrogen peak can be observed in the spectrum of both the T2kN NP and T2k NP-FOL, demonstrating the presence of the surfactant on the

surface of the NPs. The slight shift of the position of the nitrogen peak from the two NPs is possibly due to the change of the chemical environment in the vicinity of the surfactants, i.e. the presence of PLGA. The higher signal intensity from the nitrogen on T2k NP-FOL can be attributed to the presence of more nitrogen atoms in the chemical structure of folic acid (seven nitrogen atoms in one folic acid molecule).

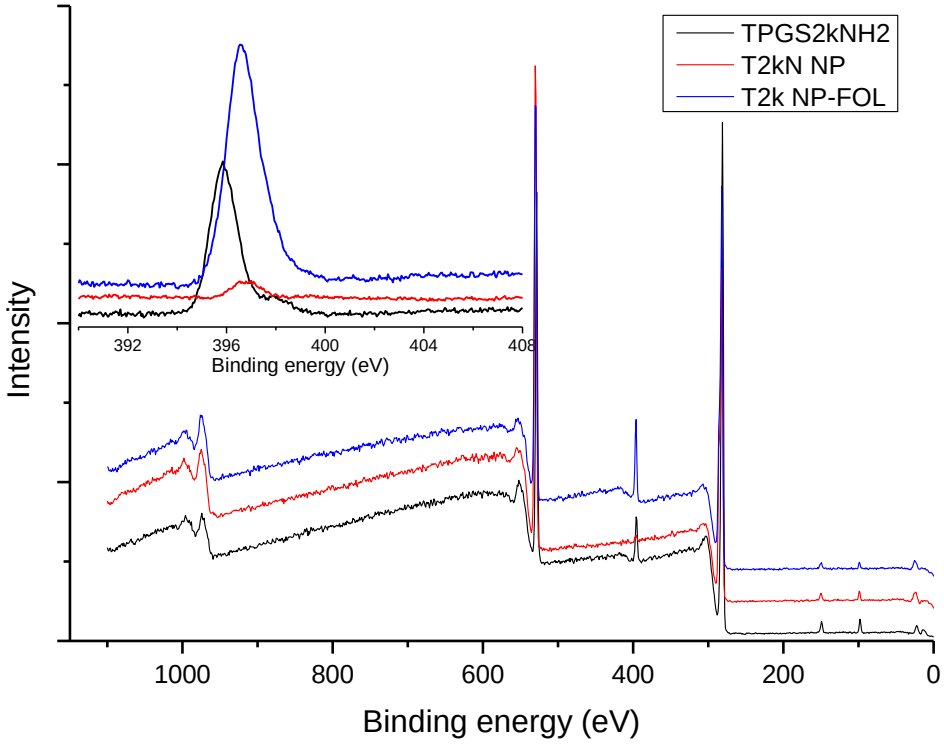

Figure 5.5 XPS widescan spectra of the synthesized product TPGS2kNH$_2$ (lower curve), T2kN NP (middle curve) and T2k NP-FOL (upper curve). The inset graph shows the N 1s spectra of those three with the same sequence.

5.3.6 *In vitro* cellular uptake

The ability of the particles to penetrate into the cells and be internalized and retained within the cell is important to achieve the objective of delivering drugs. Targeting effects of folic acid conjugation can also be examined. The qualitative cellular uptake

analysis was conducted by visualization of the internalized coumarin-6 loaded NPs using confocal laser scanning microscope. Figure 5.6 showed the images of the fluorescent nanoparticles internalized in MCF7 human adenocarcinoma cells. The images in Row A to E are of various nanoparticle formulations in the following order: NPs without surfactant, T1k NPs, T2k NPs, T5k NPs, and T2k NP-FOL. The images in column 1 were obtained using the FITC channel which reveals the green fluorescence of coumarin-6 loaded nanoparticles. Column 2 contains images obtained using the PI channel that highlights the nuclei stained by PI in red fluorescence. Column 3 lists the images that were overlaid by the FITC and PI channels. The images in column 3 show the nucleus of the cells surrounded by green fluorescence from the coumarin-6 loaded nanoparticles distributed in cytoplasm. The particles coated by the new surfactants were also successfully internalized with noticeably higher concentrations within the cell as can be seen from the brighter green fluorescence in the images. The comparison of the particles retained in the cells between folic acid conjugated NPs (T2k NP-FOL) with non-ligand attached NPs (T2k NP) demonstrated the folate receptor targeted behavior from the ligand conjugated NPs. In the condition of the same exciting laser intensity from the same confocal microscope, after incubating 2 h, the fluorescence distribution of T2k NP-FOL internalized in the cytoplasm (row E) is greater than that of T2k NP (row C). It can be explained that receptor-mediated endocytosis facilitates and promotes the entry of the NPs into cells when folate targeted NPs contact the overexpressed folate receptors on MCF7 cells (Yoo and Park, 2004). Apart from that, quantitative measurement also evidently displayed the higher cellular uptake efficiency of folic acid conjugated NPs. The efficiency is 42.8%, 14.3%, 23.1%, and 45.4% higher than the uptake of PLGA NPs,

T1k NPs, T2k NPs, and T5k NPs, respectively (two-tailed student's *t* test, $P < 0.05$). This suggests that the targeting effect of folic acid conjugation is significant after sufficient incubation time. The finding supports the hypothesis that the new surfactant provides the opportunity to conjugate with folic acid for targeted delivery to specific cancerous cells.

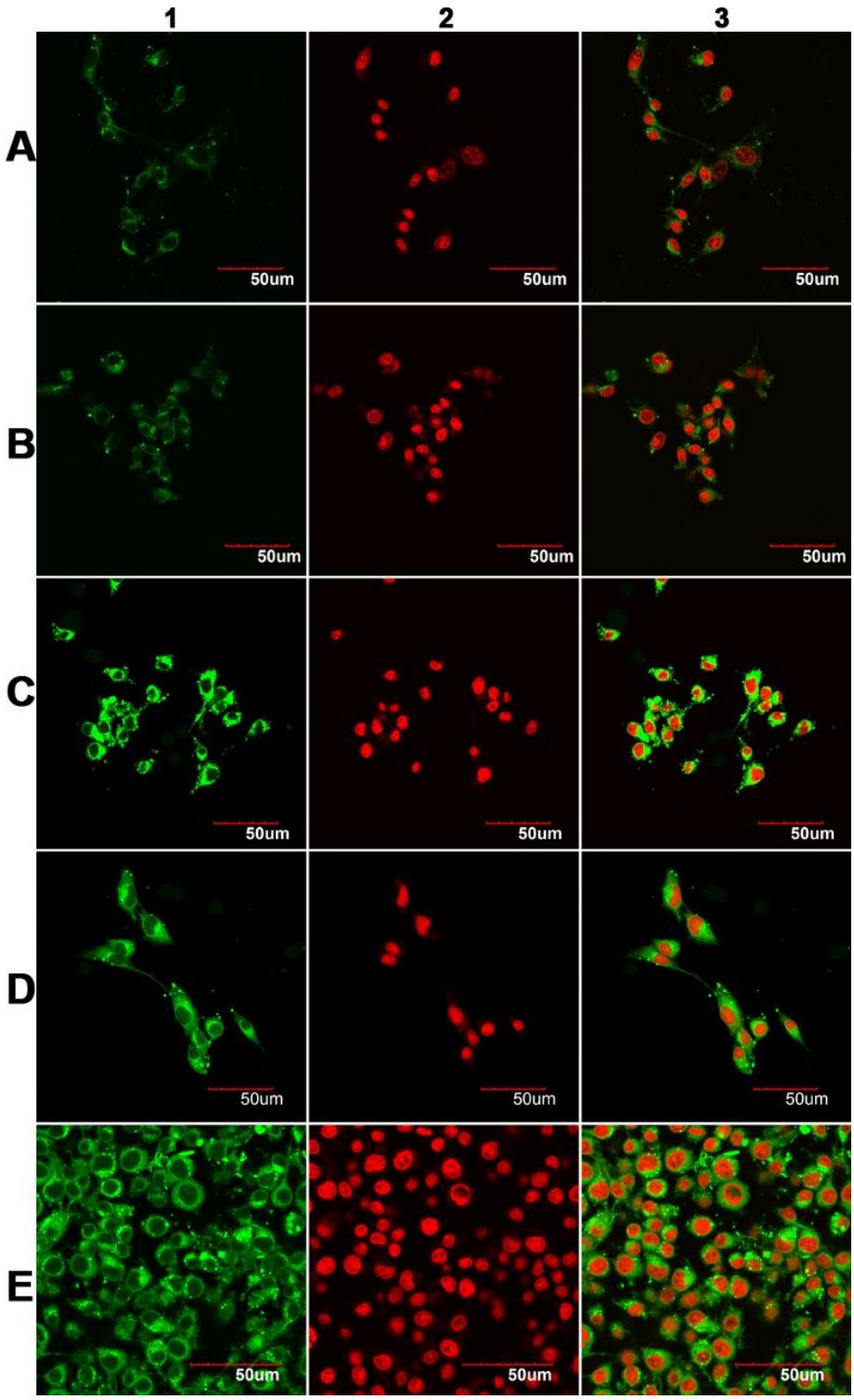

Figure 5.6 CLSM images of the particles internalized in MCF7 cells. Row A to E shows PLGA NP, T1k NP, T2k NP, T5k NP, and T2k NP-FOL used, respectively.

5.3.7 *In vitro* cytotoxicity

The efficacy of the drug delivery system was demonstrated in the cytotoxicity measurement (Figure 5.7). Lower cell viability or survival rate would translate to higher cytotoxicity. A general decreasing cell viability trend was observed with increasing incubation times for the different formulations tested. Longer incubation times would mean longer exposure of the cells to the nanoparticles carrying the drug allowing more time for the nanoparticles to internalize into the cells and release the loaded drugs in the cytoplasm, resulting in higher cell mortality. It was also observed that higher drug concentrations lead in lower cell viability, which is quite straightforward to understand. The highest cell mortality appeared at the highest concentration of the nanoparticle formulation after the longest treatment time suggesting that the drugs were released controllably and sustainably from the particles over a period of time, which is consistent with our previous study on nanoparticles (Feng et al., 2007). From this figure, the cell viabilities from the groups treated by nanoparticle formulations were found to be generally lower than that treated by Taxotere®, especially in the lower drug concentration groups, which infers the close even better capability of the nanoparticle formulations to defeat cancer cells. When compared the viability results of nanoparticles coated with the new surfactants with the traditional TPGS1k, most of the performance of T2k NPs and T5k NPs were clearly better, than T1k NPs, showing the value of those new materials to be further investigated.

In addition, we notice that cell viability is lower with the use of T2k NP-FOL as compared to all of the other formulations in all of the drug concentration cases. This situation was also repeated at all treatment times. As the concentration of the drugs is the same, the lower viability of cells implies that the result could be due to the

targeting effect of folic acid. As there was a propensity for nanoparticles conjugated with folic acid to accumulate within cancer cells, a higher concentration of the drug would be presented leading to higher cell mortality. The results also act in coordination with those shown in the cellular uptake test.

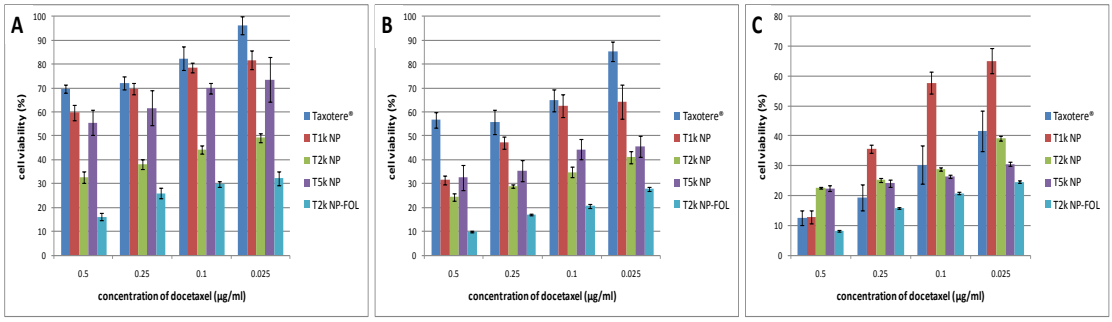

Figure 5.7 MCF7 cell viability measurement after 24 hr (A), 48 hr (B), 72 hr (C) treated by formulations of Taxotere®, T1k NP, T2k NP, T5k NP, and T2k NP-FOL at various drug concentrations.

Quantitative analysis of the dosage form for *in vitro* therapeutic effect was carried out from the *in vitro* cell viability data. The IC_{50}, defined as the drug concentration needed to kill 50% of the incubated cells in a designated time period, was calculated from the evaluation (Table 5.2). The IC_{50} value after 24 h treatment is 0.026 µg/ml for T2k NP and 0.0025 µg/ml for T2k NP-FOL. The results connote that the folic acid decorated nanoparticle formulation is 90.4% more effective than TPGS2k coated nanoparticle formulation after 24 h treatment and suggest that conjugation with folic acid to TPGS2k will significantly increase the therapeutic efficacy.

Table 5.2 IC_{50} values (μg/ml) of various formulations after different treatment times.

	Taxotere®	T1k NP	T2k NP	T5k NP	T2k NP-FOL
24 h	0.98	2.13	0.026	1.44	0.0025
48 h	0.53	0.15	0.0068	0.014	0.0026
72 h	0.016	0.082	0.0041	7.17×10^{-5}	0.0023

5.4 Conclusions

A series of new TPGS analogues, TPGS2k, TPGS5k and TPGS2kNH_2 were successfully synthesized in this study. Docetaxel loaded PLGA NPs using the new compounds as surfactant were also fabricated using the nanoprecipitation method. The NPs were characterized and the *in vitro* performance evaluated. Folic acid was conjugated as targeting ligand onto TPGS2kNH_2 coated PLGA NPs for targeted chemotherapy. Comparison of the characteristics of PLGA NPs using new TPGS as surfactants to conventional TPGS1k shows similar properties in terms of size, size distribution, surface charge and surface morphology. The new surfactant coated NPs were shown to have higher drug loading and *in vitro* evaluation revealed that the new materials were able to grant the particles greater cellular uptake efficiency and cytotoxicity. The conjugation of folic acid on the nanoparticles significantly increased the ability of targeted NPs to penetrate into cancer cells and inhibit the growth of the cells, as revealed in the higher cellular uptake efficiency and cytotoxicity results, indicating the potential of such engineered nanocarriers to achieve targeted

chemotherapy. Therefore, the major contribution of this project is that new surfactants have been successfully developed for fabrication of PLGA NPs as nanocarriers for chemotherapy with even better characteristics. Meanwhile, the strategy provides the space using potent TPGS analogues for conjugation of versatile targeting ligands on the nanocarriers to realize more effective chemotherapy.

Chapter 6 : A Strategy for Precision Engineering of Nanoparticles of Biodegradable Copolymers for Quantitative Control of Targeted Drug Delivery

Research on quantitative control of targeting effect for the drug delivery system of ligand-conjugated nanoparticles of biodegradable polymers is at the cutting edge in the design of drug delivery device. In this work, we developed a post-conjugation strategy, which makes the ligand conjugation after the preparation of the drug loaded nanoparticles of two copolymers blend. We synthesized the PLGA-PEG copolymer with PEG functioning as the linker molecule needed for herceptin conjugation. Docetaxel loaded nanoparticles of the PLGA-PEG/PLGA copolymer blend were prepared by the nanoprecipitation method. Anti-HER2 antibody (heceptin), which targets the breast cancer cells of HER2 receptor overexpression, was conjugated on the drug loaded PLGA-PEG/PLGA nanoparticles for sustained, controlled and targeted delivery of docetaxel. We demonstrated that the targeting effect can be quantitatively controlled by two ways, i.e. (1) adjusting the copolymer blend ratio of the nanoparticle matrix, and (2) adjusting the herceptin feed molar ratio to NH_2 in the linker molecules appearing on the nanoparticle surface. Compared with the pre-conjugation strategy, the post conjugation strategy provides more efficient use of the ligand and protects its bioactivity in the nanoparticle preparation process, thus resulting in better performance in drug targeting, which was assessed *in vitro* with SK-BR-3 breast cancer cells of HER2 receptor overexpression and MCF7 breast cancer cells of HER2 receptors moderate expression.

6.1 Introduction

Drug delivery device of controlled and targeted function can ideally deliver high dose of the therapeutic agent specifically to the diseased cells with the healthy cells less interfered, thus resulting in desired pharmacokinetics and biodistribution for higher therapeutic effect and fewer side effect. It has been arousing continuous interest in developing various advanced targeting strategies, among which ligand-conjugated nanocarriers may be the most prospective (Vetvicka et al., 2009; Ferrari, 2005; Sinha et al., 2006; Farokhzad and Langer, 2006; Farokhzad and Langer, 2009; Zhang et al., 2008a). Polymeric nanoparticles are able to dissolve hydrophobic drugs in polymeric matrix, solving the drug solubility problem as well as possess the advantages such as high stability, efficient drug load, sustained drug release, enhanced circulation time in bloodstream and active targeting space for cancer cells (Cho et al., 2008; Feng et al., 2007). A good example is the polymeric nanoparticle formulation of docetaxel, a potent anticancer drug approved by FDA for the treatment on a wide spectrum of cancers (Engels et al., 2007), which has aroused high attraction recently (Esmaeili et al., 2010; Zheng et al., 2010; Mei et al., 2009).

Targeted drug delivery is of necessary importance to achieve “on-site” delivery. Passive targeting can be realized by the enhanced permeation and retention effect of the leaky vessels of tumors which allows the drug carrier of appropriate size and surface properties accumulated in the tumor. Active targeting presents a more promising approach, which can be realized by conjugating molecular probes or ligands onto the surface of the nanocarriers, providing drug delivery systems for reaching and penetrating into the malignant cells which are of overexpression of the corresponding receptors on their membrane, and then releasing the encapsulated therapeutics in the

diseased cells in a controlled and sustained manner (Wang et al., 2008). Among various targeting ligands, herceptin (or Herceptin®, the clinical formulation of Trastuzumab invented by Genentech), the first humanized antibody approved by FDA for the treatment of HER2-positive metastatic breast cancers, has widely appeared in recent studies (Smith, 2001; Vogel et al., 2002). It is known that HER2 overexpresses in 25-30% invasive breast cancers. Herceptin is managed to efficiently internalize into the cells through the receptor-mediated endocytosis even when conjugated with a wide variety of molecules (Muller et al., 2009; Senter, 2009). Herceptin and its conjugates with toxins or nanoparticle formulations were widely used for selective delivery of anticancer agents to cells with positive HER2 receptors (Tsai et al., 2009; Sun et al., 2008; Sun and Feng, 2009; Phillips et al., 2008).

Tailoring of the functional nanocarriers depends on the selection of matrix materials as well as functionalization of surface property. A good example in the literature is to use PLGA as the core of the NPs and PEG to facilitate functionalization of the nanoparticle surface by antibody conjugation. The PEG layer coated over the PLGA core makes the NPs stealth property which is basic to achieve passive targeting purpose. In addition, the functional PEG chains provide the reaction site for antibody decoration on the NPs (Duncan, 2003; Yamamoto et al., 2001). The results showed the qualitative targeting effects of the nanoparticles of the copolymer blend for cancer treatment while there have been only a few reports that demonstrate a quantitative effect for drug targeting.

Precision engineering of the nanoparticles for targeted drug delivery means to develop a practical strategy that can control the quantity, i.e. the surface density, of the targeting ligand on the NP surface. Although little of such work could be found so far

from the literature, this task represents an important aspect at the cutting edge in the design of drug delivery systems for drug targeting. To certain extent, the ligand density on the surface of drug delivery systems is believed as one of the essential biophysicochemical properties as important as size, shape, charge, and surface hydrophilicity of the nanoparticle drug delivery system (Farokhzad and Langer, 2009). The control of the ligand density on the NPs surface exerts the carriers in a more precise manner as well as facilitates the balance between tissue penetration and cellular uptake, resulting in optimal therapeutic efficacy (Farokhzad and Langer, 2009). Recently, there are two strategies developed for quantitative control of the targeting effects by adjusting the ligand density on the nanoparticle surface. The first trial is through conjugation of ligand on the particle forming polymers before the nanoparticle formation, which we call the pre-conjugation method. The other is so-called the post-conjugation method, i.e. to conjugate the ligand to the particles after the nanoparticle formation. For the pre-conjugation strategy, one copolymer such as PLGA-PEG of the nanoparticle matrix was firstly conjugated with targeting ligand, the NPs was then prepared by nanoprecipitation method (Gu et al., 2008). The disadvantage of such a strategy is clear. Only part of the ligand would appear on the nanoparticle surface with some of the ligand wasted within the polymeric matrix, leading to insufficient quantity of the targeting moieties on the nanoparticle surface. Moreover, the ligand distribution on the surface of each NP would not be uniform since the polymeric macromolecules with the ligand would not be evenly distributed in each NP. Furthermore, the ligand molecules are usually fragile biomolecules of complex conformation that may be inactivated in the organic solvent used in the NP preparation process, thus weakening the targeting effects. This strategy, therefore, is not as desired to precisely control the

targeting effect. For the post-conjugation strategy, instead, it used the ligand more efficiently and protects its bioactivity.

In this study, we intend to show the feasibility of the post-conjugation strategy for quantitative control of the targeting effect by controlling the ligand density on the nanoparticle surface and to demonstrate its impact on the cellular uptake efficiency and cytotoxicity. To our knowledge, there is no report so far in the literature on the formulation of docetaxel by herceptin-conjugated nanoparticles of the PLGA-PEG/PLGA copolymer blend. We demonstrate that the surface density of the ligand molecules can be precisely controlled by adjusting the ratio of the copolymers and the antibody. In fact, a linear relation between these two parameters can be achieved within certain range of the copolymer blend ratio. We synthesized PLGA-PEG block copolymer, which was then mixed with PLGA at a designated blend ratio to prepare the docetaxel loaded NPs of the copolymer blend. The distal primary amine groups on the PEG chain were utilized to conjugate the carboxylic groups on anti-HER2 antibody as the ligand to target HER2 receptors on breast cancer cells. The control on the ligand density on the NP surface was achieved by 1) using various designated ratio of PLGA-PEG over PLGA, thus controlling the percentage of the amine groups on the surface; and 2) providing different initial amount of the antibody in the herceptin-nanoparticle conjugation process with a fixed blend ratio between the PLGA-PEG and the PLGA copolymers. The amount of the antibody conjugated on the NPs was measured by the Bradford assay. For the formulation of a designated ligand density, the ligand-conjugated, drug loaded nanoparticles were characterized for their various physicochemical properties. The *in vitro* experiment was conducted by using SK-BR-3 breast cancer cells of HER2 receptor overexpression and MCF7 breast cancer cells of

HER2 receptors moderate expression. The *in vitro* cellular uptake of the corresponding fluorescent dye loaded nanoparticles was investigated qualitatively by the confocal cell laser scanning microscope and quantitatively by the microplate reader. The *in vitro* viability was assessed by the MTT assay. The overall performance of the designed drug delivery carrier was evaluated by the whole results in consistency.

6.2 Materials and methods

6.2.1 Materials

Docetaxel (anhydrous, 99.56%) was purchased from Shanghai Jinhe Bio-Technology Co. Ltd, China. Taxotere® was provided by National Cancer Center (Singapore). Herceptin (20 mg in 0.95 ml) was offered by Singapore General Hospital. PLGA (50:50, Mw: 40,000-75,000), acetone, ethanol, dichloromethane, acetonitrile, dimethyl sulfoxide, coumarin-6, sucrose, PBS (pH 7.4), sodium borate, Bradford reagent (for 1-1,400 μg/ml protein), *N*-(3-Dimethylaminopropyl)-*N*′-ethylcarbodiimide hydrochloride (EDAC), *N*-Hydroxysulfosuccinimide (Sulfo-NHS), MTT, trypsin-EDTA solution and PI were all purchased from Sigma-Aldrich (St. Louise, MO, USA). PLGA acid terminated (PLGA-COOH, 50:50, IV=0.4 dl/g) was provided by PURAC Biomaterials (Lincolnshire, IL, USA). Poly(ethylene glycol)-2000 bis-amine (PEG_{2k} bis-amine) was offered by Laysan Bio (Arab, AL, USA). PLGA-PEG block copolymer was synthesized using PLGA-COOH and PEG bis-amine by carbodiimide chemistry as previously reported (Esmaeili et al., 2008; Murugesan et al., 2008). Tween-80 was from ICN Biomedicals, Inc. (OH, USA). Triton X-100 was provided by USB Corporation (OH, USA). FBS and penicillin-streptomycin solution was purchased

from Invitrogen. DMEM was from Sigma. All solvents used in this study were HPLC grade. SK-BR-3 and MCF7 breast cancer cells were provided by American Type Culture Collection. The water used was pretreated with the Milli-Q® Plus System (Millipore Corporation, Bedford, USA).

6.2.2 Preparation of the NPs

The NPs were prepared by the nanoprecipitation method with modification as reported in earlier publication (Cheng et al., 2007). Briefly, a weighed amount of PLGA with designated ratio between PLGA-PEG and docetaxel were dissolved in acetone to reach at 10 mg/ml concentration. 5 ml of such solution were subsequently added dropwise into 5 ml ultrapure water under vigorous stirring. The acetone was then evaporated under reduced pressure. The particle suspension was centrifuged at 8,000 rpm for 15 minutes at 4 °C to collect the NPs. After washing twice, the NPs were resuspended in the water of designated volume with 3% w/w sucrose as cryoprotectant and freeze-dried to obtain the fine powder. For blank (without drug load) NPs, only the polymers were dissolved in acetone. The fluorescent NPs were prepared in a same way with docetaxel replaced by coumarin-6.

6.2.3 Herceptin conjugation and ligand surface density control

Herceptin was diluted in borate buffer (pH 8.4) to acquire 1 mg/ml concentration as stock solution. Desired amount of various freeze-dried NPs powder was resuspended in borate buffer with designated volume of herceptin stock solution in the presence of EDAC and Sulfo-NHS to conjugate the free primary amine groups on the NPs surface with the carboxylic groups on the antibody molecules. After overnight reaction under room temperature with gentle end-to-end mixing, the NPs were collected by

centrifugation and further washed twice by borate buffer. The pellets were resuspended in ultrapure water for further characterization, while the supernatant after each centrifugation was collected and accumulated for measurement of the antibody concentration. Standard protocol of Bradford assay was employed for quantifying the concentration of the protein in the supernatant. The ligand amount on the NPs surface was thus obtained via reduction of the amount in the supernatant from the initial amount.

6.2.4 Surface chemistry analysis

The existence of herceptin on the NPs surface was confirmed by X-ray photoelectron spectroscopy (AXIS His-165 Ultra, Kratos Analytical, Shimadzu Corporation, Kyoto, Japan). The elements on the NPs surface were identified according to the specific binding energy (eV), which was recorded from 0 to 1200 eV with pass energy of 80 eV under the fixed transmission mode. The nitrogen element was particularly tested under fine mode with 0.5 eV as step. The data were processed by specific XPS software.

6.2.5 Characterization of the NPs

Data were expressed as the means with 95% confidence intervals. Statistical tests were performed with the Student's *t* test. For all tests, *P* values less than 0.05 were considered to be statistically significant. All statistical tests were two-tailed.

The particle size and size distribution of the NPs were measured by dynamic light scattering (90Plus, Brookhaven Instruments Co., TX, USA). The dispersion of NPs was diluted by ultrapure water according to the mass concentration and completely sonicated before measurement. The surface charge of the NPs was determined by ZetaPlus zeta potential analyzer (Brookhaven Instruments Co., TX, USA) at room

temperature in ultrapure water. The pH value and concentration of the NPs dispersion were determined before measurement. The amount of docetaxel encapsulated in the NPs was measured by high performance liquid chromatography (Agilent LC1100). A reversed phase Inertsil® ODS-3 column (250×4.6 mm, particle size 5 μm, GL Science Inc., Tokyo, Japan) was used. 3 mg freeze-dried NPs were dissolved in 1 ml DCM to break polymer matrix. After evaporating DCM, 3 ml mobile phase (50% ACN in water in volume ratio) was added to dissolve the extracted drugs. The solution was then filtered by 0.45 μm PVDF membrane for HPLC analysis. The column effluent was detected at 230 nm with a UV/VIS detector. The drug load is calculated as the weight of the drug encapsulated in the NPs divided the total weight of the NPs. The unit of drug load is mg drug per mg NPs.

6.2.6 Particle morphology

The shape and surface morphology of the NPs were investigated by field emission scanning electron microscope (JSM-6700F, JEOL, Tokyo, Japan). Samples were completely sonicated before dribbling onto copper tape. The thin layer of the NPs powder was obtained on copper tape for FESEM by evaporating water under reduced pressure. The dried particles were then coated by fine platinum carried out on the Auto Fine Coater (JEOL, Tokyo, Japan).

6.2.7 *In vitro* drug release

The drug loaded NPs were dispersed in PBS (0.1 M, pH 7.4) containing 0.1% (v/v) Tween-80, which improves the solubility of docetaxel in PBS to simulate the sink condition. The dispersion in tubes was then put in an orbital shaker shaking at 120 rpm in a water bath at 37℃. At designated time intervals, the tube of the suspension was

centrifuged at 10,000 rpm for 20 min. The pellet was drained and resuspended in fresh medium to continue the drug release process. The drug released in the supernatant was extracted by DCM and transferred in the same mobile phase as used in measuring drug load. After the evaporation of DCM, docetaxel quantity was determined by the same HPLC procedure as mentioned above. The error bars were obtained from triplicate samples.

6.2.8 *In vitro* evaluation

SK-BR-3 and MCF7 breast cancer cells, which are of moderate HER2 expression, were employed in this study. The Dulbecco's Modified Eagle Medium (DMEM) supplemented with 10% FBS and 1% penicillin-streptomycin solution was utilized as the cell culture medium. Cells were cultivated in humidified environment at 37 ℃ with 5% CO_2. Before experiment, the cells were pre-cultured until confluence was reached to 75%.

For quantitative cellular uptake analysis, cells were seeded into 96-well black plates (Costar, IL, USA) at 5×10^3 cells/well (0.1 ml). After the cells reached 70% confluence, the culture medium was changed to the suspension of coumarin-6 loaded NPs at a NPs concentration of 0.125 mg/ml for 0.5 and 2 hr incubation. After incubation, the NPs suspension in the testing wells was removed and the wells were washed by 0.1 ml PBS thrice to wash away the NPs outside the cells. After that, 50 μl of 0.5% Triton X-100 in 0.2 N NaOH solution was added to lyse the cells. Microplate reader (Genios, Tecan, Basel, Switzerland) was used to measure the fluorescence intensity from coumarin-6 loaded NPs in the desired wells with excitation wavelength at 430 nm and emission

wavelength at 485 nm. The cellular uptake efficiency was expressed as the percentage of the fluorescence of the testing wells over that of the positive control wells.

For fluorescent microscope study, cells were cultivated in the 4-well coverglass chamber (LAB-TEK®, Nagle Nunc, IL, USA) for 1 day. The fluorescent NPs dispersed in the cell culture medium at concentration of 0.125 mg/ml were added into the wells. Cells were washed three times after incubation for 2 hrs and then fixed by 70% ethanol for 20 mins. The cells were further washed thrice by PBS and the nuclei were then counterstained by PI for 45 mins. The fixed cell monolayer was finally washed thrice by PBS and observed by confocal laser scanning microscope (Olympus Fluoview FV1000).

For cytotoxicity measurement, cells were incubated in 96-well transparent plates (Costar, IL, USA) at 5×10^3 cells/well (0.1 ml) and after 12 hrs, the old medium was removed and the cells were incubated with prepared doses for 24, 48 and 72 hrs. The NPs were sterilized with UV irradiation for 1 day prior to using. MTT assay was used to measure the cell viability at given time intervals. The absorbance of the wells was measured by the microplate reader with wavelength at 570 nm and reference wavelength at 620 nm. Cell viability is defined as the percentage of the absorbance of the wells containing the cells incubated with the NP suspension over that of the cells only.

6.3 Results

6.3.1 Preparation and size characterization of the NPs

The nanoprecipitation method was applied for the NPs preparation with the target to make the surfactant-free system with particle size around 200 nm. We used various mass ratio of PLGA-PEG over the total mass of PLGA-PEG and PLGA from 0% to 20% to achieve different density of amine groups on the NPs surface for quantitative control of the surface density of the antibody. With the condition of 10 mg/ml polymer concentration in acetone as the oil phase and the mixing ratio of oil phase to aqueous phase (without surfactant) as 1 to 1, the particle sizes could be obtained of a size close to 200 nm in general, which has been shown in the literature for high cellular uptake efficiency (Win and Feng, 2005). Table 6.1 illustrates the particle size and size distribution of five formulations of the NPs. The general sizes of the formulations are in the range of 150 to 250 nm with polydispersity of 0.065 to 0.244, which is regarded as acceptable narrow size distribution. It can be found that the presence of various amounts of PEG chains on the NPs has little effect on the particle size while bare PLGA NPs have smallest size due to lack of PEG long chains that could enlarge the hydrodynamic diameter in water. The structure of the NPs produced in this study is a core-shell system in which PLGA chains possess the core matrix while PEG chains from PLGA-PEG copolymers stretch on the PLGA core as the shielding shell layer, which can enhance the hydrophilicity and assist to escape from the phagocytosis and opsonization. It is widely accepted that NPs of PLGA-PEG are even more biocompatible than pristine PLGA NPs.

Table 6.1 Particle size and size distribution of the PLGA-PEG/PLGA blend nanoparticles of various PLGA-PEG amounts used in the nanoprecipitation process. Data represent mean ± SE, n=3.

ratio of PLGA-PEG	Particle Size (nm)	Polydispersity
0	162.7 ± 2.9	0.065 ± 0.027
5	190.7 ± 7.6	0.191 ± 0.009
10	225.4 ± 21.9	0.244 ± 0.013
15	202.5 ± 8.7	0.141 ± 0.017
20	192.7 ± 6.0	0.119 ± 0.071

6.3.2 Herceptin conjugation and surface chemistry analysis

The conjugation of herceptin on the NPs was fulfilled by one-step carbodiimide coupling method with EDAC and Sulfo-NHS in aqueous phase (Figure 6.1) based on the abovementioned five formulations. The carboxylic groups on the antibody molecules were activated first and then reacted with the primary amine groups on the PLGA-PEG chains to form amide bonds which link the antibody molecules on the NPs surface. In order to confirm the successful conjugation, the surface chemistry of the antibody conjugated NPs was analyzed by XPS to identify the change of nitrogen signal according to the specific binding energy in that one. Herceptin molecule contains 1726 nitrogen atoms, which should respond stronger signal than that from amine groups in the PLGA-PEG molecules. A typical NPs formulation of 20% PLGA-PEG copolymer was taken as the example, which is shown in Figure 6.2. The more

distinct peak of signals from the orbital of nitrogen (N 1s) qualitatively verifies after the antibody molecules embrace the polymeric matrix cores although the non-conjugated NPs also present slight nitrogen existence due to the amine groups on the surface yet the signal intensity is much lower. Therefore, it can be confirmed that the antibody molecules have been successfully conjugated on the polymer matrix. It is quite well known that the molecular weight of herceptin is large (145 kDa) as well as the molecule size is bulky. Therefore, in conjugation process, the activated antibody molecules will scramble for the opportunity to react with the amine groups. Yet the bulky size causes steric hindrance effect to hurdle further reaction, resulting the inefficient conjugation and free antibody molecules more than stoic molar ratio. As such, we cannot control the surface density of herceptin practically. Consequently, we mixed PLGA-PEG with PLGA to lower the surface density of amine groups, making paucity for penetration of antibody molecules into PEG layer, which can enhance the reaction efficiency of amine groups and control the conjugated antibodies more precisely.

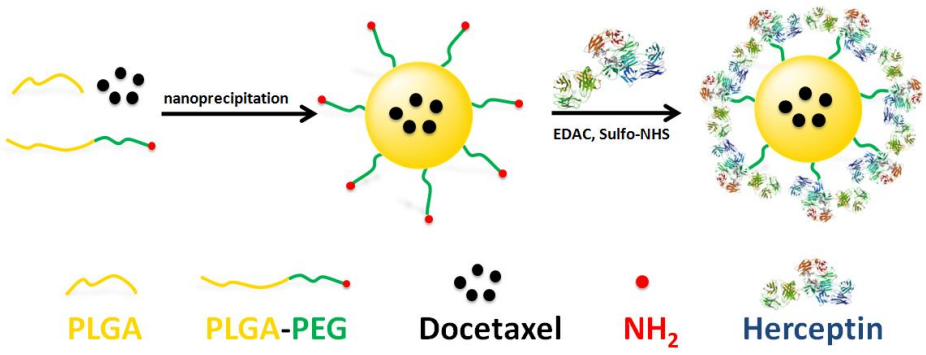

Figure 6.1 Schematic illustration of the fabrication of herceptin conjugated nanoparticles: the nanoparticles comprise a PLGA core with docetaxel loaded, a hydrophilic and stealth PEG layer shell on the surface of the core and a herceptin ligand coating.

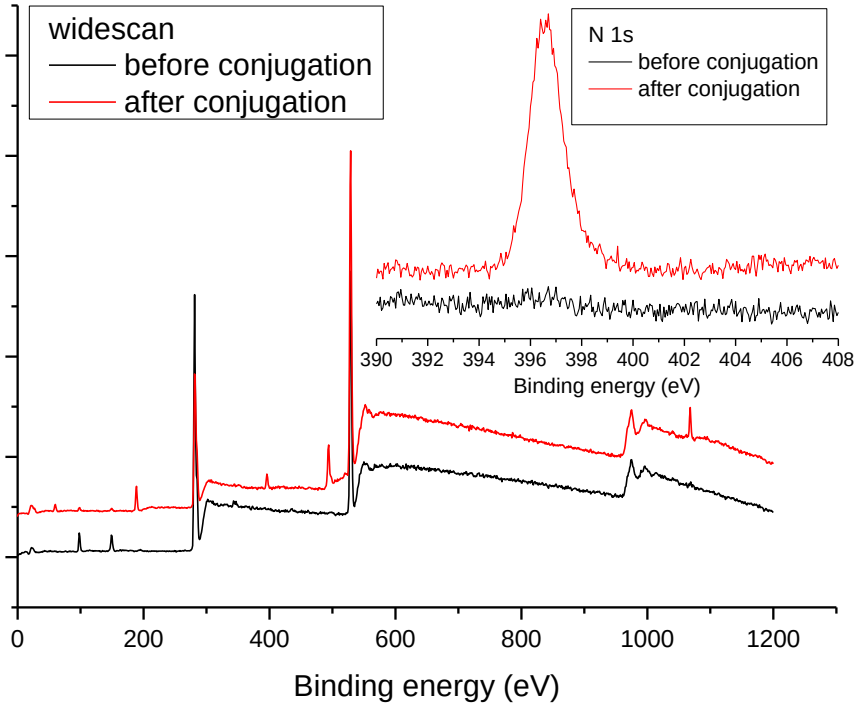

Figure 6.2 Representative XPS spectrum of widescan spectrum and N 1s peaks (the inset) from the 20% PLGA-PEG / PLGA nanoparticles before (lower curve) and after antibody conjugation (upper curve).

6.3.3 Control of ligand surface density on NPs surface

We investigated firstly the correlation of the surface quantity of the antibody conjugated on the NPs surface with the ratio of PLGA-PEG in the PLGA-PEG/PLGA copolymer blend, which has been found to have a linear proportionality and thus shows the feasibility of quantitative control of the targeting effects of the ligand-conjugated NPs. A series of PLGA-PEG/PLGA NPs of 0%, 5%, 10%, 15% and 20% PLGA-PEG in the copolymer blend were fabricated and then conjugated with herceptin of excess supply. The final amount of the antibody conjugated on the NPs surface was measured to be 0, 0.110, 0.250, 0.340, and 0.450 mg per mg of the NPs after deducting the background amount using 0% NPs as control (Figure 6.3). The

linear fit of the data points (R^2 = 0.996) reveals that it is a simple way to control the amount of the ligand conjugated on the NPs by proportional change of the ratio of the PLGA-PEG in the copolymer blend. This strategy is understandable and can be supported by the free amine groups on the NPs surface to provide the linkers for the ligand molecules in the presence of EDAC as the typical protein coupling method. With the increase of amine groups brought from the PLGA-PEG molecules, or in other words, the ratio of PLGA-PEG in the copolymer blend, more ligand molecules could be conjugated since the availability of reaction sites was proportionally higher.

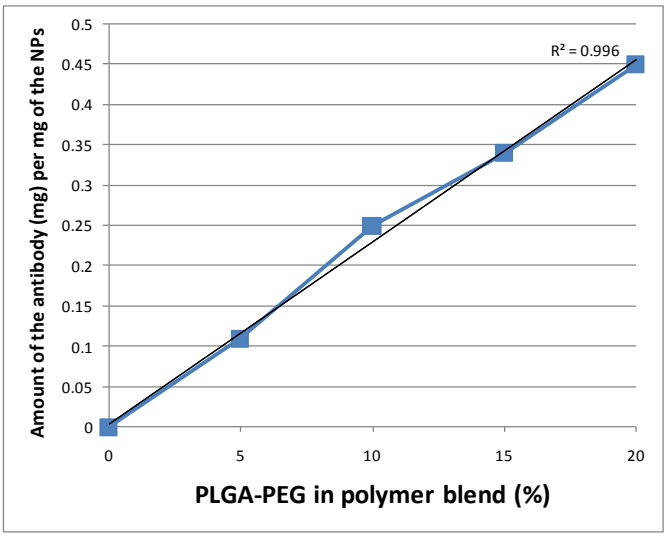

Figure 6.3 Correlation of various ratio of PLGA-PEG in the polymer blend (0, 5, 10, 15, and 20%) with the amount of the antibody conjugated on the nanoparticle surface. The black line represents the linear fitting of the five data points with R^2 = 0.996.

To confirm the feasibility of such a simple strategy for precision engineering of the nanoparticles, we chose the 20% PLGA-PEG NPs as example, which provide maximum number of the linker molecules (the free amine groups) for the ligand conjugation within our designated experimental scope, to investigate the feasibility to control the surface density of the ligand (thus the targeting effects) by changing the

feeding ratio of the ligand in the conjugation process. The results are expressed in Figure 6.4, in which, the amount of the ligand added in the conjugation process with marks at 0.0, 0.1, 0.2, 0.3, 0.4, 0.5 mg expressed in the upper horizontal axis can be converted to the molar ratio of the ligand to the NH_2 group with marks at 0.000, 0.209, 0.418, 0.627, 0.836, 1.046. Accordingly, the amount of the antibody conjugated on the NPs with marks at 0.000, 0.034, 0.084, 0.118, 0.146, 0.180 mg per mg of NPs, which is expressed in the left vertical axis, can be easily converted to the antibody density on the NPs surface in micromole (μmol) per mg NPs with marks at 0.000, 0.232, 0.581, 0.814, 1.007, 1.240 umol per mg NPs, which are expressed on the right vertical axis. It can be seen that the quantity of the ligand conjugated on the NPs surface indeed is proportionally increased with augment of the ratio of the antibody in feed to the amine groups. Supportively, it also shows a linear manner with R^2 = 0.997, which demonstrates the feasibility of the suggested copolymer blend strategy for precision engineering of the nanoparticles of biodegradable copolymer blend for targeted drug delivery as well as for targeted molecular imaging if the encapsulated drug is replaced by a designated imaging agent. In our opinion, this strategy is feasible, practical and convenient. It is a simpler and more economic method since only one type of NPs formulation, for example the 20% PLGA-PEG NPs, needs to be prepared for various designated targeting effects. The method suggested in this work is also more precise to control since the theoretical quantity of the free amine groups was fixed for the various antibody feed ratio with a designated PLGA-PEG portion say 20%, which can be easily measured by facile fluorescent method to guide the addition of the ligand amount in feed. By using this strategy, desired surface density of antibody on the NPs

surface can be conveniently obtained and precision engineering of the nanoparticles for targeted drug delivery and molecular imaging can thus be practically realized.

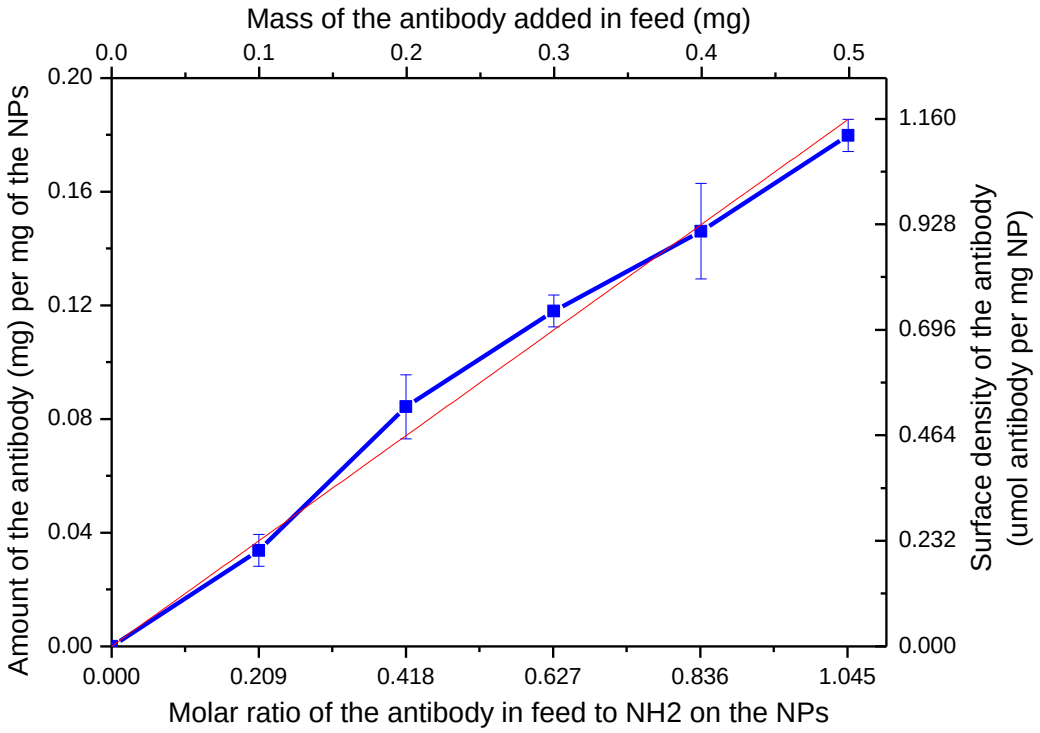

Figure 6.4 Control of the amount of the antibody conjugated or surface density of the antibody on 20% PLGA-PEG / PLGA nanoparticles through adjusting different amount of the antibody added for reaction. Data represent mean ± SE, n=3. The red line represents the linear fitting of the six data points with $R^2 = 0.997$.

6.3.4 Characterization of the docetaxel loaded NPs

The docetaxel loaded NPs of PLGA-PEG/PLGA copolymer blend of 20% PLGA-PEG which were conjugated with 1.046-fold (in stoichiometric ratio) herceptin were selected as the illustrative formulation to demonstrate the properties of so-designed nanocarrier to deliver docetaxel in the following sections. From now on, we define this formulation as HNPs (herceptin-conjugated NPs) and those with no herceptin conjugated on their surface as BNPs (bare NPs). Table 6.2 illustrates the size and size

distribution of such docetaxel loaded NPs before and after herceptin conjugation, which were obtained from DLS measurement. The general sizes of the NPs are smaller than 250 nm in diameter with polydispersity less than 0.25. The size of the conjugated NPs is in general slightly larger than the bare NPs. This could be due to the high molecular weight of herceptin (145 kDa) and thus bulky volume domain. The zeta-potential of the NPs shown in the table indicates the negative charges on the bare NPs surface, which is due to the overall negative charges of functional groups on PLGA in ultrapure water. The high negative surface charge (below -20 mV) is an important indication for the stability of a colloidal system in medium. After antibody conjugation, the zeta-potential became less negatively charged since the antibody molecules are positively charged in ultrapure water environment (pH~5.5) due to its isoelectric point of 8.45. The value of drug load of the NPs was also shown in the table. Obviously, such a formulation system demonstrates the prospect for a practically useful drug delivery carrier with appropriate size, stability and drug load capacity.

Table 6.2 Comparison of the characteristics of HNPs and BNPs: particle size, size distribution, zeta potential and drug load. Data represent mean ± SE, n=6 (For drug load results, n=3).

Formulation	Particle Size (nm)	Polydispersity	Zeta Potential (mV)	Drug load (%)
BNPs	200.7 ± 1.2	0.164 ± 0.031	-37.34 ± 2.41	34.1 ± 0.005
HNPs	243.6 ± 7.2	0.205 ± 0.029	-25.81 ± 3.01	34.1 ± 0.005

6.3.5 Surface morphology

FESEM was employed to image the morphology of the NPs (Figure 6.5). It is revealed from the images that the NPs are generally spherical in shape with narrow size distribution. Moreover, the particle size observed from these FESEM images is in good agreement with that determined by DLS. After ligand conjugation, the particles (C and D) become much more adhesive compared with the simple PLGA NPs (A) as well as the 20% PLGA-PEG NPs (B), which is possibly due to the attachment of the protein layer.

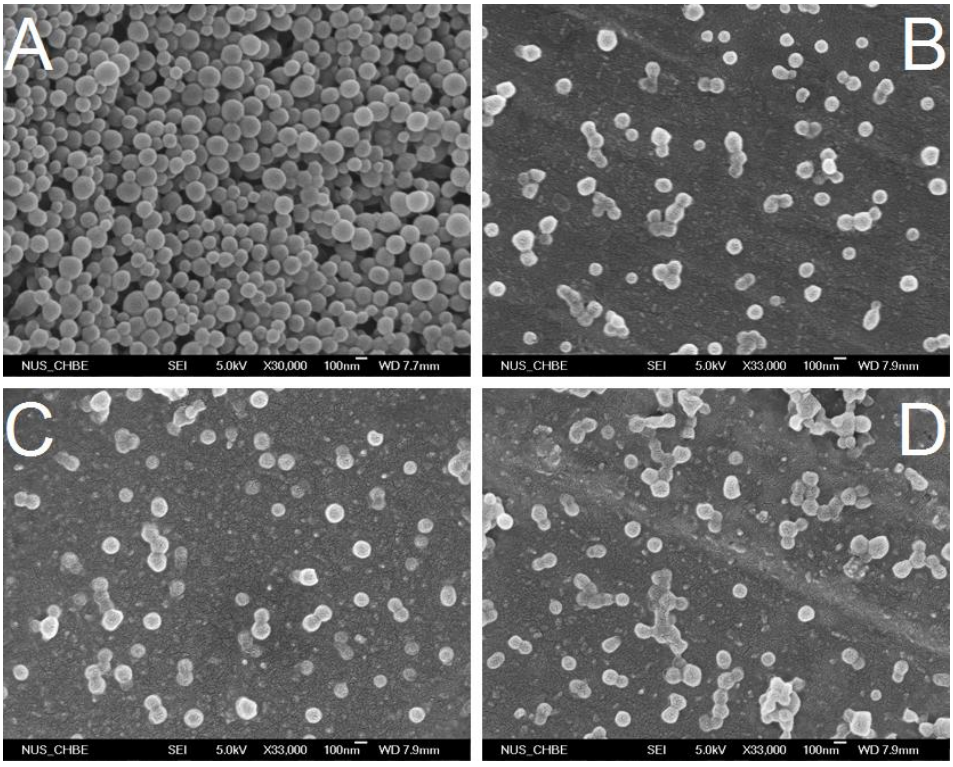

Figure 6.5 Representative FESEM images of PLGA NPs (A), BNPs (B), 0.209-fold herceptin conjugated NPs (C) and HNPs (D).

6.3.6 *In vitro* drug release

The *in vitro* drug release profile of the BNPs and HNPs in ten days was shown in Figure 6.6, from which it can be seen that there is an initial burst of 23.8% for the NPs

with no herceptin conjugation and 10.8% for the herceptin-conjugated NPs in the first 12 hours. Such the burst release may be due to the dissolution and diffusion of the drug molecules located near the surface in the NPs. The moderate initial burst could be helpful to suppress the growth of cancer cells at the beginning of the treatment. In the following 72 hours, the cumulative drug release reached 57.4% and 40.6% for the NPs without and with herceptin conjugation, respectively, and the release presents a first-order increasing manner, which can provide a sustainable treatment. The cumulative drug release approached 73% after ten days for the NPs with no herceptin conjugation, which is attributed to the diffusion of the drug localized in the PLGA core of the NPs. Comparatively, the drug release from the herceptin-conjugated NPs shows a similar manner except for the slightly slower release rate. This is due to the antibody molecule layer coated on the surface, resulting in a barrier on the polymeric cores, which lower permeation of water into the polymeric core as well as diffusion of drug outwards. Such a controlled release profile of docetaxel facilitates the NPs for the delivery of anticancer drugs.

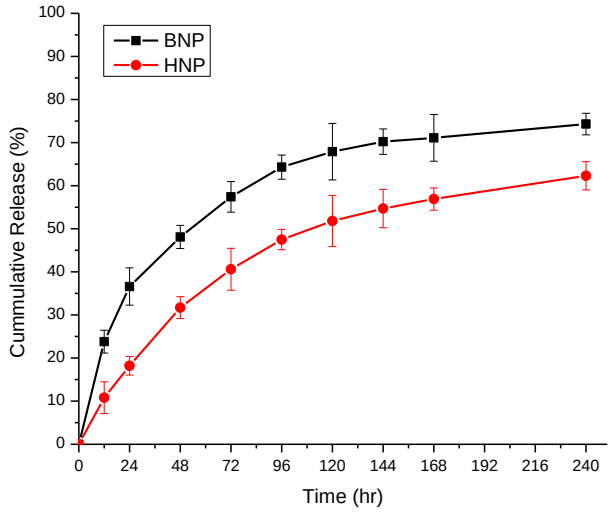

Figure 6.6 *In vitro* docetaxel release profile from the BNPs (square dots) and HNPs (round dots). Data represent mean ± SE, n=3.

6.3.7 *In vitro* cellular uptake: quantitative study

A quantitative investigation has been conducted by measuring the percentage of the coumarin-6 loaded NPs which have been entrapped in SK-BR-3 and MCF7 cells to demonstrate the possible advantages of the NPs to penetrate into the cells. The same concentration of well dispersed fluorescent PLGA-PEG/PLGA NPs (125 μg/ml) without or with herceptin conjugated on the NPs surface was used for all the cases, which was applied for incubation with the SK-BR-3 and MCF7 cells for 0.5 and 2 hr at 37 ℃. The results are summarized in Figure 6.7. It can be seen from this figure that for both of the SK-BR-3 and MCF7 cells, the intensity of the fluorescence from the NPs which has been taken up by the cells increases with the incubation time. Moreover, to demonstrate the effect of the surface density of the ligand on the NPs surface against the cellular uptake efficiency, we produced a series of the NP samples with various antibody amount coated on the surface which were described in Section 6.3.3. All antibody-conjugated NPs, regardless of the herceptin surface densities, consistently demonstrated stable internalization of the coumarin-6 loaded NPs by the MCF7 cells that moderately express HER2 receptors. Interestingly, the cells also endocytosed more NPs with the highest surface density of the ligand, indicating that even for such kind of cells of less HER2 receptors, ligand conjugation can still improve the cellular uptake of the NPs by the ligand conjugation as long as the quantity of the ligand on the NPs surface is high enough. In contrast, the amount of NPs endocytosed by SK-BR-3 cells that overexpress HER2 receptors can be controlled by adjusting the surface density of the conjugated ligand. The NPs of no antibody conjugation had virtually no uptake by the SK-BR-3 cells. On the contrary, significantly increased cellular uptake efficiency

can be observed for the NPs conjugated with herceptin. By increasing the surface density of the ligand by 104.6% of the amine groups, there was a 1.6-fold increase in the amount of the fluorescent NPs taken up by the cells compared to the bare fluorescent NPs. Furthermore, the percentage of the NPs endocytosed by the cells was almost proportionally increased to the surface density of the ligand. This shows indeed a preliminary proof-of-concept experimental result for the proposed copolymer blend strategy for precision engineering of the nanoparticles of biodegradable copolymer blend for quantitative control of targeted drug delivery. It is obvious to understand that insufficient ligand conjugation takes negative effect on efficient cellular uptake or targeted drug delivery. It is the very motivation to investigate such correlation and control the quantity of the conjugated ligands. The results of the effect of surface density of the ligand on cellular uptake efficiency demonstrate that increased surface density of the ligand promotes the cellular uptake efficiency of the targeted NPs in receptor overexpressed cancer cells. Rather, any further increase in surface density of the ligand resulted in a rare increase in the uptake. We hypothesize that it is a layer-by-layer conjugation when further increases the antibody amount in feed. The outmost layer of the ligand shields the inner molecules, resulting equivalent one layer of ligands and inevitably increased particle size, which are helpless to cellular uptake.

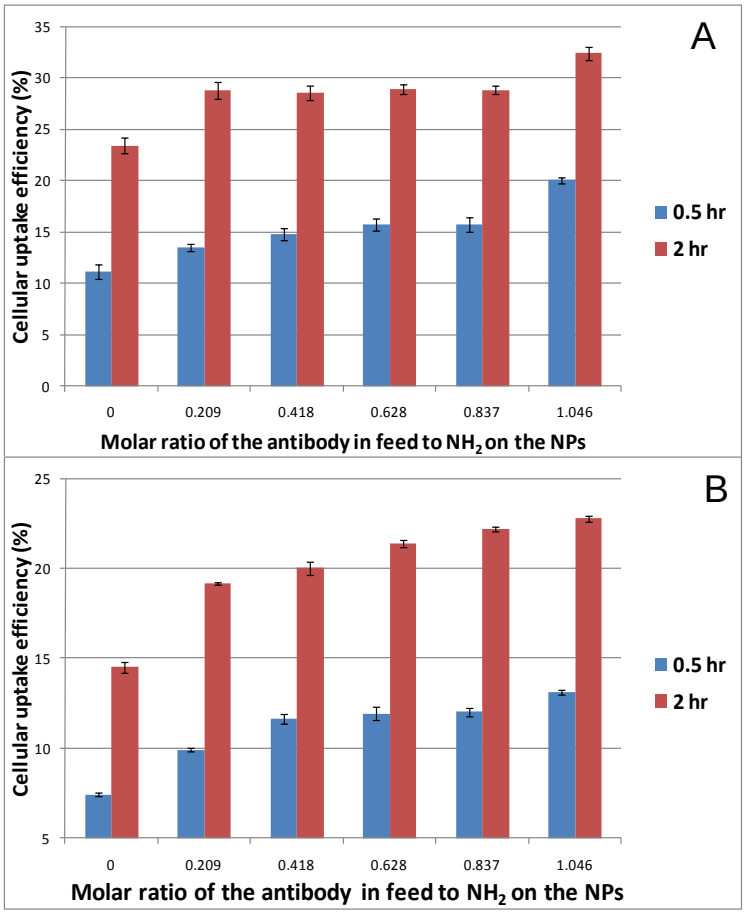

Figure 6.7 Cellular uptake efficiency of the coumarin-6 loaded 20% PLGA-PEG / PLGA nanoparticles with various molar ratio of the antibody added for conjugation to amine groups on the nanoparticles on MCF7 (A) and SK-BR-3 cells (B) after 0.5 and 2 hrs incubation at 125 μg/ml nanoparticle concentration, respectively. Data represent mean ± SE, n=6.

6.3.8 *In vitro* cellular uptake: confocal microscopy study

The cellular uptake of the BNPs and the HNPs after 2 hr incubation with the MCF7 and SK-BR-3 was further investigated by CLSM to visualize the penetration of the NPs into the cells and the targeting effects of the NPs conjugated with herceptin. The results are shown in Figure 6.8. Row A, B and C, D, respectively. Row A and C show the images of the cells incubated with the BNPs of no targeting effect, and Row B and D show the HNPs of herceptin conjugation. The images obtained from FITC channel

which shows the green fluorescence of the coumarin-6 loaded NPs are shown in column 1; column 2 lists the images obtained from the PI channel which show the nuclei in red fluorescence stained by the propidium iodide; and column 3 lists the images obtained from the merged channels of FITC and PI, from which it can be seen that, the red fluorescence representing the nucleus stained by PI is circumvented by green fluorescence representing the coumarin-6 loaded NPs internalized in the cytoplasm. Hence, the qualitative cellular uptake can be visually verified by the CLSM images. In addition, the HER2 receptor targeted behavior of the HNPs can also be observed. Under the same exciting laser intensity from the same confocal microscope, it can be seen from row C and D that the fluorescence from the HNPs in the cytoplasm (row D) is much brighter and greater than that from the BNPs (row C). It can thus be concluded that the receptor-mediated endocytosis does facilitate and promote the entry of NPs into cells when the herceptin conjugated NPs meet the overexpressed HER2 receptors on the SK-BR-3 cell surface. As for MCF7 cells with moderately expressed HER2 receptors, the fluorescence in cytoplasm does not display distinct difference between the HNPs and the BNPs.

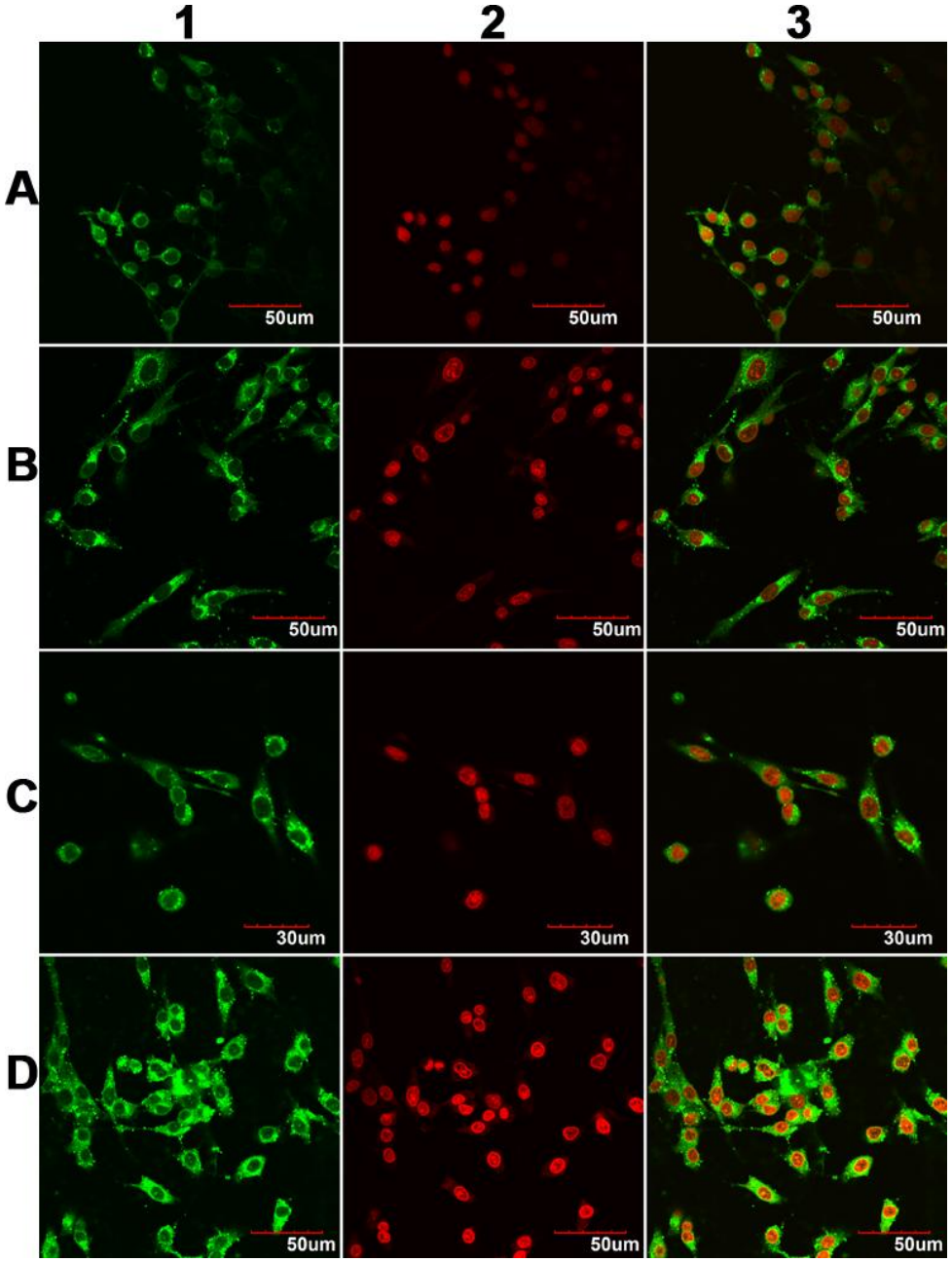

Figure 6.8 Representative CLSM images show the internalization of fluorescent nanoparticles in cells (2 hours incubation). Row A and B: MCF7 cells were used. Row C and D: SK-BR-3 cells were used. In row A and C, BNPs were incubated while in row B and D, HNPs were incubated. Scale bars were labelled on the figures.

6.3.9 *In vitro* cytotoxicity

The efficacy of the NPs formulations of docetaxel to defeat cancer cells is reflected by their cytotoxicity for the cancer cells. Figure 6.9 illustrated the quantitative analysis on the cytotoxicity of docetaxel formulated in the nanoparticles of PLGA-PEG/PLGA copolymer blend, which are of various level of surface density of herceptin as described in Section 6.3.3. Under the same antibody surface density, higher drug concentration would result in lower cell viability, or equivalently higher cell mortality. Noteworthily, the cell viability indeed decreases with increase of the surface density of the antibody, indicating the great potential to achieve the designated cytotoxicity via controlling the ligand surface densities. The 3D plot clearly presents the effects of the antibody surface density and the dose of the drug on the cytotoxicity, *i.e.* the *in vitro* therapeutic effects. The explanation is straightforward since the NPs formulation with more antibody conjugated on their surface can be more efficiently taken up by the cancer cells of the corresponding antigen overexpression. The other cause could be due to the synergistic effect of herceptin with docetaxel (Bullock and Blackwell, 2008).

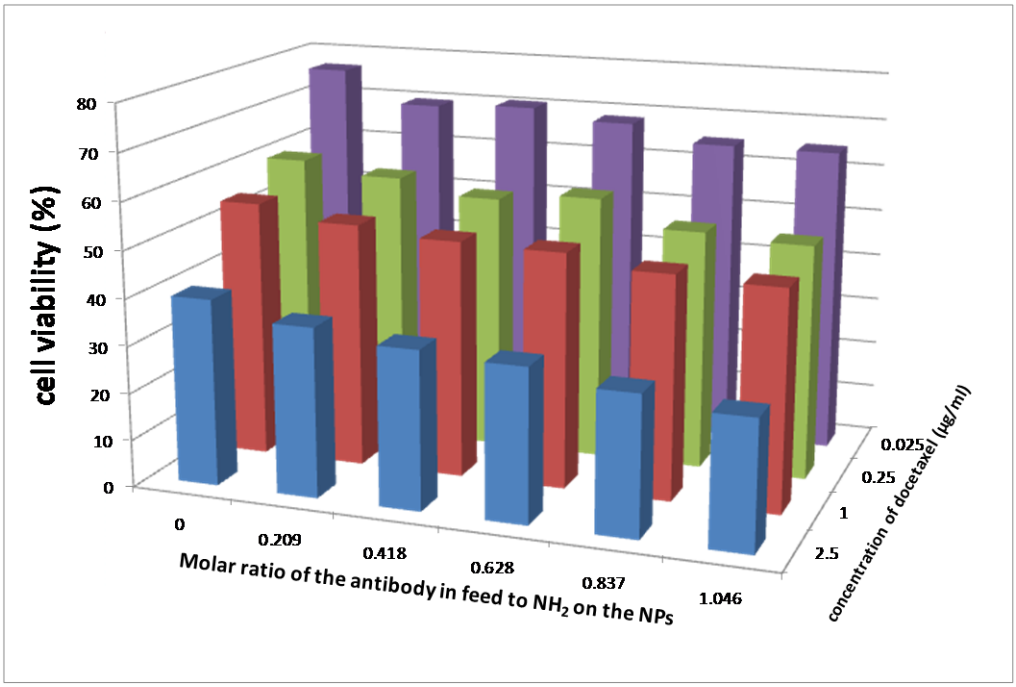

Figure 6.9 The diagram presents the cell viability of the docetaxel loaded 20% PLGA-PEG/PLGA nanoparticles with various molar ratio of the antibody added for conjugation to amine groups on the nanoparticles on SK-BR-3 cells at various concentrations of the drug under 24 hrs treatment. Data shown were taken average from six repeats.

A quantitative evaluation of the *in vitro* therapeutic effect of a dosage form is IC_{50}, which is defined as the drug concentration needed to kill 50% of the incubated cells in a designated time period. Table 6.3 summarizes the IC_{50} values of docetaxel formulated in the various nanoparticles as described in Section 6.3.3 after 24 hr treatment on SK-BR-3 cells. From this table, a consistent decrease in IC_{50} can be observed with increase of the surface density of the conjugated antibody on the NPs surface, which again demonstrates the feasibility of the proposed copolymer blend strategy for precision engineering of nanoparticles of biodegradable copolymers for quantitative control of targeted drug delivery.

Table 6.3 IC_{50} values of SK-BR-3 cells treated by various formulations after 24 hrs. The first row represents various molar ratio of the antibody in feed to NH_2 group on the NPs, and the last column shows the value of Taxotere®, which is the commercial formulation of docetaxel.

Formulation	0	0.209	0.418	0.628	0.837	1.046	Taxotere®
IC_{50} (μg/ml)	1.01	0.54	0.48	0.45	0.27	0.23	2.94

Figure 6.10 highlighted a thorough investigation on SK-BR-3 cytotoxicity of BNPs and HNPs over 24, 48 and 72 hrs period respectively. The equivalent drug concentration of 2.5, 1.0, 0.25, and 0.025 μg/ml was applied. In all cases, *P* is lower than 0.05 under the two-tailed student's *t* test. It is straightforward to understand that

higher drug concentration and longer incubation time will cause lower cell viability, or equivalently higher mortality of the cells. The lowest cell viability, i.e. the highest cell mortality, appeared at the highest drug concentration of the various formulations after treatment for the longest time, which proves the controlled and sustained efficacy of the NP formulations. Furthermore, it is clear that the HNP formulation demonstrated higher cytotoxicity than the BNP formulation at the same drug concentration and exposure time, showing the targeting effect, which means that for the same therapeutic effect, the dose needed for the HNP formulation could be less than that for the BNP formulation. It can also be calculated from the *in vitro* cell viability data that the IC_{50} for 24 hr treatment is 1.53 μg/ml using BNPs and 0.31 μg/ml using HNPs, which means the HNP formulation is 79.7% more effective than the BNP formulation in the 24 hr treatment. The more effective treatment of the HNPs formulation could be attributed to the targeting ability of the herceptin conjugation, which can thus be taken up into the cancer cells more effectively; hence the development of the HNPs formulation can enhance the therapeutic effect. The side effects can also be minimized since fewer drugs would be needed and the drug would be mainly delivered to the cancer cells with the healthy cells ignored. It is highly meaningful that the same amount of the cancer cells can be killed by using less dose of anticancer agent, thus causing fewer side effects like cardio-toxicity (Albini et al., 2010). Herceptin, the formulation intensively applied in clinical cases, is a well tolerated agent and there is minimal additional toxicity (Chan, 2007). Through the investigation, the addition of the antibody on the NP formulation of docetaxel makes the necessary amount of drug reduce to a much less toxic level, which is a very helpful solution for anticancer efficacy as well as reducing the side effects. Moreover, not only HER2 overexpressed

breast cancer cells, but also HER2 moderately expressed breast cancer cells can be applied for such systems.

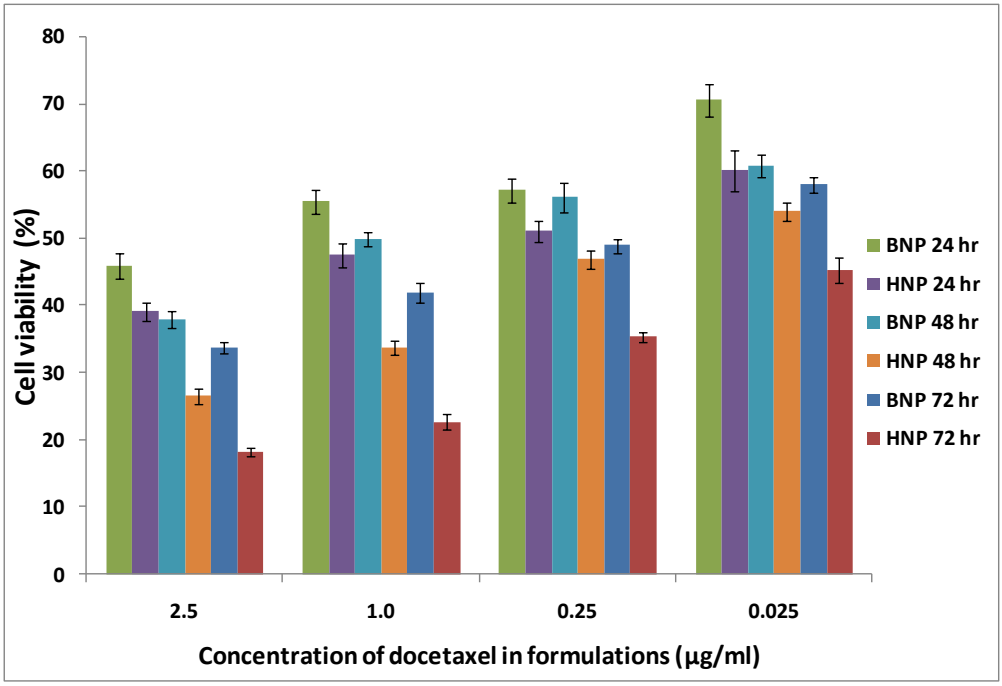

Figure 6.10 The diagram presents the cell viability at various concentrations of the drug under 24, 48 and 72 hrs treatment for SK-BR-3 cells. Data represent mean ± SE, n=6.

6.4 Conclusions

Synthesized PLGA-PEG block copolymer was mixed with PLGA as a biodegradable copolymer blend to produce NPs which were successfully developed in this research for sustainable, controlled and targeted delivery of docetaxel as a model drug. The anti-HER2 antibody, herceptin was used as the ligand to conjugate on the NPs to target HER2 receptors on breast cancer cells. The surface density of the ligand on the NPs was quantitatively controlled by using various ratio of PLGA-PEG over PLGA and different initial amount of the antibody while fixing the ratio of PLGA-PEG over

PLGA. A representative formulation with certain amount of ligand conjugated was selected for further and thorough evaluation. The formulation was found to be in favor of stealth feature and cellular uptake efficiency owning to the PEG layer and ligand attached on the surface, respectively. The targeted delivery system was also proved to be more cytotoxic to HER2 receptor overexpressed cancer cells. The overall performance of the drug delivery carrier shows significant potential and suggests that further investigation would be appropriate. Excitingly, it was shown that the surface density of the ligand on NPs positively impacts on *in vitro* performance. We thus hope that the reporting of this preliminary study demonstrates the necessity to quantify the ligand amount on nanocarriers in researches on targeted drug delivery systems as a property equally as important as, for instance, size and surface charge.

Chapter 7 : CONCLUSIONS

Throughout the thesis, the dedication of research is on the development of better performed nanotechnology based formulations for anticancer purpose. Nanoparticles of biodegradable polymers have been employed as the platform to achieve cancer nanomedicine. Multifunctional nanoparticles with the functions of therapeutics delivery, molecular imaging, and cancer cell targeting are the final target of the research toward cancer diagnosis and treatment in a targeted manner. The specific work in this project is focused on the development of novel nanoparticles through tailoring the surface properties of the nanoparticles thus obtain modified and improved overall performance for cancer nanomedicine. The lipid shell polymer core nanoparticles integrates the merits from both lipids and polymers. Particularly, the effective interaction of lipids with cell membranes was utilized for the system to achieve better cellular uptake efficiency. Moreover, space for further modification on lipids is another important feature for producing targeted nanoparticles. While for TPGS coated nanoparticles, it was designed for improving circulation life of the systems in future clinical applications. The controlling on targeting effects is more advanced, targeting to future optimal and personal therapies. Therefore the objective of developing those systems is various and the systems open up more chances to be selected for clinical trials based on their advantages.

A system of nanoparticles of lipid shell and PLGA core for sustained and controlled release of anticancer drugs was firstly developed in the work. We revisited our earlier work of using phospholipids as emulsifier for nanoparticle formation. Phospholipids, at present, has been regarded as not only efficient emulsifiers to produce colloidal

particles but also important components to provide merits for polymeric nanoparticles in terms of desired surface properties, space for conjugation of functional molecules and better cellular interaction. At beginning, the focus was on the type and amount of lipids used in the nanoparticle formation process that were believed to play a key role to determine the physicochemical properties and *in vitro* performance of the drug loaded NPs. Upon optimization, it was found that DLPC is an ideal lipid molecule to formulate the NPs with certain amount. Selective formulations were thus completely characterized to demonstrate the possibility of being employed as drug delivery systems. We also presented great advantages of phospholipid versus traditional PVA as emulsifier with higher emulsification efficiency, higher drug encapsulation efficiency and better *in vitro* performance. We demonstrated that the coumarin-6 loaded PLGA NPs of DLPC shell showed effective *in vitro* cellular uptake performance on MCF7 cells. The analysis of IC_{50} based on *in vitro* cytotoxicity evaluation demonstrated that the DLPC shell PLGA core NP formulation of paclitaxel could be 5.88-, 5.72-, 7.29×10^3- fold effective than the commercial formulation Taxol® after 24, 48, 72 hr treatment, respectively. Subsequently, the nanoparticles of mixed lipid shell and biodegradable polymer core was developed as a novel platform to construct potential multifunctional nanoparticles for cancer nanomedicine due to the versatility of attaching desired functional molecules. Ligand-conjugated nanoparticles of mixed lipid shell and PLGA core was formulated for sustainable, controlled and targeted delivery of anticancer drugs. The mixed lipid shells, DLPC, DSPE-PEG_{2k}, and functional DSPE-PEG_{5k} provide the nanoparticles with the natural property, high stability, desired surface properties in favor of cellular uptake, stealth feature of long half life in the plasma, targeted delivery property, and most importantly, possibility of

quantitative management of the targeting effect by adjusting the component ratio of the mixed lipids to provide the moieties for ligand conjugation. The IC_{50} results calculated from *in vitro* cell viability data showed that the after 24 h treatment the targeted lipid shell polymer core formulation was 50.91% more effective than the non-targeted formulation and 93.65% more effective than the commercial formulation of docetaxel, Taxotere®, respectively. Consistent evaluation and analysis on the novel formulations evolve a fascinating opportunity and promising prospect to develop these new drug delivery systems although it should be pointed out that *in vivo* investigation should be followed to collect sufficient data for the application for clinical trials.

Another type of improved materials was applied for producing polymeric nanoparticles in the followed chapter. TPGS1k, the traditional PEGylated vitamin E has been widely used to fabricate desired drug carriers; nonetheless the chain length of PEG is not sufficient for stealth property. Therefore a series of new TPGS analogues, TPGS2k, TPGS5k and TPGS2kNH_2 were synthesized in the study to fabricate drug loaded PLGA NPs. The characterization and *in vitro* evaluation demonstrated that by comparison of the PLGA NPs using new TPGS as surfactants with those using conventional TPGS1k, the former shows similar properties in terms of size, size distribution, surface charge and surface morphology. The new surfactant coated NPs were proved to have higher drug loading and greater cellular uptake efficiency and cytotoxicity. Molecular ligands are also able to be conjugated on the new TPGS coated PLGA NPs by using, for instance, TPGS2kNH_2 for targeted chemotherapy, which compensates the lack of reactive sites of TPGS1k and broadens the application of the new materials for various objectives as long as attaching desired molecules on selective TPGS analogues. The conjugation of folic acid on the nanoparticles

significantly increased the ability of the targeted NPs to penetrate into cancer cells and inhibit the growth of the cells, as revealed in the higher cellular uptake efficiency and cytotoxicity results, indicating the potential of such engineered nanocarriers to achieve targeted chemotherapy. Therefore, the major contribution of this project is that new surfactants have been successfully developed for fabrication of PLGA NPs as nanocarriers for chemotherapy with even better characteristics. Meanwhile, the strategy provides the space using potent TPGS analogues for conjugation of versatile targeting ligands on the nanocarriers to realize more effective chemotherapy. However, it is worthwhile to point out that this is only a preliminary investigation for such a novel design of the new materials coated nanoparticles. *In vivo* investigation should be followed to collect sufficient data to prove the stability and circulation time of those nanoparticles for the application for clinical trials.

The last part covers the investigation on the relationship of targeting effects with the quantity of targeting ligands on nanocarriers. A biodegradable copolymer blend of PLGA-PEG with PLGA was used to produce NPs for sustainable, controlled and targeted delivery of docetaxel. The surface density of anti-HER2 antibody, herceptin conjugated on the NPs was quantitatively controlled by using various ratio of PLGA-PEG over PLGA and different initial amount of the antibody while fixing the ratio of PLGA-PEG over PLGA. The targeted delivery system was proved to be more cytotoxic to HER2 receptor overexpressed cancer cells. The overall performance of the drug delivery carrier shows significant potential and suggests that further investigation would be appropriate. Interestingly, it was shown that the surface density of the ligand on NPs positively impacts on *in vitro* performance of the NPs. We thus hope that the reporting of this preliminary study demonstrates the necessity to quantify the ligand

amount on nanocarriers, as an important step to precisely engineering nanocarriers, in researches on targeted drug delivery systems as a property equally as important as, for instance, size and surface charge. It should be pointed out, however, that this is only a proof-of-concept investigation for such a novel design of the NPs. *In vivo* investigation should be followed to collect sufficient data for the application for clinical trials.

Chapter 8 : RECOMMENDATIONS

The preliminary results shown above evidently prove that the nanoparticles of biodegradable polymers are promising platforms for cancer treatment. However, further studies on animals are indispensible toward real clinical application. Besides, molecular imaging of tumor and cancer cells is another necessary component of multifunctional nanoparticles. Therefore in this section, *in vivo* studies and diagnosis of cancer will be proposed on the basis of the developed systems.

The blood-brain barrier (BBB) represents an insurmountable obstacle for a large number of drugs, including antibiotics, antineoplastic agents, and a variety of central nervous system (CNS)-active drugs, especially neuropeptides (Xie et al., 2010). The barrier is crucial to protect brain from the invasion of toxins in blood while it hinders the transportation of therapeutic agents into brain to cure the diseases in brain. There are several approaches to overcome the barrier and deliver drugs into brain: to modify drugs to more readily cross the barrier, to utilize the native carriers expressed at the BBB, to inject drugs directly into the brain, and to use nanoparticles as drug carriers (Tamargo and Brem, 1992; Lockman et al., 2002; Ambikanadan et al., 2003; Kreuter, 2001). Among those, nanoparticles offer a promising solution for this obstacle due to some advantages such as ease of drug encapsulation, protection of drug integrity, high drug delivery efficiency, sustained drug release in the brain, low stimulation and inflammation, and decreased peripheral toxicity (Lockman et al., 2002). One of the most widely exploited nanoparticulate formulations is probably Tween-80 coated PBCA NPs, which was shown to enhance brain uptake *in vitro* and *in vivo* (Kreuter, 2001; Kreuter, 2003; Alyaudtin et al., 2001; Sun et al., 2004). However, PBCA NPs

have potential toxicity, BBB permeabilization, and short duration of delivery and hence, PLGA NPs was regarded as a promising alternative (Olivier, 2005). And Tween-80 has also been found to be associated with severe side effects including hypersensitivity reactions, cumulative fluid retention, nausea, mouth sores, hair loss, peripheral neuropathy, fatigue and anemia (Gelderblom et al., 2001; Immordino et al., 2003; Baker et al., 2004). Therefore alternative materials have to be developed to formulate more potent PLGA NPs across BBB with higher safety. Phospholipids could be one of the candidates. The natural property could ensure the safety use for clinical trials and the high fusion with cell membranes could enhance cellular uptake efficiency, leading high interaction with the cells on BBB thus increasing the transportation efficiency. By using the NPs of lipid shell and PLGA core, it can be expected to be an effective nanocarrier across BBB with the merits of both lipids and PLGA. Furthermore, the end functional groups on certain types of lipids provide wide space for bioconjugation application to introduce molecular ligands which assist to cross BBB, such as transferring and OX-26 antibody, as reported similarly by using molecular ligands conjugated nanocariers for across BBB (Soni et al., 2008; Pang et al., 2008; Gan and Feng, 2010). It needs to conduct thorough investigation *in vivo* to confirm the ability of targeted NPs of lipid shell and PLGA core to cross BBB and deliver drugs inside the brain.

Although *in vitro* results prove the potential of the NPs of lipid shell and polymer core for cancer treatment, further in *vivo* studies should be conducted to more deeply confirm the practical applications in clinical trials. The stability of the particles in real human plasma should be firstly investigated and the release profile of the encapsulated drugs in such condition should also be studied. After that, pharmacokinetics of the

drugs loaded in the particles should be investigated to confirm the controlled and sustained release in rats. The therapeutic window of the released drug should be within the range of maximum tolerable dose and minimum effective dose of the anticancer drug. The biodistribution of such type of particles is also suggested to study. The results will demonstrate the long circulating property and possibility of accumulation of the particles in tumor. Histology study could prove the safety on the tissue level. Lastly, the ability of the particles to suppress tumor growth in rats can be tested by xenograft model study, which is the most direct evidence to show the anticancer effect. Moreover, the advantages of using PEG with longer chain length should also be demonstrated in animals by biodistribution study. If the concentration of the particles in blood is higher over long period, the merits could be proved.

We have demonstrated the impact of ligand surface density on the anticancer effect *in vitro* and the necessity of quantitatively control the ligand amount. It thus deserves further investigation *in vivo*, though the work would be as huge as decades. If we could establish the charts indicating the relationship between targeting effect and tumor inhibition performance, optimal formulation could be given to the patients of different conditions, making the personalized therapy come true.

Cancer diagnosis by molecular imaging of tumors and cancer cells is one of the most effective ways for cancer treatment. Identifying tumors or spread cancerous cells earlier will provide much more opportunity and higher probability to cure the disease. Hence some imaging agents will also be proposed to be encapsulated into the nanoparticulate systems to fulfill molecular imaging function.

QDs are verified powerful tools for imaging. There have been large numbers of work using QDs for tumor imaging recently. Our group has also accumulated certain experience of using QDs. Based on those findings, QDs will be selected to be loaded in the NPs. QDs with different emission wavelengths will be used to adapt different imaging signals called fluorescence spectrum to show different types of cancerous cells. The cancer cells detection and differentiation can be achieved by loading of QDs with different emission wavelengths in the particles anchored with different molecular ligands which are specific to certain type of cells. However, QDs still have some disadvantages. They cannot be excited repeatedly due to photo-bleaching. The safety issue still concerns due to the heavy metals. Accordingly, the imaging agents will be encapsulated into non-toxic nanoparticles or substituted by IOs, which is an MRI agent providing great contrast and spatial resolution among different soft tissues of the body. Yet, single imaging technique inevitably possesses limitations in practical applications. The idea that bridges more than one approach in an integrated system is thus inspired to compensate and complement the drawbacks, which thus provides more precise and complete information for cancer diagnosis. It is called multimodal imaging. Recently our group reported a co-encapsulation system of QDs and IOs in NPs of biodegradable polymers for tumor diagnosis (Tan et al., 2011). Similar strategy would be applied to produce multimodal imaging NPs on the platform of lipid shell and polymer core particles and evaluated *in vivo*.

After the thorough investigation and proven successful results collected from the works above, the function of drug delivery, molecular imaging and cell targeting will be combined in one nanoparticulate system to produce multifunctional nanoparticles. Since the body is a very complicated system, it is hard to predict any unexpected

disasters when using such complex systems. Several problems need also to be addressed prior to clinical application of multifunctional particles, including the batch-to-batch variation when manufacturing the particles, circulation time of the system in body, the release behavior of drugs and imaging agents, the harmful interaction between drugs and imaging agents, the accumulation of the particles in normal cells and healthy organs, fast clearance by the immune systems, resolution of the tumor detection signals, etc. To provide a more complete picture on the therapeutic effects of the fabricated particles, *in vivo* experiments such as pharmacokinetic studies, biodistribution and xenograft models should also be conducted to evaluate the practical performance of the multifunctional nanoparticles for cancer nanomedicine and determine their feasibility in clinical administration.

REFERENCES

Abra, R.M. The next generation of liposome delivery systems: recent experience with tumor-targeted, sterically stabilized immunoliposomes and active-loading gradients, J. Liposome Res., 12, pp.1-3. 2002.

Adams, G.P. and L.M. Weiner. Monoclonal antibody therapy of cancer, Nat. Biotechnol. 23, pp.1147-57. 2005.

Agarwal, A., Y. Lvov, R. Sawant and V. Torchilin. Stable nanocolloids of poorly soluble drugs with high drug content prepared using the combination of sonication and layer-by-layer technology, J. Control. Release, 128, pp.255-260. 2008.

Ahlgren, S., H. Wallberg, T.A. Tran, C. Widstrom, M. Hjertman, L. Abrahmsen, D. Berndorff, L.M. Dinkelborg, J.E. Cyr, J. Feldwisch, A. Orlova and V. Tolmachev. Targeting of HER2-expressing tumors with a site-specifically 99mTc-labeled recombinant affibody molecule, ZHER2:2395, with C-terminally engineered cysteine. J. Nucl. Med., 50, pp.781-789. 2009.

Ahmed, F. and D.E. Discher. Self-porating polymersomes of PEG-PLA and PEG-PCL: hydrolysis-triggered controlled release vesicles, J. Control. Release, 96, pp.37-53. 2004.

Albini, A., G. Pennesi, F. Donatelli, R. Cammarota, S. De Flora and D.M. Noonan. Cardiotoxicity of anticancer drugs: the need for cardio-oncology and cardio-oncological prevention, J. Natl. Cancer Inst., 120, pp.14-25. 2010.

Alexis, F. Factors affecting the degradation and drug-release mechanism of poly(lactic acid) and poly[(lactic acid)-co-(glycolic acid)], Polym. Int., 54, pp.36-46. 2005.

Alexis, F., E. Pridgen, L.K. Molnar and O.C. Farokhzad. Factors affecting the clearance and biodistribution of polymeric nanoparticles, Mol. Pharm., 5, pp.505-515. 2008.

Allen, T.M. and C. Hansen. Pharmacokinetics of stealth versus conventional liposomes: effect of dose, Biochim. Biophys. Acta, 1068, pp.133-141. 1991.

Allen, T.M. and E.H. Moase. Therapeutic opportunities for targeted liposomal drug delivery, Adv. Drug Deliv. Rev., 21, pp.117-133. 1996.

Alyaudtin, R.N., A. Reichel, R. Löbenberg, P. Ramge, J. Kreuter and D.J. Begley. Interaction of poly (butylcyanoacrylate) nanoparticles with the blood-brain barrier in vivo and in vitro, J. Drug Target., 9, pp.209-221. 2001.

Ambikanadan, M., S. Ganesh and S. Aliasgar. Drug delivery to the central nervous system: a review, J. Pharm. Pharmaceut. Sci., 6, pp.252-273. 2003.

Anderson, J.M. and M.S. Shive. Biodegradation and biocompatibility of PLA and PLGA microspheres, Adv. Drug Delive. Rev., 28, pp.5-24. 1997.

Astete, C.E. and C.M. Sabliov. Synthesis and characterization of PLGA nanoparticles. J. Biomater. Sci. Polym. Ed., 17, pp.247-89. 2006.

Avgoustakis, K. Pegylated poly(lactide) and poly(lactide-co-glycolide) nanoparticles: preparation, properties and possible application in drug delivery, Curr. Drug Deliv., 1, pp.321-333. 2004.

Bae, Y., S. Fukushima, A. Harada and K. Kataoka. Design of environment-sensitive supramolecular assemblies for intracellular drug delivery: polymeric micelles that are responsive to intracellular pH change, Angew. Chem. Int. Ed., 42, pp.4640-4643. 2003.

Bae, Y., N. Nishiyama, S. Fukushima, H. Koyama, M. Yasuhiro and K. Kataoka. Preparation and biological characterization of polymeric micelle drug carriers with intracellular pH-triggered drug release property: tumor permeability, controlled subcellular drug distribution, and enhanced in vivo antitumor efficacy, Bioconjug. Chem., 16, pp.122-130. 2005.

Baker, S.D., M. Zhao, P. He, M.A. Carducci, J. Verweij and A. Sparreboom. Simultaneous analysis of docetaxel and the formulation vehicle polysorbate 80 in human plasma by liquid chromatography/tandem mass spectrometry, Anal. Biochem., 324, pp.276-284. 2004.

Bakker-Woudenberg, I.A. Long-circulating sterically stabilized liposomes as carriers of agents for treatment of infection or for imaging infectious foci, Int. J. Antimicrob. Agents, 19, pp.299-311. 2002.

Bangham, A.D., M.M. Standish and J.C. Watkins. Diffusion of univalent ions across the lamellae of swollen phospholipids, J. Mol. Biol., 13, pp.238-252. 1965.

Barbe, C., J. Bartlett, L.G. Kong, K. Finnie, Lin H.Q., M. Larkin, S. Calleja, A. Bush and G. Calleja. Silica particles: A novel drug delivery system, Adv. Mater., 16, pp.1959-1966. 2004,

Bardhan, R., N.K. Grady and N.J. Halas. Nanoscale control of near-infrared fluorescence enhancement using Au nanoshells, Small, 4, pp.1716-1722. 2008.

Barenholz, Y. Liposome application: problems and prospects, Curr. Opin. Colloid Interface Sci., 6, pp.66-77. 2001.

Beletsi, A., P. Klepetsanis, D.S. Ithakissios, S. Kounias, A. Stavropoulos and K. Avgoustakis. Simultaneous optimization of cisplatin-loaded PLGA-mPEG nanoparticles with regard to their size and drug encapsulation, Curr. Nanosci., 4, pp.173-178. 2008.

Bianco, A., J. Hoebeke, K. Kostarelos, M. Prato and C.D. Partidos. Carbon nanotubes: On the road to deliver, Curr. Drug Deliv., 2, pp.253-259. 2005.

Bianco, A., K. Kostarelos, C.D. Partidos and M. Prato. Biomedical applications of functionalised carbon nanotubes, Chem. Commun., pp.571-577. 2005a.

Bianco, A., K. Kostarelos and M. Prato. Applications of carbon nanotubes in drug delivery, Curr. Opin. Chem. Biol., 9, 674-679. 2005b.

Bilati U., E. Allémann and E. Doelker. Development of a nanoprecipitation method intended for the entrapment of hydrophilic drugs into nanoparticles, Eur. J. Pharm. Sci., 24, pp.67-75. 2005.

Blackburn, E.H. Telomeres and telomerase: their mechanisms of action and the effects of altering their functions, FEBS Lett., 579, pp.859-862. 2005.

Blume, G. and G. Cevc. Molecular mechanism of the lipid vesicle longevity in vivo, Biochim. Biophys. Acta, 1146, pp.157-168. 1993.

Brigger, I. C. Dubernet and P. Couvreur. Nanoparticles in cancer therapy and diagnosis, Adv. Drug Deliv. Rev., 54, pp.631-651. 2002,

Brown, K.C. Peptidic tumor targeting agents: The road from phage display peptide selections to clinical applications, Curr. Pharm. Design., 16, pp.1040-1054. 2010.

Brunsvig, P.F., A. Anderson, S. Aamdal, V. Kristensen and H. Olsen. Pharmacokinetic analysis of two different docetaxel dose levels in patients with non-small cell lung cancer treated with docetaxel as monotherapy or with concurrent radiotherapy, BMC Cancer, 7, pp.197. 2007.

Bullock, K. and K, Blackwell. Clinical efficacy of taxane-trastuzumab combination regimens for HER-2-positive metastatic breast cancer, Oncologist, 13, pp.515-525. 2008.

Carmeliet, P. and R.K. Jain. Angiogenesis in cancer and other diseases, Nature, 407, pp.249-257. 2000.

Cattel, L., M. Ceruti and F. Dosio. From conventional to stealth liposomes a new frontier in cancer chemotherapy, Tumori, 89, pp.237-249. 2003,

Chan, A. A review of the use of trastuzumab (Herceptin®) plus vinorelbine in metastatic breast cancer, Ann. Oncol., 18, pp.1152-1158. 2007.

Chan, J.M., L.F. Zhang, K.P. Yuet, G. Liao, J.-W. Rhee, R. Langer and O.C. Farokhzad. PLGA-lecithin-PEG core-shell nanoparticles for controlled drug delivery, Biomaterials, 30, pp.1627-1634. 2009.

Cheng, J., B.A. Teply, I. Sherifi, J. Sung, G. Luther, F.X. Gu, E. Levy-Nissenbaum, A.F. Radovic-Moreno, R. Langer and O.C. Farokhzad. Formulation of functionalized PLGA-PEG nanoparticles for in vivo targeted drug delivery, Biomaterials, 28, pp.869-876. 2007.

Cho, K., X. Wang, S. Nie, Z.(G.) Chen and D.M. Shin. Therapeutic nanoparticles for drug delivery in cancer, Clin. Cancer Res., 14, pp.1310-1316. 2008.

Cirstoiu-Hapca, A., L. Bossy-Nobs, F. Buchegger, R. Gurny and F. Delie. Differential tumor cell targeting of anti-HER2 (Herceptin®) and anti-CD20 (Mabthera®) coupled nanoparticles, Int. J. Pharm., 331, pp.190-196. 2007.

Cirstoiu-Hapca, A., F. Buchegger, L. Bossy, M. Kosinski, R. Gurny and F. Delie. Nanomedicines for active targeting: Physico-chemical characterization of paclitaxel-

loaded anti-HER2 immunonanoparticles and in vitro functional studies on target cells, Eur. J. Pharm. Sci., 38, pp.230-237. 2009.

Collnot, E.M., C. Baldes, M.F. Wempe, J. Hyatt, L. Navarro, K.J. Edgar, U.F. Schaefer and C.M. Lehr. Influence of vitamin E TPGS poly(ethylene glycol) chain length on apical efflux transporters in Caco-2 cell monolayers, J. Control. Release, 111, pp.35-40. 2006.

Danhier, F., N. Lecouturier, B. Vroman, C. Jérôme, J. Marchand-Brynaert, O. Feron and V. Préat. Paclitaxel-loaded PEGylated PLGA-based nanoparticles: In vitro and in vivo evaluation, J. Control. Release, 133, pp.11-17. 2009.

de la Zerda, A. and S.S. Gambhir. Drug delivery: Keeping tabs on nanocarriers, Nat. Nanotechnol., 2, pp.745-746. 2007.

De Miguel, I., L. Imbertie, V. Rieumajou, M. Major, R. Kravtzoff and D. Betbeder. Proofs of the structure of lipid coated nanoparticles (SMBV) used as drug carriers, Pharm. Res., 17, pp.817-824. 2000.

Debbage, P. and W. Jaschke. Molecular imaging with nanoparticles: giant roles for dwarf actors, Histochem. Cell Biol., 130, pp.845-875. 2008.

Decuzzi, P. and M. Ferrari. The role of specific and non-specific interactions in receptor-mediated endocytosis of nanoparticles, Biomaterials, 28, pp.2915-2922. 2007.

Dintaman, J.M. and J.A. Silverman. Inhibition of P-Glycoprotein by D-α-Tocopheryl Polyethylene Glycol 1000 Succinate (TPGS), Pharm. Res., 16, pp.1550-1556. 1999.

Discher, D.E. and A. Eisenberg. Polymer vesicles, Science, 297, pp.967-973. 2002.

Discher, D.E. and F. Ahmed. Polymersomes, Annu. Rev. Biomed. Eng., 8, pp.323-341. 2006.

Donehower, R.C., E.K. Rowinsky, L.B. Grochow, S.M. Longnecker and D.S. Ettinger. Phase I trial of Taxol in patients with advanced cancer, Cancer Treat. Rep., 71, pp.1171-1177. 1987.

Dreher, M.R., W. Liu, C.R. Michelich, M.W. Dewhirst, F. Yuan and A. Chilkoti. Tumor vascular permeability, accumulation, and penetration of macromolecular drug carriers, J. Natl. Cancer Inst., 98, pp.335-344. 2006.

Duncan, R., L.W. Seymour, K.B. O'Hare, P.A. Flanagan, S. Wedge, I.C. Hume, K. Ulbrich, J. Strohalm, V. Subr, F. Spreafico, M. Grandi, M. Ripamonti, M. Farao and A. Suarato. Preclinical evaluation of polymer-bound doxorubicin, J. Control. Release, 19, pp.331-346. 1992.

Duncan, R. The dawning era of polymer therapeutics, Nat. Rev. Drug Discov., 2, pp.347-360. 2003.

Duncan, R. Polymer conjugates as anticancer nanomedicines, Nat. Rev. Cancer, 6, pp.688-701. 2006

Dusinska, M., M Dusinska, L.M. Fjellsbø, Z. Magdolenova, A. Rinna, E. Runden Pran, A. Bartonova, E. Heimstad, M. Harju, L. Tran, B. Ross, L. Juillerat, B. Halamoda Kenzaui, F .Marano, S. Boland, R. Guadaginini, M. Saunders, L. Cartwright, S. Carreira, M. Whelan, Ch. Kelin, A. Worth, T. Palosaari, E. Burello, C. Housiadas, M. Pilou, K. Volkovova, J. Tulinska, A. Kazimirova, M. Barancokova, K. Sebekova, M. Hurbankova, Z. Kovacikova, L. Knudsen, M. Poulsen, T. Mose, M. Vilà, L. Gombau, B. Fernandez, J. Castell, A. Marcomini, G. Pojana, D. Bilanicova and D. Vallotto. Testing strategies for the safety of nanoparticles used in medical applications, Nanomedicine, 4, pp.605-607. 2009.

Engels, F.K., R.A.A. Mathot and J. Verweij. Alternative drug formulations of docetaxel: a review, Anticancer Drugs, 18, pp.95-103. 2007.

Esfand, R. and D.A. Tomalia. Poly(amidoamine) (PAMAM) dendrimers: from biomimicry to drug delivery and biomedical applications, Drug Discov. Today, 6, pp.427-436. 2001.

Esmaeili, F., M.H. Ghahremani, S.N. Ostad, F. Atyabi, M. Seyedabadi, M.R. Malekshahi, M. Amini and R. Dinarvand. Folate-receptor-targeted delivery of docetaxel nanoparticles prepared by PLGA-PEG-folate conjugate, J. Drug Target., 16, pp.415-423. 2008.

Esmaeili, F., R. Dinarvand, M.H. Ghahremani, S.N. Ostad, H. Esmaily and F. Atyabi. Cellular cytotoxicity and in-vivo biodistribution of docetaxel poly(lactide-co-glycolide) nanoparticles, Anticancer Drugs, 21, pp.43-52. 2010.

Evora, C., I. Soriano, R.A. Rogers, K.M. Shakesheff, J.Hanes and R. Langer. Relating the phagocytosis of microparticles by alveolar macrophages to surface chemistry: the effect of 1,2-dipalmitoylphosphatidylcholine, J. Control. Release, 51, pp.143-152. 1998.

Farokhzad, O.C. and R. Langer. Nanomedicine: Developing smarter therapeutic and diagnostic modalities, Adv. Drug Deliv. Rev., 58, pp.1456-1459. 2006.

Farokhzad, O.C., J. Cheng, B.A. Teply, I. Sherifi, S. Jon, P.W. Kantoff, J.P. Richie and R. Langer. Targeted nanoparticle-aptamer bioconjugates for cancer chemotherapy in vivo, Proc. Natl. Acad. Sci., 103, pp.6315-6320. 2006a.

Farokhzad, O.C. and R. Langer. Impact of Nanotechnology on Drug Delivery, ACS Nano, 3, pp.16-20. 2009.

Feng, S.S. and G. Huang. Effects of emulsifiers on the controlled release of paclitaxel (Taxol®) from nanospheres of biodegradable polymers, J. Control. Release, 71, pp.53-69. 2001.

Feng, S.S., L. Mu, B.H. Chen and D. Pack. Polymeric nanospheres fabricated with natural emulsifiers for clinical administration of an anticancer drug paclitaxel (Taxol®), Mater. Sci. Eng. C, 20, pp.85-92. 2002.

Feng, S.S. and S. Chien. Chemotherapeutic engineering: Application and further development of chemical engineering principles for chemotherapy of cancer and other diseases, Chem. Eng. Sci., 58, pp.4087-4114. 2003.

Feng, S.S. Nanoparticles of biodegradable polymers for new-concept chemotherapy, Expert Rev. Med. Dev., 1, pp.115-125. 2004.

Feng, S.S., L. Mu, K.Y. Win and G. Huang, Nanoparticles of biodegradable polymers for clinical administration of paclitaxel, Curr. Med. Chem., 11, pp.413-424. 2004.

Feng, S.S. New-concept chemotherapy by nanoparticles of biodegradable polymers: where are we now? Nanomedicine, 1, pp. 297-309. 2006.

Feng, S.S., L. Zhao, Z. Zhang, G. Bhakta, K.Y. Win, Y.Dong and S. Chien. Chemotherapeutic engineering: Vitamin E TPGS-emulsified nanoparticles of biodegradable polymers realized sustainable paclitaxel chemotherapy for 168 h in vivo, Chem. Eng. Sci., 62, pp.6641-6648. 2007.

Feng, S.S., L. Mei, P. Anitha, C.W. Gan and W.Y. Zhou. Poly(lactide)-vitamin E derivative/montmorillonite nanoparticle formulations for the oral delivery of Docetaxel, Biomaterials, 30, 3297-3306. 2009.

Ferrari, M. Cancer nanotechnology: opportunities and challenges, Nat. Rev. Cancer, 5, pp.161-171. 2005.

Fessi, H., F. Puisieux, J.P. Devissaguet, N. Ammoury and S. Benita. Nanocapsule formation by interfacial polymer deposition following solvent displacement, Int. J. Pharm., 55, pp.R1-R4. 1989.

Fjallskog, M. L., L. Frii and J. Bergh. Is cremophor, solvent for paclitaxel, cytotoxic? Lancet, 342, pp.876. 1993.

Fonseca, C., S. Simões and R. Gaspar. Paclitaxel-loaded PLGA nanoparticles: preparation, physicochemical characterization and in vitro anti-tumoral activity, J. Control. Release, 83, pp.273-286. 2002.

Gabizon, A. Emerging role of liposomal drug carrier systems in cancer chemotherapy, J. Liposome Res., 13, pp.17-20. 2003.

Gabizon, A.A. Pegylated liposomal doxorubicin: metamorphosis of an old drug into a new form of chemotherapy, Cancer Invest., 19, pp.424-436. 2001.

Galindo-Rodriguez, S., E. Allémann, H. Fessi and E. Doelker. Physicochemical parameters associated with nanoparticle formation in the salting-out, emulsification-diffusion, and nanoprecipitation methods, Pharm. Res., 21, pp.1428-1439. 2004.

Gan, C.W. and S.S. Feng. Transferrin-conjugated nanoparticles of Poly(lactide)-D-a-Tocopheryl polyethylene glycol succinate diblock copolymer for targeted drug delivery across the bloodebrain barrier, Biomaterials, 31, pp.7748-7757. 2010.

Gan, C.W., S. Chien and S.S. Feng. Nanomedicine: Enhancement of chemotherapeutical efficacy of docetaxel by using a biodegradable nanoparticle formulation, Curr. Pharm. Design, 16, pp.2308-2320. 2010.

Gao, X.H., Y.Y. Cui, R.M. Levenson, L.W.K. Chung and S.M. Nie. In vivo cancer targeting and imaging with semiconductor quantum dots, Nat. Biotechnol., 22, pp.969-976. 2004.

Gao, Y., L.B. Li and G. Zhai. Preparation and characterization of Pluronic/TPGS mixed micelles for solubilization of camptothecin, Colloid Surf., 64, pp.194-199. 2009.

Garti, N. What can nature offer from an emulsifier point of view: trends and progress? Colloids Surf., 152, pp.125-146. 1999.

Gelderblom, H., J. Verweij, K. Nooter and A. Sparreboom. Cremophor EL: the drawbacks and advantages of vehicle selection for drug formulation, Eur. J. Cancer, 37, pp.1590-1598. 2001.

Gelmon, K. The taxoids: paclitaxel and docetaxel, Lancet, 344, pp.1267-1272. 1994.

Geng, Y., P. Dalhaimer, S. Cai, R. Tsai, M. Tewari, T. Minko and D.E. Discher. Shape effects of filaments versus spherical particles in flow and drug delivery, Nat. Nanotechnol., 2, pp.249-255. 2007.

Govender, T., S. Stolnik, M.C. Garnett, L. Illum and S.S. Davis. PLGA nanoparticles prepared by nanoprecipitation: drug loading and release studies of a water soluble drug, J. Control. Release, 57, pp.171-185. 1999.

Greenwald, R.B., Y.H. Choe, J. McGuire and C.D. Conover. Effective drug delivery by PEGylated drug conjugates, Adv. Drug Deliv. Rev. 55, pp.217-250. 2003.

Gref, R., Y. Minamitake, M.T. Peracchia, V. Trubetskoy, V. Torchilin and R. Langer. Biodegradable long-circulating polymeric nanospheres, Science, 263, pp.1600-1603. 1994.

Gros, L., H. Ringsdorf and H. Schupp. Polymeric anti-tumor agents on a molecular and on a cellular-level, Angew. Chem. Int. Ed., 20, pp.305-325. 1981.

Gu, F., L. Zhang, B.A. Teply, N. Mann, A. Wang, A.F. Radovic-Moreno, R. Langer and O.C. Farokhzad. Precise engineering of targeted nanoparticles by using self-assembled biointegrated block copolymers, Proc. Natl. Acad. Sci. USA, 105, pp.2586-2591. 2008.

Hagan, S.A., A.G.A. Coombes, M.C. Garnett, S.E. Dunn, M.C. Davis, L. Illum, S.S. Davis, S.E. Harding, S. Purkiss and P.R. Gellert. Polylactide-poly(ethylene glycol) copolymers as drug delivery systems. 1. Characterization of water dispersible micelle-forming systems, Langmuir, 12, pp.2153-2161. 1996.

Hanauske, A.-R., H. Depenbrock, D. Shirvani and J. Rastetter. Effects of the microtubule-disturbing agents docetaxel (Taxotere), vinblastine and vincristine on epidermal growth factor-receptor binding of human breast cancer cell lines in vitro, Eur. J. Cancer, 30, pp.1688-1694. 1994.

Hans, M.L. and A.M. Lowman. Biodegradable nanoparticles for drug delivery and targeting, Curr. Opin. Solid St. M., 6, pp.319-327. 2002.

Hatakeyama, H., A. Kikuchi, M. Yamato and T. Okano. Bio-functionalized thermoresponsive interfaces facilitating cell adhesion and proliferation, Biomaterials, 27, pp.5069-5078. 2006.

Hennenfent, K.L. and R. Govindan. Novel formulations of taxanes: a review. Old wine in a new bottle? Ann. of Oncol., 17, pp.735-749. 2006.

Hoare, T.R. and D.S. Kohane. Hydrogels in drug delivery: Progress and challenges, Polymer, 49, pp.1993-2007. 2008.

Holowka, E.P., V.Z. Sun, D.T. Kamei and T.J. Deming. Polyarginine segments in block copolypeptides drive both vesicular assembly and intracellular delivery, Nat. Mater., 6, pp.52-57. 2006.

Huang, H.Y., E.E. Remsen, T. Kowalewski and K.L. Wooley. Nanocages derived from shell cross-linked micelle templates, J. Am. Chem. Soc., 121, pp.3805-3806. 1999.

Hudis, C.A. Trastuzumab-mechanism of action and use in clinical practice, N. Engl. J. Med., 357, pp.39-51 (2007).

Huh, Y.M., Y.W. Jun, H.T. Song, S. Kim, J.S. Choi, J.H. Lee, S. Yoon, K.S. Kim, J.S. Shin, J.S. Suh and J. Cheon. In vivo magnetic resonance detection of cancer by using multifunctional magnetic nanocrystals, J. Am. Chem. Soc., 127, pp.12387-12391. 2005.

Immordino, M.L., P. Brusa, S. Arpicco, B. Stella, F. Dosio and L. Cattel. Preparation, characterization, cytotoxicity and pharmacokinetics of liposomes containing docetaxel, J. Control. Release, 91, pp.417-429. 2003.

Ito, J.-I., T. Kato, Y. Kamio, H. Kato, T. Kishikawa, T. Toda, S. Sasaki and R. Tanaka. A cellular uptake of cis-Platinum encapsulating liposome through endocytosis by human neuroblastoma cell, Neurochem. Int., 18, pp.257-264. 1991.

Jain, R.K. Physiological barriers to delivery of monoclonal antibodies and other macromolecules in tumors, Cancer Res., 50, pp.814-819. 1990.

Jain, R.K. Delivery of molecular and cellular medicine to solid tumors, Adv. Drug Deliv. Rev., 46, pp.149-168. 2001.

Jalil, R. and J. Nixon. Biodegradable poly (lactic acid) and poly (lactide-co-glycolide) microcapsules: Problems associated with preparative techniques and release properties, J. Microencapsul., 7, pp.297-325. 1990.

Jemal, A., R. Siegel, E. Ward, Y. Hao, J. Xu and M. J. Thun. Cancer statistics, 2009, CA Cancer J. Clin., 59, pp.225-249. 2009.

Jemal, A., R. Siegel, J. Xu and E. Ward. Cancer statistics, 2010, CA Cancer J. Clin., 60, pp.277-300. 2010.

Jemal, A., F. Bray, M.M. Center, J. Ferlay, E. Ward and D. Forman. Global cancer statistics, CA Cancer J. Clin., 61, pp.69-90. 2011.

Jiang, J., X. Tong and Y. Zhao. A new design for light-breakable polymer micelles, J. Am. Chem. Soc., 127, pp.8290-8291. 2005.

Jones, S. Head-to-head: docetaxel challenges paclitaxel, Eur. J. Cancer, Supp 4, pp.4-8. 2006.

Jones, S.E., J. Erban, B. Overmoyer, G.T. Budd, L. Hutchins, E. Lower, L. Laufman, S. Sundaram, W.J. Urba, K.I. Pritchard, R. Mennel, D. Richards, S. Olsen, M.L. Meyers and P.M. Ravdin. Randomized phase III study of docetaxel compared with paclitaxel in metastatic breast cancer, J. Clin. Oncol., 23, pp.5542-5551. 2005.

Kabanov, A.V., E.V. Batrakova and V.Y. Alakhov. Pluronic® block copolymers as novel polymer therapeutics for drug and gene delivery, J. Control. Release, 82, pp.189-212. 2002.

Kah, J.C.Y., K.Y. Wong, K.G. Neoh, J.H. Song, J.W. Fu, S. Mhaisalkar, M. Olive and C.J. Sheppard. Critical parameters in the pegylation of gold nanoshells for biomedical applications: an in vitro macrophage study, J. Drug Target., 17, pp.181-193. 2009.

Kakizawa, Y. and K. Kataoka. Block copolymer micelles for delivery of gene and related compounds, Adv. Drug Deliv. Rev., 54, pp.203-222. 2002.

Kataoka, K., A. Harada and Y. Nagasaki. Block copolymer micelles for drug delivery: Design, characterization and biological significance, Adv. Drug Deliv. Rev., 47, pp.113-131. 2001.

Kirpotin, D.B., D.C. Drummond, Y. Shao, M.R. Shalaby, K. Hong, U.B. Nielsen, J.D. Marks, C.C. Benz and J.W. Park. Antibody targeting of long-circulating lipidic nanoparticles does not increase tumor localization but does increase internalization in animal models, Cancer Res., 66, pp.6732-6740. 2006.

Klein, C.A. Cancer: The metastasis cascade, Science, 321, pp.1785-1787. 2008.

Klibanov, A.L., K. Maruyama, V.P. Torchilin and L. Huang. Amphipatic polyethyleneglycols effectively prolong the circulation time of liposomes, FEBS Lett., 268, pp.235-237. 1990.

Klouda, L. and A.G. Mikos. Thermoresponsive hydrogels in biomedical applications, Eur. J. Pharm. Biopharm., 68, pp.34-45. 2008.

Koo, Y.E.L., G.R. Reddy, M. Bhojani, R. Schneider, M.A. Philbert, A. Rehemtulla, B.D. Ross and R. Kopelman. Brain cancer diagnosis and therapy with nanoplatforms, Adv. Drug Deliv. Rev., 58, pp.1556-1577. 2006.

Kopecek, J. and J. Yang. Hydrogels as smart materials, Polym. Int., 56, pp.1078-1098. 2007.

Kopecek, J. Hydrogel biomaterials: A smart future? Biomaterials, 28, pp.5185-5192. 2007.

Kopelman, R., Y.E.K. Lee, M. Philbert, B.A. Moffat, G.R. Reddy, P. McConville, D.E. Hall, T.L. Chenevert, M.S. Bhojani, S.M. Buck, A. Rehemtulla and B.D. Ross. Multifunctional nanoparticle platforms for in vivo MRI enhancement and photodynamic therapy of a rat brain cancer, J. Magn. Magn. Mater., 293, pp.404-410. 2005.

Kostarelos, K. The long and short of carbon nanotube toxicity, Nat. Biothechnol., 26, pp.774-776. 2008.

Kreuter, J. Nanoparticulate systems for brain delivery for drugs, Adv. Drug Deliv. Rev., 47, pp.65-81. 2001.

Kreuter, J., P. Ramge, V. Petrov, S. Hamm, S.E. Gelperina, B. Engelhardt, R. Alyautdin, H. von Briesen and D.J. Begley. Direct evidence that polysorbate-80-coated poly (butylcyanoacylate) nanoparticles deliver drugs to the CNS via specific mechanisms requiring prior binding of drugs to the nanoparticles, Pharm. Res., 20, pp.409-416. 2003.

Krishna, R., and L.D. Mayer. Multidrug resistance (MDR) in cancer - Mechanisms, reversal using modulators of MDR and the role of MDR modulators in influencing the pharmacokinetics of anticancer drugs, Eur. J. Pharm. Sci., 11, pp.265-83. 2000.

Kukowska-Latallo, J.F., K.A. Candido, Z.Y. Cao, S.S. Nigavekar, I.J. Majoros, T.P. Thomas, L.P. Balogh, M.K. Khan and J.R. Baker, Nanoparticle targeting of anticancer drug improves therapeutic response in animal model of human epithelial cancer, Cancer Res., 65, pp.5317-5324. 2005.

Langer, R. Drug delivery and targeting, Nature, 392, pp.5-10. 1998.

Langer, R. Drug delivery: Drugs on target, Science, 293, pp.58-59. 2001.

Lasic, D.D. Liposomes: from physics to applications, Elsevier. 1993.

Lavasanifar, A., J. Samuel, G.S. Kwon. Poly(ethylene oxide)-block-poly(L-amino acid) micelles for drug delivery, Adv. Drug Deliv. Rev., 54, pp.169-190. 2002.

Lavelle, F., M.C. Bissery and C. Combeau. Preclinical evaluation of docetaxel (Taxotere), Semin. Oncol., 22, pp.3-16. 1995.

Leamon, C.P. and P.S. Low. Delivery of macromolecules into living cells: a method that exploits folate receptor endocytosis, Proc. Natl. Acad. Sci., 88, pp.5572-5576. 1991.

Lee, C.C., J.A. MacKay, J.M.J. Frechet and F.C. Szoka. Designing dendrimers for biological applications, Nat. Biotechnol., 23, pp.1517-1526. 2005,

Lee, C.C., E.R. Gillies, M.E. Fox, S.J. Guillaudeu, J.M.J. Frechet, E.E. Dy and F.C. Szoka. A single dose of doxorubicin-functionalized bow-tie dendrimer cures mice bearing C-26 colon carcinomas, Proc. Natl. Acad. Sci., 103, pp.16649-16654. 2006.

Lee, E., K. Na, Y.H. Bae. Polymeric micelle for tumor pH and folate-mediated targeting, J. Control. Release, 91, pp.103-113. 2003.

Lee, R.J. and P.S. Low. Folate-mediated tumor cell targeting of liposome-entrapped doxorubicin in vitro, Biochim. Biophys. Acta, 1233, pp.134-144. 1995.

Lee, S.H., Z. Zhang and S.S. Feng. Nanoparticles of poly(lactide)-tocopheryl polyethylene glycol succinate (PLA-TPGS) copolymers for protein drug delivery, Biomaterials, 28, pp.2041-2050. 2007.

Li, C., D.F. Yu, R.A. Newman, F. Cabral, L.C. Stephens, N. Hunter, L. Milas and S. Wallace. Complete regression of well-established tumors using a novel water-soluble poly(L-glutamic acid)-paclitaxel conjugate, Cancer Res., 58, pp.2404-2409. 1998.

Li, Y.Q., H.L. Wong, A.J. Shuhendler, A.M. Rauth and X.Y. Wu. Molecular interactions, internal structure and drug release kinetics of rationally developed polymer-lipid hybrid nanoparticles, J. Control. Release, 128, pp.60-70. 2008.

Liu, Y.Y., Y.H. Shao and J. Lu. Preparation, properties and controlled release behaviors of pH-induced thermosensitive amphiphilic gels, Biomaterials, 27, pp.4016-4024. 2006.

Liu, Z., C. Davis, W. Cai, L. He, X. Chen and H. Dai. Circulation and long-term fate of functionalized, biocompatible single-walled carbon nanotubes in mice probed by Raman spectroscopy, P. Natl. Acad. Sci., 105, pp.1410-1415. 2008.

Lockman, P.R., R.J. Mumper, M.A. Khan and D.D. Allen. Nanoparticle technology for drug delivery across the blood-brain barrier, Drug Dev. Ind. Pharm., 28, pp.1-13. 2002.

Longo, R., F. Torino and G. Gasparini. Targeted therapy of breast cancer, Curr. Pharma. Design, 13, pp.497-517. 2007.

Lopes, N.M., E.G. Adams, T.W. Pitts and B.K. Bhuyan. Cell kill kinetics and cell cycle effects of Taxol on human and hamster ovarian cell lines, Cancer Chemoth. Pharm., 32, pp.235-242. 1993.

Lukyanov, A.N. and V.P. Torchilin. Micelles from lipid derivatives of water-soluble polymers as delivery systems for poorly soluble drugs, Adv. Drug Deliv. Rev., 56, pp.1273-1289. 2004.

Müller, R.H., C. Jacobs and O. Kayser. Nanosuspensions as particulate drug formulations in therapy: Rationale for development and what we can expect for the future, Adv. Drug Deliv. Rev., 47, pp.3-19. 2001.

Maeda, H., J. Wu, T. Sawa, Y. Matsumura and K. Hori. Tumor vascular permeability and the EPR effect in macromolecular therapeutics: a review, J. Control. Release, 65, pp.271-284. 2000.

Maeda, H. The enhanced permeability and retention (EPR) effect in tumor vasculature: the key role of tumor-selective macromolecular drug targeting, Adv. Enzyme Regul., 41, pp.189-207. 2001.

Makino, K., T. Yamada, M. Kimura, T. Oka, H. Ohshima and T. Kondo. Temperature- and ionic strength-induced conformational changes in the lipid head group region of liposomes as suggested by zeta potential data, Biophys. Chem., 41, pp.175-183. 1991.

Malik, N., E. G. Evagorou and R. Duncan. Dendrimer-platinate: A novel approach to cancer chemotherapy, Anticancer Drugs, 10, pp.767-776. 1999.

Manske, R. and H. Holmes. The Alkaloids: Chemistry and Physiology. The American Journal of Medical Sciences. 1952.

Marty, J.J., R.C. Oppenheim and P. Speiser. Nanoparticles: New colloidal drug delivery system, Pharm. Acta Helv., 53, pp.17-23. 1978.

Matsumura, Y. and H. Maeda. A new concept for macromolecular therapeutics in cancer chemotherapy: mechanism of tumoritropic accumulation of proteins and the antitumor agent smancs, Cancer Res., 46, 6387-6392. 1986.

Mbeunkui, F. and D.J. Johann. Cancer and the tumor microenvironment: a review of an essential relationship, Cancer Chemother. Pharmacol., 63, pp.571-582. 2009.

Meerum Terwogt, J. M., W.W. ten Bokkel Huinink, J.H. Schellens, M. Schot, I.A. Mandjes, M.G. Zurlo, M. Rocchetti, H. Rosing, F.J. Koopman and J.H. Beijnen. Phase I clinical and pharmacokinetic study of PNU166945, a novel water soluble polymer-conjugated prodrug of paclitaxel, Anticancer Drugs, 12, pp.315-323. 2001.

Mei, L., Y.Q. Zhang, Y. Zheng, G. Tian, C.X. Song, D.Y. Yang, H. Chen, H. Sun, Y. Tian, K. Liu, Z. Li and L. Huang. A novel docetaxel-loaded poly (epsilon-caprolactone)/Pluronic F68 nanoparticle overcoming multidrug resistance for breast cancer treatment, Nanoscale Res. Lett., 4, pp.1530-1539. 2009.

Miller, C.A. Spontaneous emulsification produced by diffusion: A review, Colloids Surf., 29, pp.89-102. 1988.

Minchinton, A.l. and I.F. Tannock. Drug penetration in solid tumours, Nat. Rev. Cancer, 6, pp.583-592. 2006.

Moghimi, S.M., A.C. Hunter and J.C. Murray. Nanomedicine: Current status and future prospects, FASEB J., 19, pp.311-330. 2005.

Mu, L. and S.S. Feng. Vitamin E TPGS used as emulsifier in the solvent evaporation/extraction technique for fabrication of polymeric nanospheres for controlled release of paclitaxel, J. Control. Release, 80, pp.129-144. 2002.

Mu, L. and S.S. Feng. A novel controlled release formulation for the anticancer drug Paclitaxel (Taxol®): PLGA nanoparticles containing vitamin E TPGS, J. Control. Release, 86, pp.33-48. 2003.

Mu, L., P.H. Seow, S.N. Ang and S.S. Feng. Study on surfactant coating of polymeric nanoparticles for controlled delivery of anticancer drug, Colloid Polym. Sci., 283, pp.58-65. 2004.

Mu, L., T.A. Elbayoumi and V.P. Torchilin. Mixed micelles made of poly(ethylene glycol)-phosphatidylethanolamine conjugate and D-α-tocopherol succinate polyethylene glycol 1000 succinate as pharmaceutical nanocarriers for camptothecin, Int. J. Pharm., 306, pp.142-149. 2005.

Mu, L. and P.H. Seow. Application of TPGS in polymeric nanoparticulate drug delivery system, Colloid Surf., 47, pp.90-97. 2006.

Muller, V., I. Witzel and E. Stickeler. Immunological approaches in the treatment of metastasized breast cancer, Breast Care, 4, pp.358-366. 2009.

Murugesan, S., P. Mishra and N.K. Jain. Development of folate-conjugated PEGylated poly (d, l-lactide-co-glycolide) nanoparticulate carrier for docetaxel, Curr. Nanosci., 4, pp.402-408. 2008.

Musumeci, T., C.A. Ventura, I. Giannone, B. Ruozi, L. Montenegro, R. Pignatello and G. Puglisi. PLA/PLGA nanoparticles for sustained release of docetaxel, Int. J. Pharm., 325, pp.172-179. 2006.

Na, K., J.H. Park, S.W. Kim, B.K. Sun, D.G. Woo, H.M. Chung and K.H. Park. Delivery of dexamethasone, ascorbate, and growth factor (TGF beta-3) in thermo-reversible hydrogel constructs embedded with rabbit chondrocytes, Biomaterials, 27, pp.5951-5957. 2006.

Nahta, R. and F.J. Esteva. Herceptin: mechanisms of action and resistance, Cancer Lett., 232, pp.123-138. 2006.

Neradovic, D., O. Soga, C.F. van Nostrum and W.E. Hennink. The effect of the processing and formulation parameters on the size of nanoparticles based on block copolymers of poly(ethylene glycol) and poly(N-isopropylacrylamide) with and without hydrolytically sensitive groups, Biomaterials, 25, pp.2409-2418. 2004.

New, R.R.C. Liposomes a practical approach, Oxford University Press. 1990.

Nie, S. Understanding and overcoming major barriers in cancer nanomedicine. Nanomedicine 5, pp.523-528. 2010.

Nishiyama, N. and K. Kataoka. Current state, achievements, and future prospects of polymeric micelles as nanocarriers for drug and gene delivery, Pharmacol. Ther., 112, pp.630-648. 2006.

Noble, C.O., D.B. Kirpotin, M.E. Hayes, C. Mamot, K. Hong, J.W. Park, C.C. Benz, J.D. Marks and D.C. Drummond. Development of ligand-targeted liposomes for cancer therapy, Expert Opin. Ther. Targets, 8, pp.335-353. 2004.

Ochoa, L., A. Tolcher, J. Rizzo, G. Schwartz, A. Patnaik, L. Hammond, H. McCreery, L. Denis, M. Hidalgo, J. Kwiatek, J. McGuire and E. Rowinsky. A Phase I study of PEG-camptothecin (PEG-CPT) in patients with advanced solid tumours: A novel formulation for an insoluble but active agent, Proc. Am. Soc. Clin. Oncol., 19, pp.700. 2000.

Olivier, J. Drug transport to brain with targeted nanoparticles, NeuroRx, 2, pp.108-119. 2005.

Owens, D.E. and N.A. Peppas. Opsonization, biodistribution, and pharmacokinetics of polymeric nanoparticles. Int. J. Pharm., 307, pp.93-102. 2006.

Pan, J. and S.S. Feng. Folate-decorated poly (lactide)-vitamin E TPGS nanoparticles for targeted delivery of paclitaxel, Biomaterials, 29, pp.2663-2672. 2008.

Pan, J. and S.S. Feng. Targeting and imaging cancer cells by Folate-decorated, quantum dots (QDs) - loaded nanoparticles of biodegradable polymers, Biomaterials, 30, pp.1176-1183. 2009.

Pang, Z., W. Lu, H. Gao, K. Hu, J. Chen, C. Zhang, X. Gao, X. Jiang and C. Zhu. Preparation and brain delivery property of biodegradable polymersomes conjugated with OX26, J. Control. Release, 128, pp.120-127. 2008.

Park, J. W., C.C. Benz. and F.J. Martin. Future directions of liposome and immunoliposome based cancer therapeutics, Semin. Oncol., 31, pp.196-205. 2004.

Park, K., S. Lee, E. Kang, K. Kim, K. Choi and I.C. Kwon. New generation of multifunctional nanoparticles for cancer imaging and therapy, Adv. Func. Mater., 19, pp.1553-1566. 2009.

Parveen, S. and S.K. Sahoo. Polymeric nanoparticles for cancer therapy, J. Drug Target., 16, pp.108-123. 2008.

Pasut, G. and F.M. Veronese. Polymer-drug conjugation, recent achievements and general strategies, Prog. Polym. Sci., 32, pp.933-961. 2007.

Patel, G. B. and G.D. Sprott. Archaeobacterial ether lipid liposomes (archaeosomes) as novel vaccine and drug delivery systems, Crit. Rev. Biotechnol., 19, pp.317-357. 1999.

Patil, A., I.M. Shaikh, V.J. Kadam and K.R. Jadhav. Nanotechnology in therapeutics - Current technologies and applications, Curr. Nanosci., 5, pp.141-153. 2009.

Pelicano, H., D.S. Martin, R.H. Xu and P. Huang. Glycolysis inhibition for anticancer treatment, Oncogene, 25, pp.4633-4646. 2006.

Phillips, G.D.L., G.M. Li, D.L. Dugger, L.M. Crocker, K.L. Parsons, E. Mai, W.A. Blättler, J.M. Lambert, R.V. Chari, R.J. Lutz, W.L. Wong, F.S. Jacobson, H. Koeppen, R.H. Schwall, S.R. Kenkare-Mitra, S.D. Spencer and M.X. Sliwkowski. Targeting HER2-positive breast cancer with Trastuzumab-DM1, an antibody-cytotoxic drug conjugate, Cancer Res., 68, pp.9280-9290. 2008.

Pratten, M., J. Lloyd, G. Horpel, H. Ringsdorf. Micelle forming block copolymers: Pinocytosis by macrophages and interaction with model membranes, Makromol. Chem. Macromol. Chem. Phys., 186, pp.725-733. 1985.

Qiu, L.Y. and Y.H. Bae. Polymer architecture and drug delivery, Pharm. Res., 23, pp.1-30. 2006.

Rai, S., R. Paliwal, P.N. Gupta, K. Khatri, A.K. Goyal, B. Vaidya and S.P. Vyas. Solid lipid nanoparticles (SLNs) as a rising tool in drug delivery science: one step up in nanotechnology, Curr. Nanosci., 4, pp.30-44. 2008.

Rapoport, N. Physical stimuli-responsive polymeric micelles for anti-cancer drug delivery, Prog. Polym. Sci., 32, pp.962-990. 2007.

Rijcken, C.J., C.J. Snel, R.M. Schiffelers, C.F. van Nostrum and W.E. Hennink. Hydrolysable core-crosslinked thermosensitive polymeric micelles: Synthesis, characterisation and in vivo studies, Biomaterials, 28, pp.5581-5593. 2007.

Riou, J.F., A. Naudin and E. Lavelle. Effects of Taxotere on murine and human tumor cell lines, Biochem. Biophys. Res. Commun., 187, pp.164-170. 1992.

Riou, J.F., O. Petitgenet, C. Combeau and F. Lavelle. Cellular uptake and efflux of Docetaxel (Taxotere®) and Paclitaxel (Taxol®) in P388 cell line, Proc. Am. Assoc. Cancer Res., 35, pp.385. 1994.

Ross, J.S., J.A. Fletcher, K.J. Bloom, G.P. Linette, J .Stec, W.F. Symmans, L. Pusztai and G.N. Hortobagyi. Targeted therapy in breast cancer: the HER-2/neu gene and protein, Mol. Cell Proteomics, 3, pp.379-98. 2004.

Rowinsky, E.K., L.A. Cazenave and R.C. Donehower. Taxol: a novel investigational antimicrotubule agent, J. Natl. Cancer Inst., 82, pp.1247-1259. 1990.

Rowinsky, E.K., N. Onetto, R.M. Canetta and S.G. Arguck. Taxol - the 1st of the taxanes, an important new class of antitumor agents, Semin. Oncol., 6, pp.646-662. 1992.

Sadoqi, M., C.A. Lau-Cam and S.H. Wu. Investigation of the micellar properties of the tocopheryl polyethylene glycol succinate surfactants TPGS 400 and TPGS 1000 by steady state fluorometry, J. Colloid Interface Sci., 333, pp.585-589. 2009.

Scholes, P.D., A.G.A. Coombes, L. Illum, S.S. Daviz, M. Vert and M.C. Davies. The preparation of sub-200 nm poly (lactide-co-glycolide) microspheres for site specific drug delivery, J. Control. Release, 25, pp.145-153. 1993.

Seidman, A.D., M.N. Fornier, F.J. Esteva, L. Tan, S. Kaptain, A. Bach, K.S. Panageas, C. Arroyo, V. Valero, V. Currie, T. Gilewski, M. Theodoulou, M.E. Moynahan, M. Moasser, N. Sklarin, M. Dickler, G. D'Andrea, M. Cristofanilli, E. Rivera, G.N. Hortobagyi, L. Norton and C.A. Hudis. Weekly trastuzumab and paclitaxel therapy for metastatic breast cancer with analysis of efficacy by HER2 immunophenotype and gene amplification, J. Clin. Oncol., 19, pp.2587-2595. 2001.

Senter, P.D. Potent antibody drug conjugates for cancer therapy, Curr. Opin. Chem. Biol., 13, pp.235-244. 2009.

Senthilkumar, M., P. Mishra and N.K. Jain. Long circulating PEGylated poly(d,l-lactide-co-glycolide) nanoparticulate delivery of Docetaxel to solid tumors, J. Drug Target., 16, pp.424-435. 2008.

Sethuraman, V.A. and Y.H. Bae. Tat peptide-based micelle system for potential active targeting of anti-cancer agents to acidic solid tumors, J. Control. Release, 118, pp.216-224. 2007.

Seymour, L.W. for the Cancer Research Campaign Phase I/II Clinical Trials Committee. Hepatic drug targeting: Phase I evaluation of polymer-bound doxorubicin, J. Clin. Oncol., 20, pp.1668-1676. 2002.

Shi, G., Q. Cai, C. Wang, N. Lu, S. Wang and J. Bei. Fabrication and biocompatibility of cell scaffolds of poly(L-lactic acid) and poly(L-lactic-co-glycolic acid), Polymer Adv. Tech., 13, pp.227-232. 2002.

Shiokawa, T., Y. Hattori, K. Kawano, Y. Ohguchi, H. Kawakami, K. Toma and Y. Maitani. Effect of polyethylene glycol linker chain length of folate-linked microemulsions loading aclacinomycin A on targeting ability and antitumor effect in vitro and in vivo, Clin. Cancer Res., 11, pp.2018-2025. 2005.

Sinha, R., G.J. Kim, S. Nie and D.M. Shin. Nanotechnology in cancer therapeutics: bioconjugated nanoparticles for drug delivery, Mol. Cancer Ther., 5, pp.1909-1917. 2006.

Smart, S.K., A.I. Cassady, G.Q. Lu and D.J. Martin. The biocompatibility of carbon nanotubes, Carbon, 44, pp.1034-1047. 2006.

Smith, I.E. Efficacy and safety of Herceptin in women with metastatic breast cancer: results from pivotal clinical studies, Anticancer Drugs, 12, pp.S3-S10. 2001.

Soni, V., D.V. Kohli and S.K. Jain. Transferrin-conjugated liposomal system for improved delivery of 5-fluorouracil to brain, J. Drug Target., 16, pp.73-78. 2008.

Soppimath, K., T. Aminabhavi, A. Kulkarni and W. Rudzinski. Biodegradable polymeric nanoparticles as drug delivery devices, J. Control. Release, 70, pp.1-20. 2001.

Stohrer, M., Y. Boucher, M. Stangassinger and R.K. Jain. Oncotic pressure in solid tumors is elevated, Cancer Res., 60, pp.4251-4255. 2000.

Strebhardt, K. and A. Ullrich. Paul Ehrlich's magic bullet concept: 100 years of progress, Nat. Rev. Cancer, 8, pp.473-480. 2008,

Sun, B., B. Ranganathan and S.S. Feng. Multifunctional poly(D,L-lactide-co-glycolide)/montmorillonite (PLGA/MMT) nanoparticles decorated by trastuzumab for targeted chemotherapy of breast cancer, Biomaterials, 29, pp.475-486. 2008.

Sun, B. and S.S. Feng. Trastuzumab-functionalized nanoparticles of biodegradable copolymers for targeted delivery of docetaxel, Nanomedicine, 4, pp.431-445. 2009.

Sun, W., C. Xie, H. Wang and Y. Hu. Specific role of polysorbate 80 coating on the targeting of nanoparticles to the brain, Biomaterials, 25, pp.3065-3071. 2004.

Svenson, S., D.A. Tomalia. Dendrimers in biomedical applications-reflections on the field, Adv. Drug Deliv. Rev., 57, pp.2106-2129. 2005.

Tamargo, R.J. and H. Brem. Drug delivery to the central nervous system: a review, Neurosurg. Quat. 2, pp.259-279. 1992.

Tan, Y.F., P. Chandrasekharan, D. Maity, C.X. Yong, K.H. Chuang, Y. Zhao, S. Wang, J. Ding and S.S. Feng. Multimodal tumor imaging by iron oxides and quantum dots formulated in poly (lactic acid)-d-alpha-tocopheryl polyethylene glycol 1000 succinate nanoparticles, Biomaterials, 32, pp.2969-2978. 2011.

Tang, N., G. Du, N. Wang, C. Liu, H. Hang and W. Liang. Improving Penetration in Tumors With Nanoassemblies of Phospholipids and Doxorubicin, J. Natl. Cancer Inst., 99, pp.1004-1015. 2007.

Thevenot, J., A.L. Troutier, L. David, T. Delair and C. Ladaviere. Steric stabilization of lipid/polymer particle assemblies by poly(ethylene glycol)-lipids, Biomacromolecules, 8, pp.3651-3660. 2007.

Tong, R. and J. Cheng. Anticancer polymeric nanomedicines, Polym. Rev., 47, pp.345-381. 2007.

Torchilin, V.P. and V.S. Trubetskoy. Which polymers can make nanoparticulate drug carriers long-circulating? Adv. Drug Deliv. Rev., 16, pp.141-155. 1995.

Torchilin, V.P. Block copolymer micelles as a solution for drug delivery problems, Expert Opin. Ther. Patents, 15, pp.63-75. 2005.

Torchilin, V.P. Recent Advances with liposomes as pharmaceutical carriers, Nat. Rev. Drug Discov, 4, pp.145-160. 2005a.

Tsai, C.P., C.Y. Chen, Y. Hung, F.H. Chang and C.Y. Mou. Monoclonal antibody-functionalized mesoporous silica nanoparticles (MSN) for selective targeting breast cancer cells, J. Mater. Chem., 19, pp.5737-5743. 2009.

van Vlerken, L.E., T.K. Vyas and M.M. Amiji. Poly(ethylene glycol)-modified nanocarriers for tumor-targeted and intracellular delivery, Pharm. Res., 24, pp.1405-1414. 2007.

Vasey, P. and on behalf of the Cancer Research Campaign Phase I/II Committee. Phase I clinical and pharmacokinetic study of PK1 [N-(2-hydroxypropyl)methacrylamide copolymer doxorubicin]: first member of a new class of chemotherapeutic agents-drug-polymer conjugates, Clin. Cancer Res., 5, pp.83-94. 1999.

Veronese, F.M. and A. Mero. The impact of PEGylation on biological therapies, Biodrugs, 22, pp.315-329. 2008.

Vetvicka, D., M. Hruby, O. Hovorka, T. Etrych, M. Vetrik, L. Kovar, M. Kovar, K. Ulbrich and B. Rihova. Biological evaluation of polymeric micelles with covalently bound doxorubicin, Bioconjug. Chem., 20, pp.2090-2097. 2009.

Vogel, C.L., M.A. Cobleigh, D. Tripathy, J.C. Gutheil, L.N. Harris, L. Fehrenbacher, D.J. Slamon, M. Murphy, W.F. Novotny, M. Burchmore, S. Shak, S.J. Stewart and M. Press. Efficacy and safety of trastuzumab as a single agent in first-line treatment of HER2-overexpressing metastatic breast cancer, J. Clin. Oncol., 20, pp.719-726. 2002.

Wang, X., L. Yang, Z. Chen and D.M. Shin. Application of nanotechnology in cancer therapy and imaging, CA Cancer J. Clin., 58, pp.97-110. 2008.

Webster, L., M. Linsenmeyer, M. Millward, C. Morton, J. Bishop, and D. Woodcock. Measurement of cremopnor EL following taxol: Plasma levels sufficient to reverse

drug exclusion mediated by the multidrug-resistant phenotype, J. Natl. Cancer Inst., 85, pp.1685-1690. 1993.

Wichterle, O. and D. L ím. Hydrophilic gels for biological use, Nature, 185, pp.117-118. 1960.

Win, K.Y. and S.S. Feng. Effects of particle size and surface coating on cellular uptake of polymeric nanoparticles for oral delivery of anticancer drugs, Biomaterials, 26, pp.2713-2722. 2005.

Win, K.Y. and S.S. Feng. In vitro and in vivo studies on vitamin E TPGS-emulsified poly(D,L-lactic-co-glycolic acid) nanoparticles for paclitaxel formulation, Biomaterials, 27, pp.2285-2291. 2006.

Wong, H.L., R. Bendayan, A.M. Rauth and X.Y. Wu. Simultaneous delivery of doxorubicin and GG918 (Elacridar) by new polymer-lipid hybrid nanoparticles (PLN) for enhanced treatment of multidrug-resistant breast cancer, J. Control. Release, 116, pp.275-284. 2006.

Wong, H.L., R. Bendayan, A.M. Rauth, H.Y. Xue, K. Babakhanian and X.Y. Wu. A mechanistic study of enhanced doxorubicin uptake and retention in multidrug resistant breastcancer cells using a polymer-lipid hybrid nanoparticle system, J. Pharmacol. Exp. Ther., 317, pp.1372-1381. 2006a.

Wong, H.L., A.M. Rauth, R. Bendayan and X.Y. Wu. In vivo evaluation of a new polymer-lipid hybrid nanoparticle (PLN) formulation of doxorubicin in a murine solid tumor model, Eur. J. Pharm. Biopharm., 65, pp.300-308. 2007.

Wu, J., Q. Liu and R.J. Lee. A folate receptor-targeted liposomal formulation for paclitaxel, Int. J. Pharm., 316, pp.148-153. 2006.

Xie, J., C. Lei, Y. Hu, G.K. Gay, N.H.B. Jamali and C.H. Wang. Nanoparticulate formulations for paclitaxel delivery across MDCK cell monolayer, Curr. Pharm. Design, 16, pp.2331-2340. 2010.

Xu, C. and J. Kopecek. Self-assembling hydrogels, Polymer Bulletin, 58, pp.53-63. 2007.

Yamamoto, Y., Y. Nagasaki, Y. Kato, Y. Sugiyama and K. Kataoka. Long-circulating poly(ethylene glycol)-poly(D,L-lactide) block copolymer micelles with modulated surface charge, J. Control. Release, 77, pp.27-38. 2001.

Yang, K., S. Zhang, G. Zhang, X. Sun, S.T. Lee and Z. Liu. Graphene in mice: Ultrahigh in vivo tumor uptake and efficient photothermal therapy, Nano Lett., 10, pp.3318-3323. 2010.

Yang, S.T., K.A. Fernando, J.H. Liu, J. Wang, H.F. Sun, Y. Liu, M. Chen, Y. Huang, X. Wang, H. Wang and Y.P. Sun. Covalently PEGylated carbon nanotubes with stealth character in vivo, Small, 4, pp.940-944. 2008.

Yang, T., M.K. Choi, F.D. Cui, S.J. Lee, S.J. Chung, C.K. Shim and D.D. Kim. Antitumor effect of paclitaxel-loaded PEGylated immunoliposomes against human breast cancer cells, Pharm. Res., 24, pp.2402-2411. 2007.

Yarden, Y. The EGFR family and its ligands in human cancer: signalling mechanisms and therapeutic opportunities, Eur. J. Cancer, 37, pp.S3-S8. 2001.

Yatvin, M.B., W. Kreutz, B.A. Horwitz and M. Shinitzky. pH-sensitive liposomes: possible clinical implications, Science, 210, pp.1253-1255. 1980.

Yin, X., A.S. Hoffman and P.S. Stayton. Poly(N-isopropylacrylamide-copropylacrylic acid) copolymers that respond sharply to temperature and pH, Biomacromolecules, 7, pp.1381-1385. 2006.

Yoo, H.S. and T.G. Park. Folate-receptor-targeted delivery of doxorubicin nanoaggregates stabilized by doxorubicine-PEG-folate conjugate, J. Control. Release, 100, pp.247-56. 2004.

Zalipsky, S., M. Qazen, J.A. Walker, N. Mullah, Y.P. Quinn and S.K. Huang. New detachable poly(ethylene glycol) conjugates: cysteine-cleavable lipopolymers regenerating natural phospholipid, diacyl phosphatidylethanolamine, Bioconjug. Chem., 10, pp.703-707. 1999.

Zhang, L., F.X. Gu, J.M. Chan, A.Z. Wang, R. Langer and O.C. Farokhzad. Nanoparticles in medicine: therapeutic applications and developments, Clin. Pharmacol. Ther., 83, pp.761-769. 2008a.

Zhang, L., J.M. Chan, F.X. Gu, J.-W. Rhee, A.Z. Wang, A.F. Radovic-Moreno, F. Alexis, R. Langer and O.C. Farokhzad. Self-assembled lipid-polymer hybrid nanoparticles: a robust drug delivery platform, ACS Nano, 2, pp.1696-1702. 2008b.

Zhang, Z. and S.S. Feng. The drug encapsulation efficiency, in vitro drug Release, cellular uptake and cytotoxicity of paclitaxel-loaded poly(lactide)-tocopheryl polyethylene glycol succinate nanoparticles, Biomaterials, 27, pp.4025-4033. 2006.

Zhang, Z. and S.S. Feng. Nanoparticles of poly(lactide)/vitamin E TPGS copolymer for cancer chemotherapy: Synthesis, formulation, characterization and in vitro drug release, Biomaterials, 27, pp.262-270. 2006a.

Zhang, Z., S.H. Lee and S.S. Feng. Folate-decorated poly(lactide-co-glycolide)-vitamin E TPGS nanoparticles for targeted drug delivery, Biomaterials, 28, pp.1889-1899. 2007.

Zhang, Z., S.H. Lee, C.W. Gan and S.S. Feng. *In vitro* and *in vivo* investigation on PLA-TPGS nanoparticles for controlled and sustained small molecule chemotherapy, Pharm. Res., 25, pp.1925-1935. 2008.

Zhao, H.Z., and L.Y.L. Yung. Selectivity of folate conjugated polymer micelles against different tumor cells, Int. J. Pharm., 349, pp.256-268. 2008.

Zhao, H.Z., and L.Y.L. Yung. Addition of TPGS to folate-conjugated polymer micelles for selective tumor targeting, J. Biomed. Mater. Res., 91A, pp.505-518. 2009.

Zhao, Y., J. Neuzil and K. Wu. Review: Vitamin E analogues as mitochondria-targeting compounds: From the bench to the bedside? Mol. Nutr. Food Res., 53, pp.129-139. 2009.

Zhen, X.M., G.P. Martin and C. Marriott. The controlled delivery of drugs to the lung, Int. J. Pharm., 124, pp.149-164. 1995.

Zheng, D.H., D. Li, X.W. Lu and Z.Q. Feng. Enhanced antitumor efficiency of docetaxel-loaded nanoparticles in a human ovarian xenograft model with lower systemic toxicities by intratumoral delivery, Oncol. Rep. 23, pp.717-724. 2010.

Zweers, M.L.T., G.H.M. Engbers, D.W. Grijpma and J. Feijen. In vitro degradation of nanoparticles prepared from polymers based on dl-lactide, glycolide and poly(ethylene oxide), J. Control. Release, 100, pp.347-356. 2004.

LIST OF PUBLICATIONS

JOURNAL PUBLICATIONS

Liu Y, Siow JYF, Feng SS*. Chemotherapeutic engineering on nanoparticles of biodegradable polymers for anticancer drug delivery: Effects of newly applied surfactant macromolecules. Submitted.

Liu Y, Mi Y, Zhao J, Feng SS*. Multifunctional silica nanoparticles for targeted delivery of hydrophobic imaging and therapeutic agents. Accepted by Int J Pharm.

Liu Y, Mi Y, Feng SS*. Editorial: Nanotechnology for multimodal imaging. Nanomedicine 2011;6:1141-1144.

Mi Y, Li K, **Liu Y**, Pu KY, Liu B, Feng SS*. Herceptin Functionalized Polyhedral Oligomeric Silsesquioxane - Conjugated Oligomers - Silica/Iron Oxide Nanoparticles for Tumor Cell Sorting and Detection. Biomaterials 2011;32:8226-8233.

Li K, Jiang Y, Ding D, Zhang X, **Liu Y**, Hua J, Feng SS, Liu B*. Folic acid-functionalized two-photon absorbing nanoparticles for targeted MCF-7 cancer cell imaging. Chem Commun 2011;47:7323-7325.

Pan J, Mi Y, Wan D, **Liu Y**, Feng SS, Gong J*. PEGylated liposome coated QDs/mesoporous silica core-shell nanoparticles for molecular imaging. Chem Commun 2011;47:3442-3444.

Mi Y, **Liu Y**, Feng SS*. Research highlights: Herceptin®-conjugated nanocarriers for targeted imaging and treatment of HER2-positive cancer. Nanomedicine 2011;6:311-315.

Mi Y, **Liu Y**, Feng SS*. Formulation of Docetaxel by folic acid-conjugated D-α-tocopheryl polyethylene glycol succinate 2000 (Vitamin E TPGS2k) micelles for targeted and synergistic chemotherapy. Biomaterials 2011;32:4058-4066.

Li K, **Liu Y**, Pu KY, Feng SS, Zhan R, Liu B*. Polyhedral oligomeric silsesquioxanes-containing conjugated polymer loaded PLGA nanoparticles with Trastuzumab (Herceptin) functionalization for HER2-positive cancer Cell detection. Adv Funct Mater 2011;21:287-294.

Liu Y, Li K, Liu B, Feng SS*. Leading Opinion: A strategy for precision engineering of nanoparticles of biodegradable copolymers for quantitative control of targeted drug delivery. Biomaterials 2010;31:9145-9155.

Liu Y, Feng SS*. Research highlights: Multimodal imaging for cancer detection. Nanomedicine 2010;5:687-691.

Liu Y, Pan J, Feng SS*. Nanoparticles of lipid monolayer shell and biodegradable polymer core for controlled release of paclitaxel: Effects of surfactants on particles size, characteristics and in vitro performance. Int J Pharm 2010;395:243-250.

Pan J, **Liu Y**, Feng SS*. Multifunctional biodegradable copolymer nanoparticles blend for cancer diagnosis. Nanomedicine 2010;5:347-360.

Liu Y, Li K, Pan J, Liu B, Feng SS*. Folic acid conjugated nanoparticles of mixed lipid monolayer shell and biodegradable polymer core for targeted delivery of Docetaxel. Biomaterials 2010;31:330-338. (Top 25 Hottest Article published on Biomaterials in Q3 2009.)

Li K, Pan J, Feng SS, Wu AW, Pu KY, **Liu Y**, Liu B*. Generic strategy of preparing fluorescent conjugated-polymer-loaded poly(DL-lactide-co-Glycolide) nanoparticles for targeted cell imaging. Adv Funct Mater 2009;19:3535-3542.

CONFERENCE PUBLICATIONS

Liu Y*, Feng SS. Nanoparticles of lipid monolayer shell and biodegradable polymer core for anticancer drug delivery. The 13th Asia Pacific Confederation of Chemical Engineering Congress. Oct. 2010, Taipei, ROC.

Liu Y*, Feng SS. The synergistic effect of herceptin and docetaxel in polylactide-D-α-tocopheryl polyethylene glycol succinate (PLA-TPGS) nanoparticles. Symposium on Innovative Polymers for Controlled Delivery. Sept. 2010, Suzhou, PRC. (Contributed as an inside cover image of conference proceeding book)

Phyo WM, **Liu Y**, Mi Y, Feng SS*. Formulations of lipid shell and polymer core nanoparticles for drug delivery. MRS-S Trilateral Conference on Advances in Nanoscience: Energy, Water and Healthcare. Aug. 2010, Singapore.

Liu Y*, Feng SS. Formulation of phospholipid coated PLGA nanoparticles for anticancer drug delivery. International Conference on Materials for Advanced Technologies 2009. Jun. 2009, Singapore.

BOOK CHAPTERS

Sun B, Rachmawati H, **Liu Y**, Zhao J, Feng SS. Antibody-Conjugated Nanoparticles of Biodegradable Polymers for Targeted Drug Delivery. Bionanotechnology II. In press.